

https://dspace.org/

The role of electrostatic interactions in the stability and structural integrity of human CLIC1

Legg-E'Silva, Derryn Audrey

2012-02-23
http://hdl.handle.net/10539/11336

Downloaded from a DSpace repository. https://dspace.org/

THE ROLE OF ELECTROSTATIC INTERACTIONS IN THE STABILITY AND STRUCTURAL INTEGRITY OF HUMAN CLIC1

Derryn Audrey Legg-E'Silva

A thesis submitted to the Faculty of Science, University of the Witwatersrand, Johannesburg, in fulfilment of the requirements for the degree of Doctor of Philosophy.

Johannesburg, 2011

DECLARATION

I declare that this thesis is my own, unaided work. It is being submitted for the Degree of Doctor of Philosophy in the University of the Witwatersrand, Johannesburg. It has not been submitted before for any degree or examination at any other University.



Derryn Audrey Legg-E'Silva

9 December 2011.

ABSTRACT

Chloride intracellular channel proteins (CLICs) are able to exist in a soluble or membrane-bound state. The mechanism by which the transition between the two states takes place is yet to be elucidated. It is proposed that structural rearrangements of the N-terminal domain take place when CLICs encounter the lower pH environment of the membrane surface (pH 5.5). This prompts the CLICs to form a soluble membrane-ready state prior to pore formation and membrane transversion. Since the insertion of CLIC1 into membranes occurs at low pH, perhaps protonation and electrostatic effects of key conserved residues at the domain interface situated within the transmembrane region bring about the structural changes necessary for this transition. Structural and sequence alignments revealed that a conserved salt-bridge interaction between conserved residues on helices 1 and 3 of the N-terminal domain is present at the domain interface of CLICs. Therefore, this interaction was proposed to play an important role in maintaining the structural integrity and conformational stability of the N-terminal domain. This hypothesis was tested by mutating conserved CLIC1 residues Arg29 and salt-bridge partner Glu81 to methionine, thus removing the salt-bridge interaction. The conformational stabilities of each mutant at pH 7 (cytosol) and pH 5.5 (membrane surface) in the absence of membranes was then measured and compared to that of the wild type protein. The mutations did not impact upon the structural integrity of the protein. However, removal of the salt-bridge and hydrogen bonding interactions caused a loss in the cooperativity of unfolding from the native to unfolded state that resulted in the formation of an intermediate species. The intermediate species are less stable than the intermediate species of wild type CLIC1 at pH 5.5. Nevertheless, the properties (secondary and tertiary structure, ANS binding and cooperative unfolding (N ↔ U)) of the intermediate species are the same for all mutants and wild type protein. It can be concluded that the salt-bridge and more importantly hydrogen bonding interactions between helices 1 and 3 stabilise the N-terminal domain of CLIC1. It can be hypothesised that in the absence of membranes under acidic conditions, such as those at the surface of the membrane, protonation of acidic amino acid residues at the domain interface cause destabilisation of the N-terminal domain. This causes a reduction in the activation energy barrier for the conversion of soluble CLIC1 to its membrane-insertion conformation.

I dedicate this work to the people who have always supported and encouraged me: my soul mate Elio, my mother Maryanne, my brother Tyrone, grandparents Dorothy and John, and my late father Edward, this is for you!

"It is not the critic who counts, not the man who points out how the strong man stumbled, or where the doer of deeds could have done better. The credit belongs to the man who is actually in the arena, whose face is marred by dust and sweat and blood, who strives valiantly, who errs and comes short again and again, who knows the great enthusiasms, the great devotions, and spends himself in a worthy cause, who at best knows achievement and who at the worst if he fails at least fails while daring greatly so that his place shall never be with those cold and timid souls who know neither victory nor defeat."

~ Theodore Roosevelt

ACKNOWLEDGEMENTS

I would like to thank the following people:

Professor Heini Dirr for his guidance, patience, motivation and support over the course of my studies. Thank-you for constantly inspiring me with the boundless enthusiasm and passion you have for this subject. It has been a privilege and honour working in your lab.

The members of the Protein Structure-Function Research Unit, University of the Witwatersrand for all their assistance and friendship.

Dr. Yasien Sayed for his support, motivation and friendship.

Dr Elizabeth Brenner and Dr Samantha Gildenhuys who always had time to listen, to discuss and to proof read.

I would like to recognise the contributions of Dr Sylvia Fanucchi and Dr Ikechukwu Achilonu, School of Molecular and Cell Biology, University of the Witwatersrand and Dr Manuel Fernandes, School of Chemistry, University of the Witwatersrand for their work on the CLIC1-R29M/E81M crystal structure.

Dr Mahmoud Soliman from the Computational Chemistry & Modelling Department of Chemistry, University of Bath for his expert work with LIGPLOT.

The University of the Witwatersrand and the South African National Research Foundation for financial support.

TABLE OF CONTENTS

DECLARATION i

ABSTRACT ii

ACKNOWLEDGEMENTS iv

TABLE OF CONTENTS v

LIST OF FIGURES vii

LIST OF TABLES ix

ABBREVIATIONS x

CHAPTER 1

INTRODUCTION 1
1.1. CLIC1 structure 4
1.2. CLIC1 channel formation 7
1.2.1. Regulation of channel formation 9
1.3. The stability of soluble CLIC1 10
1.4. Objectives 19

CHAPTER 2

MATERIALS AND METHODS 20
2.1. Materials 20
2.2. Methods 20
2.2.1. Oligonucleotide primer design 20
2.2.2. Site-directed mutagenesis 22
2.2.3. DNA sequencing 23
2.2.4. Protein over-expression and purification 24
2.2.4.1. Induction studies 24
2.2.4.2. Over-expression and purification 25
2.2.5. Protein concentration determination 26
2.2.6. Purification analysis 27
2.2.7. Structural characterisation 28
2.2.7.1. Circular dichroism spectroscopy 28
2.2.7.2. Fluorescence spectroscopy 30
2.2.8. Conformational stability studies 33
2.2.8.1. Equilibrium-unfolding data fitting 35
2.2.8.1.1. Two-state fitting model ($N \leftrightarrow U$) 36
2.2.8.1.2. Three-state fitting model ($N \leftrightarrow I \leftrightarrow U$) 38
2.2.9. Software for structural, sequence and protein property analysis 40

CHAPTER 3

RESULTS 41
3.1. Verification of the CLIC1 mutations 41
3.2. Protein over-expression and purification 41
3.3. Protein concentration determination 45
3.4. Structural integrity of the CLIC1 mutant proteins 45

3.4.1. Far-UV and near-UV CD spectroscopy 45
3.4.2. Fluorescence spectroscopy 47
3.5. Conformational stability of the CLIC1-WT and mutant proteins 54
3.5.1. Recovery 54
3.5.2. Urea-induced equilibrium unfolding 54
3.5.3. Fitting of equilibrium unfolding data 59
3.5.3.1. Two-state unfolding model 59
3.5.3.2. Three-state unfolding model 61
3.6. ANS binding 65
3.7. Properties of unfolding intermediate 70

CHAPTER 4

DISCUSSION 74
4.1. Impact of the mutations on the structural integrity of CLIC1 76
4.2. Impact of the mutations on the stability of CLIC1 78
4.3. Conclusion 94

CHAPTER 5

REFERENCES 95

CHAPTER 6

APPENDIX 115
6.1. Purification of CLIC1 R29M/E81M 116
6.2. R29M/E81M crystal structure 116
6.2.1. Crystallisation of CLIC1-R29M/E81M 116
6.2.2. Structure solution 117
6.3. Crystal structure of R29M/E81M 117

LIST OF FIGURES

Figure	Title	Page
1	Ribbon representation of the crystal structure of reduced CLIC1	5
2	Superimposed structures of the reduced and oxidised forms of soluble CLIC1	6
3	The proposed model for the CLIC1 transition from its soluble to membrane-bound form	11
4	Sequence alignment of the TMR and helix 3 of CLIC proteins	15
5	Residues which are topologically equivalent to Arg29, Asn78 and Glu81 in CLIC1	16
6	Structure-based sequence alignment of the N-terminal domain of CLIC proteins	18
7	Verification of the CLIC1-R29M, E81M, N78A and R29M/E81M mutations	42
8	Over-expression and induction study of CLIC1-R29M	43
9	SDS-PAGE gel and calibration curve	44
10	Far-UV CD spectra of the native CLIC1-WT and mutant proteins at pH 7 and 5.5	46
11	Near-UV CD spectra of the native CLIC1-WT and mutant proteins at pH 7 and 5.5	48
12	Fluorescence spectra of the native CLIC1-WT and mutant proteins	49
13	Fluorescence spectra of the unfolded CLIC1-WT and mutant proteins in the presence of 8 M urea	51
14	Stern-Volmer plots of the native CLIC1-WT and mutant proteins at pH 7 and 5.5	52
15	Urea-induced equilibrium unfolding of CLIC1-WT and mutant proteins monitored by far-UV CD and fluorescence spectroscopy	56
16	Maximum emission wavelengths of CLIC1-WT and mutant proteins	58

17	Rayleigh scatter measured during urea-induced equilibrium unfolding	60
18	Global fitting of unfolding data obtained at pH 7 and pH 5.5	62
19	Residual plots of the globally-fitted data	63
20	Chemical structure of 1-anilinonaphthalene-8-sulfonate (ANS)	66
21	ANS binding during unfolding	68
22	Rayleigh scatter plots for unfolding in the presence of ANS	69
23	Fractional populations of N, U and I states of CLIC1-WT and mutant proteins	71
24	Far-UV CD spectra of the intermediate species of CLIC1-WT and mutant proteins	72
25	Fluorescence spectra of the intermediate species of CLIC1-WT and mutant proteins	73
26	Ribbon representations of the tertiary environment around Trp35 of CLIC1-WT and CLIC1-R29M/E81M	77
27	Schematic of the thermodynamic unfolding pathways of the CLIC1-WT and mutant proteins	79
28	Hydrogen bonds between residues 29, 78, 81 and water	84
29	A schematic representation of the electrostatic network of CLIC1-WT and CLIC1-R29M/E81M with reference to residues 29 and 81	85
30	Salt-bridges at the domain interface of CLIC1	90
31	A schematic representation of the electrostatic network at the domain interface of CLIC1	91

LIST OF TABLES

Table	Title	Page
1	Summary of CLIC proteins locations and functions	3
2	K_{sv} values for the quenching of fluorescence by acrylamide	53
3	Percentage recoveries of the native folds of the CLIC1-WT and mutant proteins	55
4	Thermodynamic parameters and statistical data from global fitting	64
5	Residues interacting with residues 29 and 81 in CLIC1-WT and CLIC1-R29M/E81M	83

ABBREVIATIONS

Å	Ångström (10^{-10} m)
A_{280}	absorbance at 280 nm
ANS	8-anilino-1-napthalene sulfonate
C^{α}	alpha carbon
c	concentration / centi
^{o}C	degrees celsius
CD	circular dichroism
cDNA	complementary DNA
CLIC	chloride intracellular channel protein
DEAE	diethylaminoethyl
DNA	deoxyribose nucleic acid
DTT	dithiothreitol
dH_2O	distilled water
ds	double stranded
E_{222}	ellipticity at 222 nm
EDTA	ethylenediaminetetraacetic acid
E81M	glutamic acid 81 replaced with a methionine
F	fluorescence intensity in the presence of quencher
F_0	fluorescence intensity in the absence of quencher
F310	fluorescence emission intensity at 310 nm
F320	fluorescence emission intensity at 320 nm
F330	fluorescence emission intensity at 330 nm
F345	fluorescence emission intensity at 345 nm
g	gram

ΔG	the change in Gibbs free energy
$\Delta G(H_2O)$	the change in Gibbs free energy of unfolding in the absence of denaturant
GSH	glutathione
GST	glutathione *S*-transferase
I	intermediate conformation
K_{sv}	Stern-Volmer quenching constant
mdeg	milli degree
ss	single stranded
IPTG	isopropyl β-D-1-thiogalactopyranoside
kDa	kilo daltons
l	litre / path length
LB	Luria-Bertani
μ	micro
m	milli
min	minute
mol	mole
M	molar
ε	molar absorption coefficient
m-value	the dependence of the free energy of unfolding on denaturant concentration
θ	mean residue ellipticity
N	folded native conformation
n	non bonding molecular orbital/ number of residues/ nano
N78A	asparagine 78 replaced with an alanine

OD_{600}	optical density at 600 nm
p	pico
π	pi bonding orbital
π*	pi anti-bonding orbital
PDB	protein data bank
p*K*	ionisation state
pK_a	acid ionisation state
PTMR	putative transmembrane region
Q	quencher
R	universal gas constant
rmsd	root mean square distance
rpm	revolutions per minute
R29M	arginine 29 residue replaced with a methionine
R29M/E81M	arginine 29 and Glu81 replaced with methionine
SDS	sodium dodecyl sulfate
SDS-PAGE	sodium dodecyl sulfate-polyacrylamide gel electrophoresis
T	temperature in kelvin
T_m	temperature induced transition midpoint
U	unfolded conformation / units
UV	ultra violet
YT	yeast tryptone

The one- and three-letter symbolism for amino acids (IUPAC-IUB, 1984), and the one-letter symbolism for deoxyribonucleic acids (IUPAC-IUB, 1974) have been used in accordance with the IUPAC-IUBMB system of nomenclature.

CHAPTER 1

INTRODUCTION

Chloride ion channels occur on the plasma membrane of most eukaryotic cells as well as in other intracellular membranes (Cromer *et al.*, 2002; Harrop *et al.*, 2001). There are various chloride channels, the most recent of which to be characterised are the chloride intracellular channel (CLIC) proteins (al-Awgati, 1995; Jentsch and Gunther, 1997). CLICs are implicated in many physiological processes such as the control of the absorption and secretion of salt, normalisation of membrane potentials, cell volume homeostasis and organellar acidification (Strange *et al*., 1996). Disruption of their functioning can cause severe disease conditions such as Dents disease (Lloyd *et al.*, 1996), Bartters' syndrome (Simon *et al.*, 1997) and cystic fibrosis (Riordan *et al.*, 1998).

Metamorphic proteins are proteins that are able to assume different conformations under native conditions (Murzin, 2008). These different conformations do, however, contain the same amino acid sequence. These conformational changes are reversible for metamorphic proteins and have been shown to be influenced by changes in environmental conditions such as pH, temperature and redox (Murzin, 2008). CLIC proteins are categorised as metamorphic proteins as they are able to assume a reduced and oxidised conformation under native conditions (Littler *et al*., 2004). The soluble form of CLIC1 undergoes a structural transition with the concomitant loss of conformational stability when exposed to low pH conditions (Fanucchi *et al*., 2008). This transition involved the flexibility of certain regions of the protein (Fanucchi *et al*., 2008; Stoychev *et al*., 2009) and the transition state revealed new binding sites (ANS binding) (Fanucchi *et al*., 2008). The above-mentioned changes have been observed for a number of other metamorphic or fold-switching proteins (Mottonen *et al*., 1992; Yamasaki *et al*., 2008; Bullough *et al*., 1994; Tuinstra *et al*., 2008). Fold-switching proteins such as CLIC1, appear to adopt different folds or forms in order to increase their functionality by developing new binding interactions (Bryan and Orban, 2010). Not only are CLIC proteins metamorphic, but they are also able to adopt a membrane-bound conformation (see reviews, Berryman and Bretscher, 2000; Cromer *et al.*, 2002; Ashley, 2003). This membrane conformation has been shown to be

enhanced at the surface of membranes, where the pH is low (5.5) (Van der Goot *et al.*, 1991). However, the mechanism whereby CLIC changes from its soluble to membrane-bound form is still unknown.

The CLIC protein family consists of seven members; namely, p64 (CLIC5B in humans), parchorin (CLIC6 in humans) and CLICs 1-5A are conserved in vertebrates (Littler *et al.*, 2004; Littler *et al.*, 2010). However, there is a certain amount of variation between the vertebrate CLIC family members with bony ray-finned (teleost) fish having a second copy of CLIC5 (CLIC5L) while birds and lizards lack CLIC1 (Littler *et al.*, 2010). There are also several variants of CLIC proteins that are spliced, a process whereby introns in pre-mRNA are removed to produce a continuous protein coding sequence (Green, 1986). Examples are CLIC2, CLIC5 and CLIC6 (Littler *et al.*, 2010).

Members of the CLIC family show high sequence identity of between 47% and 76% (Cromer *et al.*, 2002). This conservation between the vertebrate CLIC proteins suggests that they originated from rounds of duplication from a single ancestral protein in an ancient chordate (Littler *et al.*, 2010). This notion is corroborated by the fact that the urochordate *Ciona intestinalis* contains a single CLIC protein that is decidedly homologous to the vertebrate CLIC family members with whom it shares three conserved cysteine residues (Littler *et al.*, 2010).

Invertebrates also possess CLIC-like proteins. The sequences of these proteins are rather different from the vertebrate CLIC proteins with sequence identities of roughly 35%, even though in most instances the three characteristic cysteine residues of the CLIC protein family are conserved (Littler *et al.*, 2010). In a number of nematodes, the active site cysteine located in vertebrate CLIC proteins has been substituted by aspartate, examples being EXC-4 and EXL-1 (Littler *et al.*, 2010). The cellular locations, molecular functions and biological processes of the CLIC protein family are summarised in Table 1.

The CLIC protein family does not show sequence identity with that of other membrane proteins but has shown structural homology to the glutathione *S*-transferase (GST) super-family (Harrop *et al.*, 2001). The most closely sequence-

Table 1: Summary of CLIC proteins locations and functions

CLIC	LOCATION	MOLECULAR FUNCTION	BIOLOGICAL PROCESS	REFERENCES
1	Membrane and soluble fraction Integral to membrane Nucleus Nuclear envelope and membrane Cytoplasm	Ion channel activity Voltage-gated ion activity Chloride channel activity Protein binding	Ion transport Transport Signal transduction Chloride transport	Harrop *et al.* , 2001
2	Nucleus Cytoplasm Membrane Chloride channel complex	Ion channel activity Voltage-gated ion activity Chloride channel activity Electron carrier activity	Ion transport Transport Signal transduction Cell redox homeostasis	Mi *et al.* , 2008
3	Membrane Integral to membrane Nucleus Chloride channel complex Cytoplasm	Ion channel activity Voltage-gated ion channel activity Chloride channel activity Protein binding	Ion transport Transport Signal transduction Chloride transport	Littler *et al.* , 2010b
4	Soluble fraction Nucleus Cytoskeleton	Ion channel activity Voltage-gated ion channel activity Protein complex binding Protein binding	Ion transport Cell differentiation Cytoskeleton organisation Cellular response to calcium ion	Howell *et al.* , 1996 Li *et al.* , 2006
5A	Microvillus cytoskeleton Cortical actin cytoskeleton	Ion channel activity (*in vitro*)	Ion transport Chloride transport (not efflux)	Shanks *et al* ., 2002 Berryman and Bretsher 2000 Berryman *et al* ., 2004
5B (p64)	Plasma membrane Cytosol of HeLa cells Intracellular membrane	Ion channel activity	Ion transport	Shanks *et al.* , 2002 Landry *et al* ., 1993 Edwards *et al* ., 1998
6 (parchorin)	Gastric parietal epithelia cells Airway epithelial cells Membrane bound	Regulate chloride ion transport	Secretory epithelium	Ashley, 2003 Nishizawa *et al* ., 2000
EXC-4	Cytoplasm Lysosome Integral to membrane Membrane Apical plasma membrane	Ion channel activity Voltage-gated ion channel activity Chloride channel activity	Epithelial cell development Ion transport Regulation of tube size	Littler *et al* ., 2008
DmCLIC	_	Chloride channel activity Calcium ion binding Lipid binding	_	Littler *et al* ., 2008

related GST proteins to the CLIC proteins are GST from *Zea mays* (PDB code 1AW9) (Neuefeind *et al*., 1997) and the Omega class GST (PDB code 1EEM) (Board *et al*., 2000). The major difference between the CLIC and GST proteins is that CLIC proteins are monomeric whereas GST proteins are dimeric (Harrop *et al.*, 2001).

1.1. CLIC1 structure

CLIC family members 1-5A, are approximately 240 amino acid residues in length. However, p64 and parchorin have long N–terminal expansions (Cromer *et al*., 2002). Perhaps the most extensively studied CLIC family member is CLIC1. The crystal structure of reduced CLIC1, the first for the CLIC family, was solved at 1.4 Å by Harrop *et al*. in 2001 (Figure 1). CLIC1 was shown to be monomeric and consists of an N-terminal domain with a thioredoxin-like fold and an all α-helical C–terminal domain, which is typical of the GST super-family (Figure 1) (Cromer *et al.*, 2002; Harrop *et al.*, 2001). CLIC1 contains an intact glutathione (GSH) binding site and, therefore, it is likely to be under redox control. This is due to the ability of the redox active Cys24 residue to form a mixed disulfide bond with GSH. The thioredoxin fold of the N-terminal domain is shared by families of redox-active proteins (Littler *et al.*, 2010).

The structure of the soluble form of CLIC1 indicates that it is most similar to that of the Omega class GST (Board *et al*., 2000). Although, Omega class GST has not yet been shown to form ion channels it has been shown to modulate ryanodine-sensitive calcium ion release channels (Dulhunty *et al.*, 2001). As mentioned previously, one of the major differences between CLIC1 and GST proteins is that CLICs are monomeric and GSTs are dimeric. Another distinguishing characteristic of CLIC1 that makes it different to the GST proteins is a long loop between helices 5 and 6 (Pro147–Gln164) at the “foot” of CLIC1. This loop is negatively charged with seven acidic residues giving CLIC1 a net charge of negative 7 (Harrop *et al*., 2001).

In 2004, Littler *et al*. solved the crystal structure of the oxidised form of CLIC1 (Figure 2). It was observed that under oxidising conditions, in the absence of membranes, CLIC1 undergoes a reversible but major structural transition whereby the

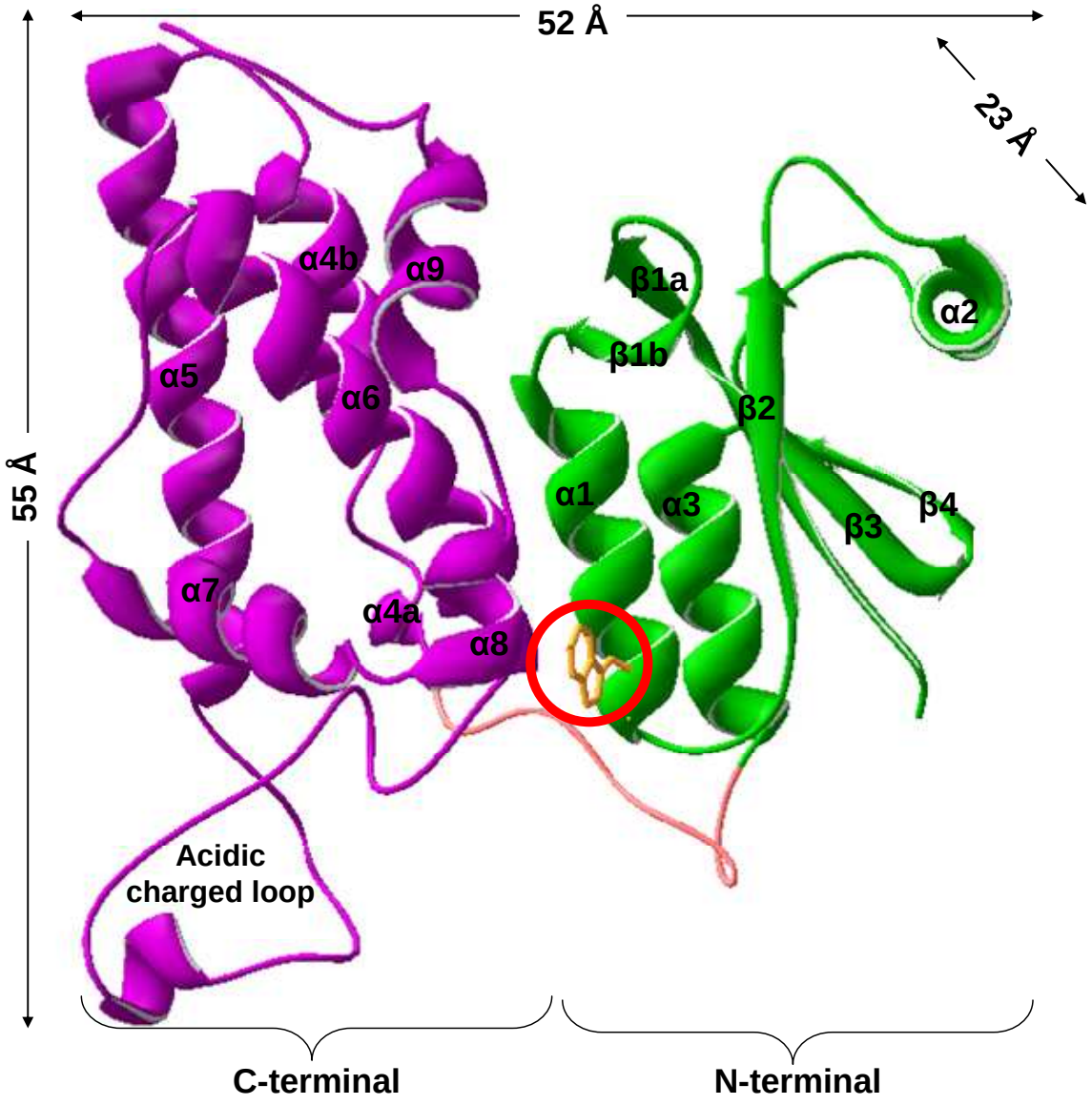


Figure 1: Ribbon representation of the crystal structure of reduced CLIC1.

The N-terminal domain is shown in green, the C-terminal domain in purple and the linker region in light pink. The lone tryptophan residue is circled in red and represented by an orange stick molecule. The α-helices and β-strands are labelled accordingly. This image was generated using Swiss PDB Viewer (Guex and Peitsch, 1997) using PDB code 1K0M (Harrop *et al.*, 2001).

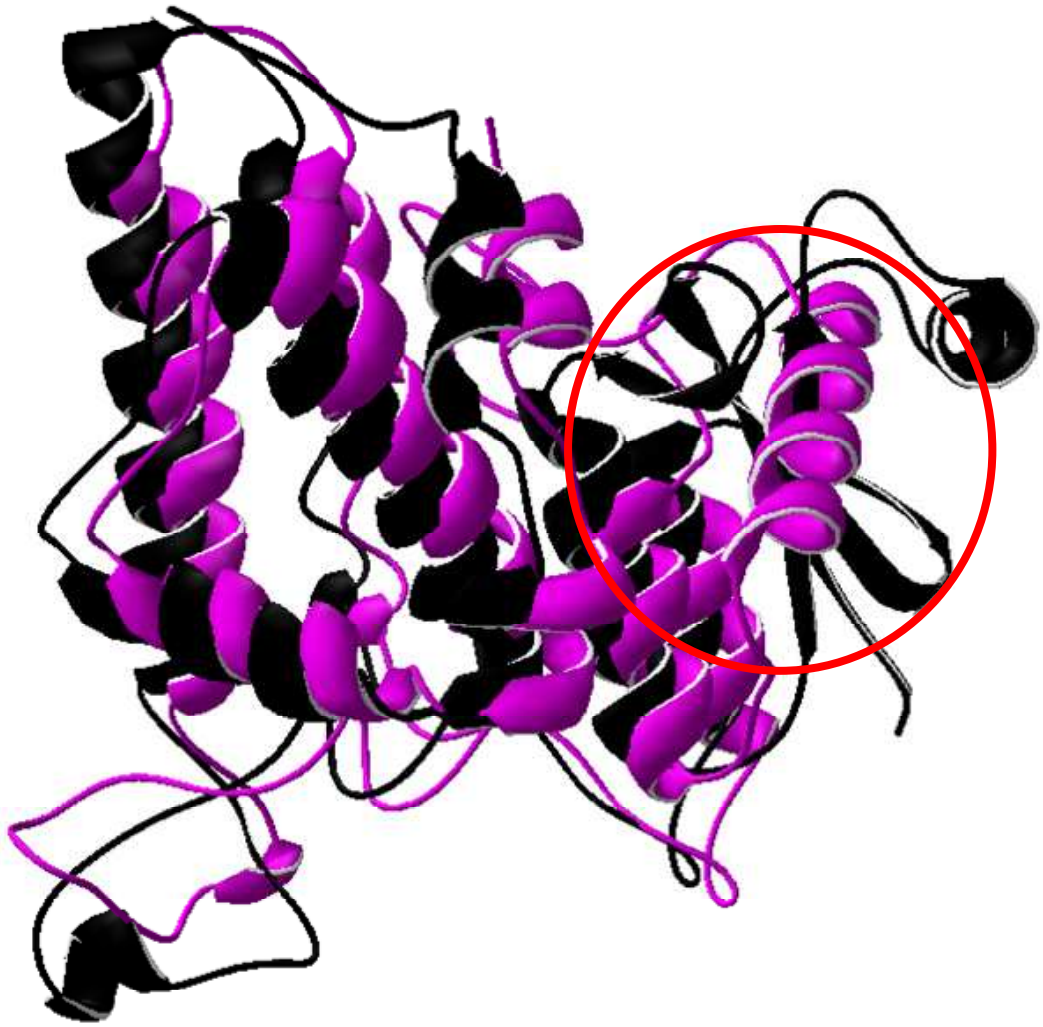


Figure 2: Superimposed structures of the reduced and oxidised forms of soluble CLIC1

Reduced CLIC1 is shown in purple and oxidised CLIC1 is shown in black. The region of structural change from the thioredoxin fold to an all α-helical arrangement is circled in red. This image was generated using Swiss PDB Viewer (Guex and Peitsch, 1997) using PDB codes 1K0M (Harrop *et al*., 2001) and 1RK4 (Littler *et al*., 2004).

N-terminal domain becomes all α-helical with the concomitant formation of an intramolecular disulfide bond between Cys24 and Cys59 (Littler *et al*., 2004) (Figure 2). This structural transition resulted in the exposure of a large hydrophobic surface that forms the domain interface. It has been hypothesised that the large hydrophobic surface of the oxidised dimeric state of CLIC1 would insert into a lipid bilayer more readily then forming a protein dimer (Littler *et al*., 2004). Therefore, the exposed hydrophobic surface area has been proposed to be similar to a membrane insertion "intermediate state" that forms upon oxidation of the monomer (Littler *et al*., 2004; Goodchild *et al*., 2009). A similar intermediate state of CLIC1 in the monomeric form was recently suggested by Fanucchi *et al*. (2008). Studies also revealed that the oxidised dimeric form of CLIC1 forms chloride ion channels in artificial lipid bilayers (Littler *et al*., 2004). Littler *et al*. (2004) went on to show that if either Cys24 or Cys59 were mutated to serine, CLIC1 no longer formed active ion channels. Other work on CLIC proteins under oxidising conditions revealed that oxidation enhances the binding of CLIC4 and DmCLIC to artificial membrane bilayers when compared to that under reducing conditions (Littler *et al*., 2005 and Littler *et al*., 2008). Also see section 1.2.1.

1.2. CLIC1 channel formation

A 23 amino acid region corresponding to the sequence Cys24 to Val46 comprising helix 1 and β-strand 2 that is likely to form a single transmembrane helix in the channel form of CLIC1 has been identified (Valenzuela *et al*., 1997; Edwards *et al*., 1998; Harrop *et al*., 2001). Many studies have since been conducted that support the notion that CLIC1 has a single transmembrane region. These include sequence alignments and hydrophobicity plots of CLIC1 and CLIC4 (Ashley, 2003; Shorning *et al*., 2003), protease digestion work on membrane-bound CLIC4 (Duncan *et al*., 1997), electrophysiological studies by Tonini *et al*. (2000) and by truncation, mutagenesis and membrane localisation work on EXC-4 by Berry *et al*. (2003) and Berry and Hobert (2006). Probably the most convincing evidence of a single transmembrane region in CLIC proteins came about when Singh and Ashley (2007) showed a truncated version of CLIC4 that consisted of the first 61 residues of the N-terminal domain including the TMR formed functional ion channels in planar membranes.

Therefore, there is convincing evidence that indicates that the TMR of CLIC1 consists of helix 1 and β-strand 2 (Duncan *et al*., 1997; Harrop *et al*., 2001; Warton et al., 2002; Berry *et al*., 2003 and Littler *et al*., 2004; Berry and Hobert, 2006; Singh and Ashley, 2007). AGADIR, a helix-coil transition algorithm (Lacroix *et al*., 1998) also predicted that helix 1 and β-strand 2 of CLIC1 have high propensities to form helical structures even in isolation and, therefore, they are probably helical in membranes (Fanucchi *et al*., 2008 and Stoychev *et al*., 2009) much like the TMRs of other membrane proteins (White and Wimley, 1999) and pore forming toxins (Parker and Feil, 2005). AGADIR also showed that helix 1 and β-strand 2 of CLIC1 have high propensities to form N- and C-capping motifs (Stoychev *et al*., 2009). These structural motifs have been shown to stabilise helical structures (Scholtz and Baldwin, 1992) and so provide further support that the CLIC1 TMR is most likely to be helical when membrane-bound.

The structural homology between CLIC proteins and the enzyme active GST proteins as well as the location of the TMR (helix 1 and β-strand 2) within the central part of the N-terminal domain, leads to the hypothesis that in order for CLIC proteins to transverse the membrane and form channels, major structural rearrangements of the N-terminal domain would have to occur. Despite the fact that the mechanism by which CLIC proteins change from the soluble to insoluble membrane-bound state remains unknown, their ability to associate with membranes has been observed. The ability of soluble CLIC1, CLIC2, CLIC4 and CLIC5 to assimilate into synthetic lipid bilayers and demonstrate ion channel activity has been demonstrated (Harrop *et al*., 2001; Tulk *et al*., 2002; Warton *et al*., 2002; Berryman et al., 2004; Littler *et al*., 2004; Littler *et al*., 2005; Singh and Ashley, 2006; Cromer, 2007; Singh and Ashley, 2007; Singh *et al*., 2007). It was also recently shown that the CLIC homologs, DmCLIC and EXC-4, produce ion channels in artificial bilayers (Littler *et al*., 2008).

Monomeric CLIC1 co-reconstitutes into asolectin liposomes (Tulk *et al*., 2000). The insertion also occurs spontaneously and does not require a receptor (Tulk *et al.*, 2000; Warton *et al.*, 2002; Harrop *et al.*, 2001). CLIC1 may or may not insert into phosphatidylcholine liposomes, but cannot function as a channel without acidic lipids such as phosphatidylserine (Tulk *et al.*, 2002). Although CLIC1 monomers are able to insert into different lipid membranes, native membrane CLIC1 may only

accumulate into functional ion channels in organelles or membrane domains that contain specific lipid components (Singh and Ashley, 2006). This may be due to different affinities towards different membranes such as those shown by dermaseptin S4 and human-like cecropin LL-37 towards zwitterionic phosphatidylchloline phospholipid membranes (Shai, 1999). So, although the exact mechanism whereby CLICs transcend into membranes remains unknown, it is logical to say that the transition must be a strictly controlled and well-regulated process.

1.2.1. Regulation of channel formation

As mentioned previously in section 1.1 the N-terminal domain of CLIC1 contains a redox active site that covalently binds GSH by means of a conserved cysteine residue, Cys24, to form a mixed disulfide (Cromer *et al.*, 2002; Littler *et al.*, 2004). A comparable site on GST proteins implies that GSH binding sites may be a general characteristic of proteins with a GST fold (Board *et al*., 2000). CLIC protein structures confirm that the position of the cysteine sulfhydryl is in a basic environment and that it forms hydrogen bonds to the backbone amides of helix 1, probably creating a reactive thiolate group (Harrop *et al*., 2001; Littler *et al*., 2005; Cromer *et al*., 2007; Littler *et al*., 2008; Li *et al*., 2006 and Mi *et al*., 2008). Singh and Ashley (2007) showed that Cys24 is situated on the *trans* side (exterior lumen) of membranes and may produce disulfide-linked dimers that oligomerise and thereby form pores within membranes (Singh and Ashley, 2006). This may explain the redox sensitivity of ion channels and the operation of CLIC1 under redox control (Littler *et al.*, 2004; Singh and Ashley, 2007; Cromer *et al*., 2007; Littler *et al*., 2008). Furthermore, mutating residues at the GSH-like binding site obliterates the ability of CLIC4 to localise towards the plasma membrane (Berry and Hobert, 2006).

CLIC proteins that contain a Cys residue at the redox active site bind to lipid bilayers under oxidising conditions (Littler *et al*., 2004; Littler *et al*., 2005; Cromer *et al*., 2007; Littler *et al*., 2008; Goodchild *et al*., 2009). Goodchild *et al*. (2009) showed that monomeric CLIC1 under reducing conditions associates poorly with membranes and does not form ion conducting pores. However, the same monomer under oxidising conditions exhibits greatest membrane association and insertion and forms effective ion channels. Interestingly, the CLIC-like protein EXC-4 does not require redox conditions in order to bind to the lipid bilayer (Littler *et al*., 2008). This may be

rationalised due to the fact that EXC-4 contains an Asp residue and not a Cys residue in the redox active site, unlike the other CLIC and CLIC-like proteins (Berry *et al*., 2003; Berry and Hobert, 2006).

Low pH has also been shown to be a requirement for membrane insertion in other metamorphic proteins such as colicin A (Muga *et al*., 1993), diphtheria toxin (Sandvig and Olsnes, 1980) and Bcl-$_{XL}$ (Thuduppathy *et al*., 2006). pH has been observed to affect CLIC membrane insertion, with more frequent insertions occurring at low and high pH values which suggests that the event could be non-specific (Tulk *et al.*, 2000; Warton *et al.*, 2002; Littler *et al*., 2005; Cromer *et al*., 2007; Littler *et al*., 2008). pH has also been shown to influence the ion conductivity of ion channels with higher channel activity at low pH (Tulk *et al*., 2002; Cromer *et al*., 2007 and Littler *et al*., 2007). More recently, unfolding studies (see section 1.3) (Fanucchi *et al*., 2008) and HXMS work (see section 1.3) (Stoychev *et al*., 2009) on soluble CLIC1 specify that low pH primes the N-terminal domain for membrane insertion. However, pH alone does not seem to trigger structural changes in CLIC proteins. This can be verified by looking at the crystal structures of CLIC proteins and mutations thereof solved under various pH conditions ranging from pH 4.5 to pH 8.5 (Harrop *et al*., 2001; Littler *et al*., 2004; Li *et al*., 2006; Mi *et al*., 2008; Littler *et al*., 2010). Also, experimental work done on CLIC1 confirms that the structure of CLIC1 is unchanged at pH 5.5 when compared to pH 7 (Fanucchi *et al*., 2008; Stoychev *et al*., 2009).

Therefore, perhaps the low pH environment of the membrane surface primes the soluble monomeric form of CLIC1 to undergo structural changes which permit its transition to the unknown membrane-bound form (Figure 3). Consequently, if the transition of CLIC1 from its soluble to insoluble membrane form (N-terminal rearrangement) is controlled by redox conditions and pH, what maintains the structural integrity and conformational stability of the soluble form of CLIC1 and, more, specifically the N-terminal domain?

1.3. The stability of soluble CLIC1

"The three-dimensional structure of a native protein in its normal physiological milieu (solvent, pH, ionic strength, presence other components such as metal ions or prosthetic groups, temperature, and other) is one in which the Gibbs free energy is the

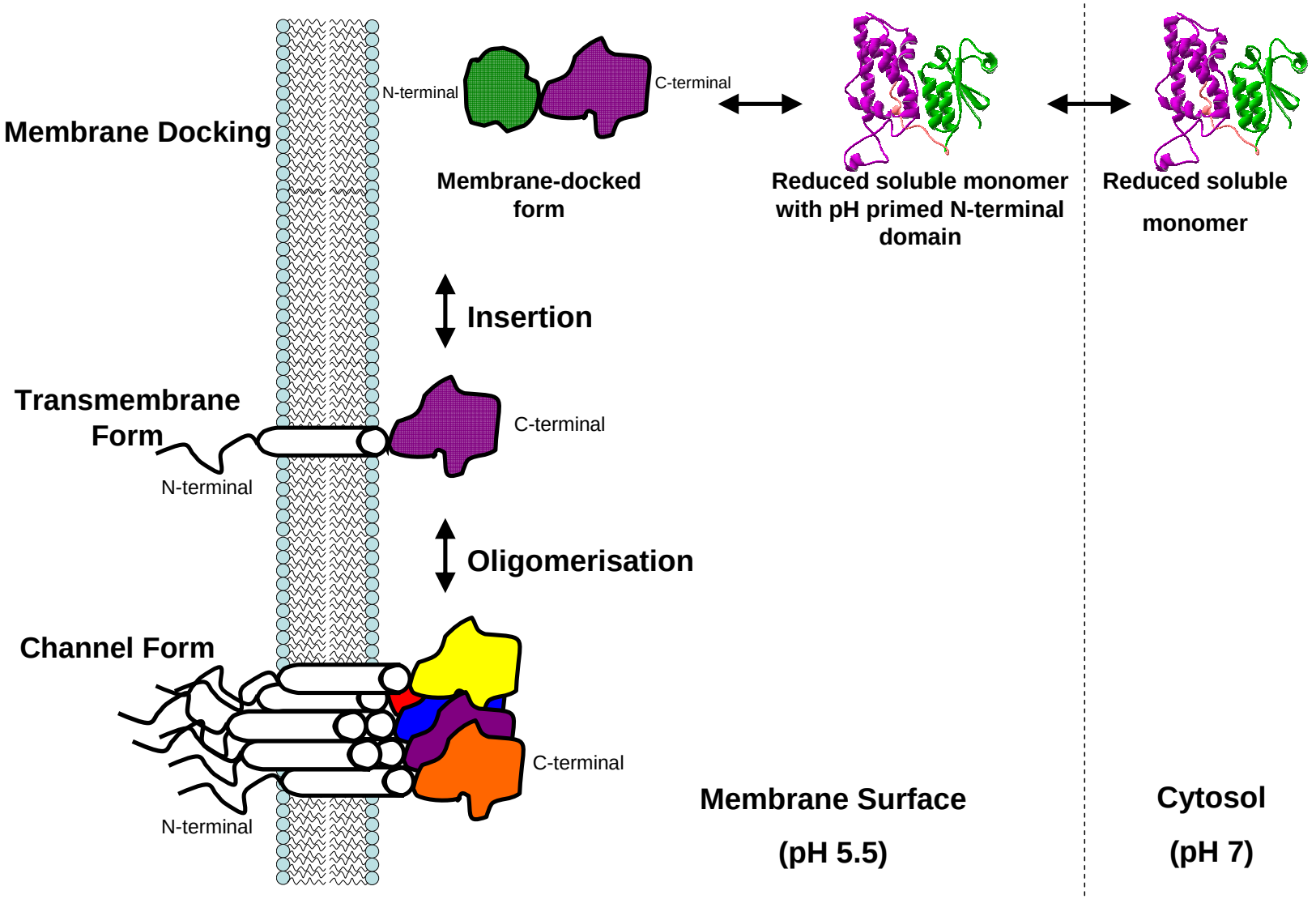


Figure 3: The proposed model for the CLIC1 transition from its soluble to membrane-bound form.
This figure was adapted from Littler *et al.* (2010).

lowest; that is, that the native conformation is determined by the totality of interatomic interactions and hence by the amino acid sequence, in a given environment" (Anfinsen, 1973). Accordingly, the stabilities of the three-dimensional structures of proteins arise due to the fine balance of opposing forces between the amino acid residues in a protein sequence. These forces are described in detail by Dill (1990). It should also be noted that, depending on the balance of these forces, regions within proteins may differ in flexibility and rigidity.

Flexible and inflexible regions of proteins are important for protein function as inflexible regions provide a frame-work while flexible regions are important for protein movements and function (Sinha *et al*., 2001a; Sinha *et al*., 2001b; Sinha *et al*., 2001c). This has been highlighted by the studies done on CLIC1 that show that the N-terminal domain may provide the flexibility needed for the structural changes that are necessary for CLIC1 to change from its soluble to its membrane form. This concept was first proposed by Harrop *et al*. (2001).

Helices 1 and 3 form the domain interface of CLIC1 and are proposed to provide plasticity in the molecule (Harrop *et al*., 2001). Therefore, CLIC1 is more susceptible to undergo a conformational change in order to form a membrane-bound state much like that of oxidised dimeric CLIC1. It is also important to highlight here that helix 1 provides most of the interdomain interactions. Therefore, this region of the protein may be more vulnerable to structural changes as part of CLIC1's function *in vivo* and may provide a means whereby environmental factors alter the stability of reduced soluble CLIC1. This may in turn prime CLIC1 to undergo the changes it requires to perform a different function such as ion channel formation.

The structure, stability, solubility and functions of proteins are also influenced by the net charge and ionisation states of individual residues and hence are pH-dependent (Pace *et al*., 2009). Therefore, the degree of flexibility and rigidity of proteins is greatly impacted upon by the number of hydrogen bonds and salt-bridges, as well as the stabilising and destabilising nature of those salt-bridges (Sinha *et al*., 2001a). Since the ability of CLIC1 to transverse membranes and form functional membrane pores has been shown to be pH-dependent (as discussed previously, section 1.2.1), perhaps changes in the ionisation states of residues within the flexible regions

(outlined above) due to changes in pH may alter the conformational stability of soluble CLIC1 thereby enabling it to be "primed" for membrane insertion. This may occur when CLIC1 moves from the cytosol (pH 7) to the membrane surface (pH 5.5) prior to membrane insertion.

Recently, urea-induced equilibrium unfolding studies on reduced soluble CLIC1 in the absence of membranes revealed that the protein molecule became destabilised at low pH (5.5) illustrated by a loss in cooperativity (Fanucchi *et al*., 2008). However, at pH 7 CLIC1 unfolds via a two-state transition in a cooperative manner much like the dimeric GST proteins (Wallace *et al*., 1998; Wallace *et al*., 2000; Hornby *et al*., 2000) and monomeric glutaredoxin 2 (Gildenhuys *et al*., 2008). Therefore, the conformational stability of CLIC1 has been shown to be pH-dependent. The destabilised form of soluble CLIC1 at low pH results in the formation of an intermediate with a solvent-exposed hydrophobic surface (Fanucchi *et al*., 2008). The intermediate is not a molten globule as it was shown to have a defined tertiary structure and unfolded in a cooperative manner at high urea concentrations. Fanucchi *et al*. (2008) concluded that acid-induced destabilisation and partial unfolding of CLIC1 involve helix 1. This is interesting because as mentioned previously, helix 1 forms part of the TMR and may provide the plasticity the molecule requires to partially unfold. Fanucchi *et al*. (2008) also suggested that the acidic environment found at the membrane surface may prime the CLIC1 TMR of the N-terminal domain by protonating certain amino acids thereby lowering the energy barrier for the conversion of soluble CLIC1 to its membrane-bound form.

Another study that highlights the flexibility of the domain interface (helix 1 and helix 3) of CLIC1 made use of amide hydrogen-deuterium exchange mass spectrometry (HXMS). This technique was used to investigate the structural dynamics of soluble CLIC1 (Stoychev *et al*., 2009). The core structure of CLIC1 at pH 5.5 (the pH at which CLIC1 forms channels in membranes (Tulk *et al*., 2000; Warton *et al*., 2002)) appears unchanged compared to that at pH 7 (Stoychev *et al*., 2009). However, the data also showed that the N-terminal domain of CLIC1 is less stable than the all α-helical C-terminal domain and although the structural integrity of CLIC1 is unchanged at pH 5.5, its conformational flexibility increases as the pH of the environment becomes more acidic (Stoychev *et al*., 2009). Peptide segments 11-31 (β-

strand 1 and helix 1) and 68-82 (β-strand 3, β-strand 4 and helix 3) showed substantially increased hydrogen-deuterium exchange rates at pH 5.5. Stoychev *et al*. (2009) proposed that this may be due to protonation of acidic amino acid residues that may be involved in salt-bridges. Interestingly, peptide segments 31-34 (helix 1) and 83-86 (helix 3) display almost no deuterium incorporation. This implies that these regions are extremely stable and may, therefore, play an important role in maintaining the conformational stability of the domain interface and more specifically the N-terminal domain in the soluble form of CLIC1.

In order to explore this idea, conserved residues within the structural elements represented by the peptide segments (helices 1 and 3) were closely inspected as conserved residues are hypothesised to play structural and hence functional roles in proteins. In an attempt to identify residues that maintain the structural stability of the N-terminal domain in the soluble form of CLIC1, a multiple sequence alignment of the CLIC protein family using the ClustalW multiple sequence alignment tool (Thompson *et al*., 1994) was conducted as shown in Figure 4. The alignments were done in order to identify residues which are conserved across a range of species within the TMR and N-terminal domain of CLIC proteins. The sequence alignments identified a number of residues that are conserved which includes Arg29 and Glu81. This was rather an exciting finding, as these residues form part of helices 1 and 3 and the TMR at the domain interface and that these helices are proposed to form interactions with the C-terminal domain. It is important to note that Arg29 is not conserved within the invertebrate CLIC proteins as it is substituted with Glu. Glu81, however, is conserved throughout all CLICs in the alignment. Within the N-terminal domain Arg29 forms hydrogen bonds and a partially buried salt-bridge with Glu81 (helix 3) and Asn78 (helix 3). The hydrogen bonds and salt-bridge interactions between these residues were identified visually using SwissPDB viewer (Figure 5) (Guex and Peitsch, 1997), and were confirmed using iMOLTalk (http://imoltalk.org) and the PPI server (http://www.biochem.ucl.ac.uk/bsm/PP/server/index.html). Salt-bridge interactions are assumed to occur between a pair of oppositely charged residues (Asp or Glu with Arg, Lys, His) if (i) the centroids of the side-chains of the charged residues are within 4 Å of one another (Barlow and Thornton, 1983) and (ii) if no less than one pair of Asp or Glu side-chain carboxyl oxygen atoms and side-chain nitrogen atoms of Arg, Lys or His are within 4 Å (Kumar and Nussinov, 1999).

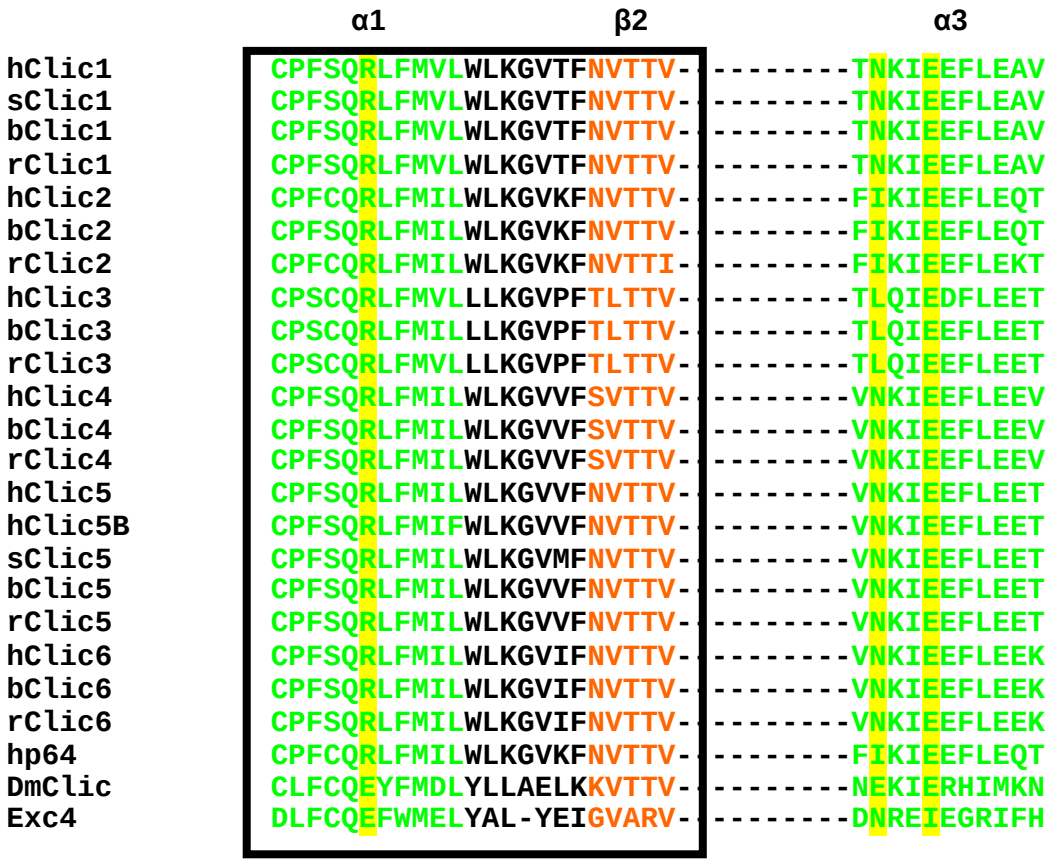


Figure 4: **Sequence alignment of the TMR and helix 3 of CLIC proteins.**

The 23 amino acid residues making up the TMR are framed in black. The black dashed line represents the amino acids between the TMR and helix 3. The letters preceding the protein names are indicative of the protein species, that is, h (*Homo sapien*), b (*Bos taurus*), r (*Rattis norvegicus*) and s (*Sus scrofa*). The residues making up the α-helices and β-strands are shown in green and orange, respectively. The CLIC1 residues Arg29, Asn78, Glu81 are highlighted in yellow.

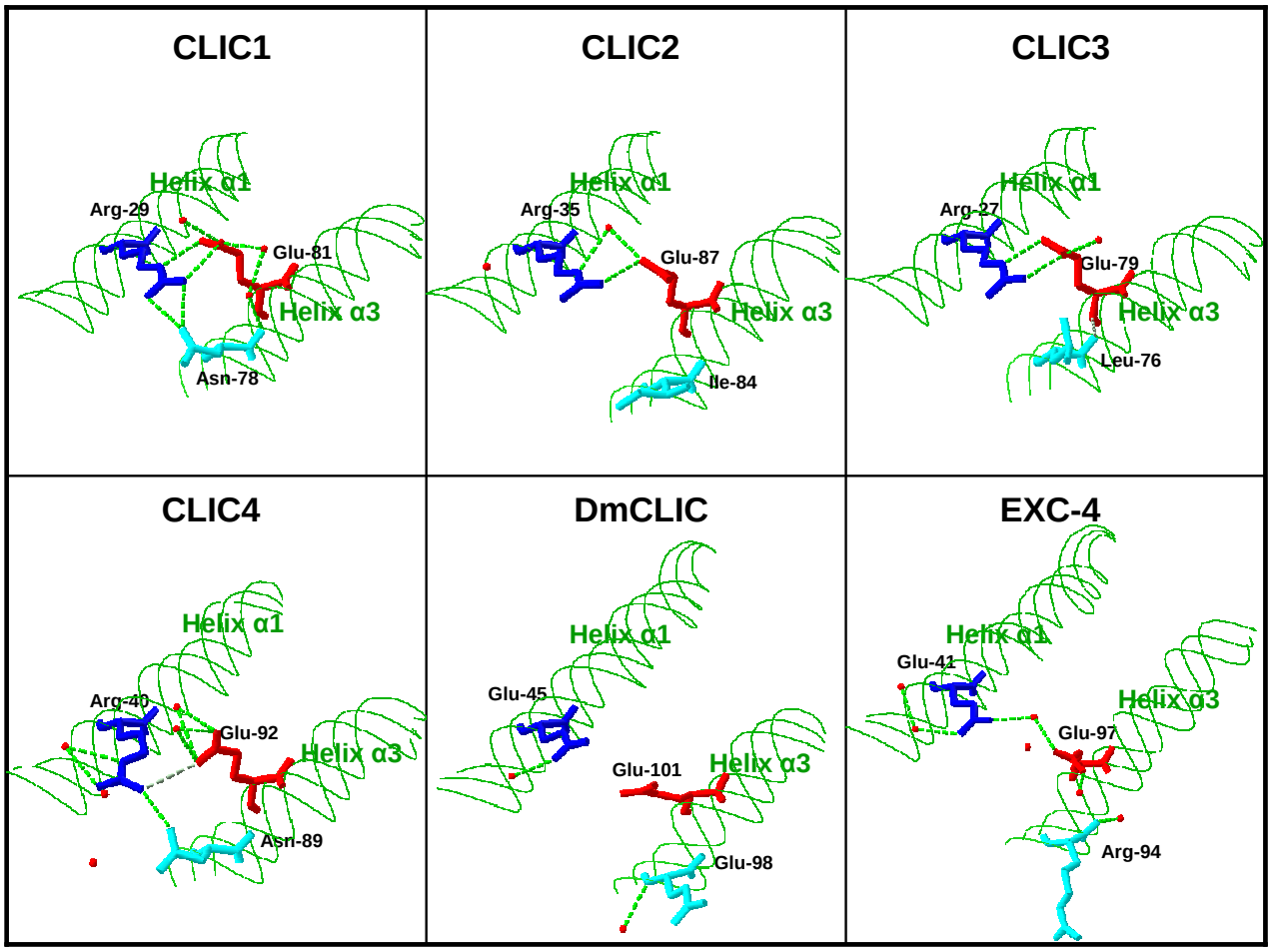


Figure 5: Residues which are topologically equivalent to Arg29, Asn78 and Glu81 in CLIC1

Amino acid residues are represented by sticks and labelled accordingly. Hydrogen bonds are represented by green and grey broken lines. Water molecules are represented by red spheres. This image was generated using Swiss PDB Viewer (Guex and Peitsch, 1997) using PDB codes 1K0M (Harrop *et al*., 2001), 2PER (Mi *et al*., 2008), 3FY7 (Little *et al*., 2010), 2AHE (Littler *et al*., 2005), 2YV7 and 2YV9 (Littler *et al*., 2008).

A structure-based sequence alignment was conducted using Cn3D 4.1 (Wang *et al.*, 2000) in order to check if the conserved residues were topologically equivalent across the CLIC protein family (Figure 6). The structure-based sequence alignment revealed that the hydrogen bonds and salt-bridge interaction are topologically conserved across the CLIC proteins with the exception of the CLIC invertebrate proteins.

Since residues R29 and E81 of CLIC1 contain ionisable groups, the intrinsic pK values of their ionisable groups could change depending on a number of environmental factors. This could, therefore, impact upon the structure, stability, solubility and/or function of CLIC1. Since many ionisable groups are buried in the interior of proteins, they frequently influence the function and stability of proteins (Pace *et al*., 2009). Just as the ionisation state of the side chains of charged residues is pH-dependent, so too are the free energy contributions of salt-bridges to the stability of proteins. Also, salt-bridges can supply the conformational specificity for folding and function (Hendsch and Tidor, 1994) in that they restrict the number of allowable conformations to those in which charge compensatory interactions can take place (Paul, 1982).

Therefore, perhaps the role of the hydrogen bonds and the conserved salt-bridge interaction between Arg29, Glu81 and Asn78 of CLIC1 is to provide stabilising interactions in the soluble form of CLIC1 thereby maintaining the structural integrity and stability of the N-terminal domain. This is significant since it is the N-terminal domain that is involved in membrane insertion and is the region of CLIC1 that is required to change in order for CLIC1 to adopt its membrane-bound topology. Therefore, one may speculate that the membrane-bound topology is somehow “trapped” within the soluble topology of the N-terminal domain.

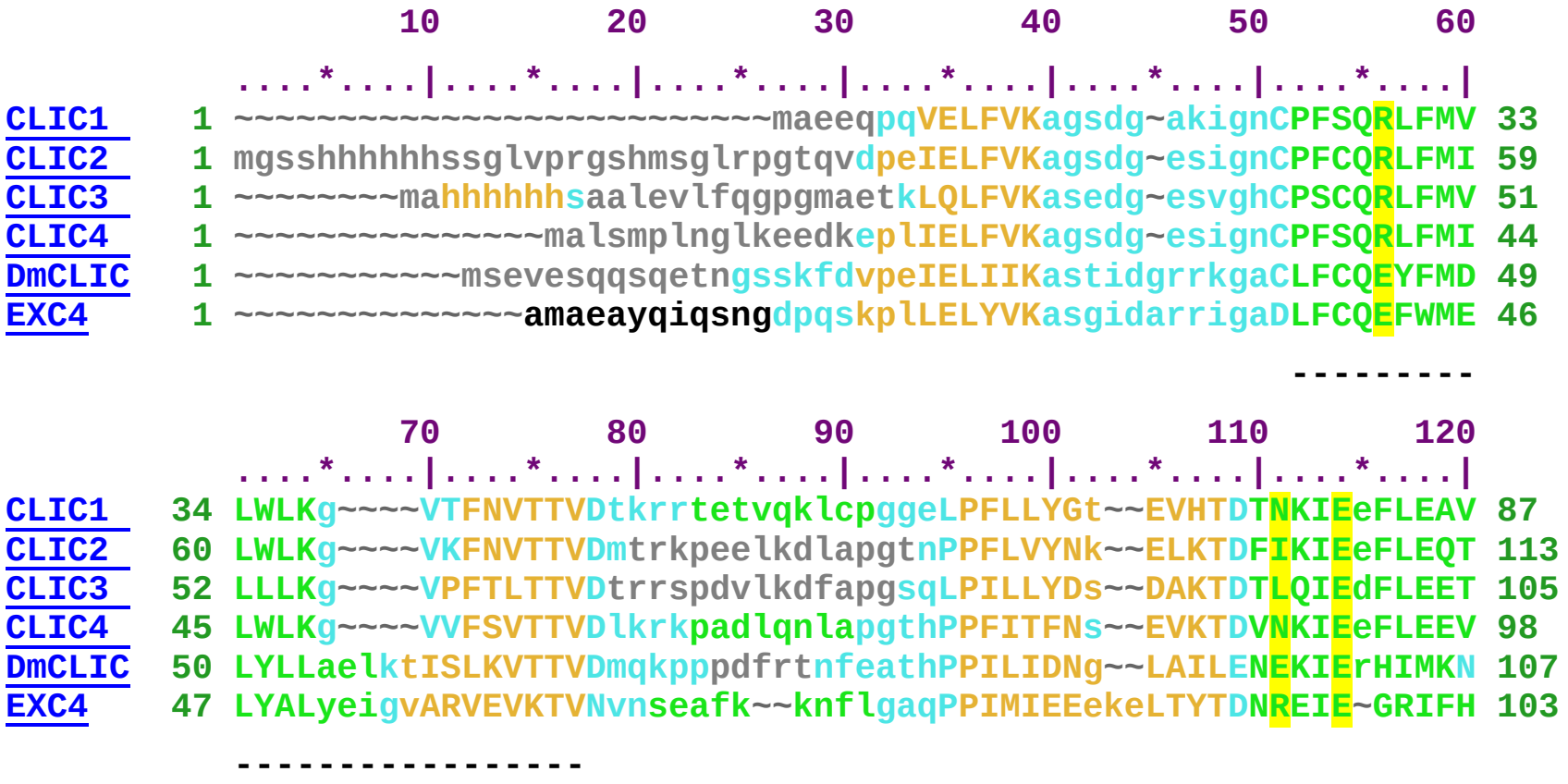


Figure 6: Structure-based sequence alignment of the N-terminal domain of CLIC proteins.

Alignment was conducted with sequences of CLIC family members using the PDB codes 1K0M (CLIC1) (Harrop *et al*., 2001), 2PER (CLIC2) (Mi *et al*., 2008), 3FY7 (CLIC3) (Little *et al*., 2010), 2AHE (CLIC4) (Littler *et al*., 2005), 2YV7 (DmCLIC) and 2YV9 (EXC4) (Littler *et al*., 2008). The α-helices and β-strands are shown in green and in orange, respectively. The residues selected for mutagenesis in this study are highlighted in yellow.

1.4. Objectives

The oxidised CLIC1 dimer structure has been proposed to resemble a membrane insertion "intermediate state" (Goodchild *et al.*, 2009). This membrane insertion "intermediate state" was shown to have a completely altered N-terminal domain. Therefore, it seems that in order for CLIC1 to change from its soluble to insoluble form, the N-terminal domain requires major structural rearrangements which requires a degree of flexibility (Littler *et al.*, 2001; Fanucchi *et al.*, 2008; Stoychev *et al.*, 2009). This flexibility has been shown in the soluble form of CLIC1 (Stoychev *et al.*, 2009).

The main objective of this project was to identify and characterise residues and/or interactions that stabilise the structure and stability of the soluble form of the N-terminal domain of CLIC1, since it appears as though the membrane-bound topology is "trapped" within the soluble topology of CLIC1. This was performed as a function of pH in order to gain a better understanding of how the conformational stability of soluble (cytosolic) CLIC1 at pH 7 changes when it is exposed to the acidic (pH 5.5) environment at the surface of the membrane. This may provide insight as to what triggers CLIC1 to be primed for membrane insertion thereby revealing its "trapped" membrane-bound topology.

Therefore, the primary aim of this research project was to engineer three single amino acid mutations in CLIC1, namely; R29M, E81M and N78A. These mutations were designed to break the salt-bridge between Arg29 and Glu81 as well as the hydrogen bonds connecting Arg29, Glu81 and Asn78. In addition, a double mutant R29M/E81M which would remove the salt-bridge and hydrogen bonds between the three residues was also engineered. The rationale for this was that mutants R29M and E81M would essentially maintain bulk but alter charge, whereas N78A would alter both the bulk and polarity. The effect of the mutations on the N-terminal domain and the protein's structure was assessed spectroscopically using fluorescence and circular dichroism spectroscopy, acrylamide quenching and ANS binding. The impact of the mutations on the structural stability was assessed by urea-induced equilibrium unfolding studies. The crystal structure of the R29M/E81M mutant was used to further interpret the structural and stability data. The data obtained were compared with that of the wild type protein.

CHAPTER 2

MATERIALS AND METHODS

2.1. Materials

cDNA encoding the GST-CLIC1 fusion protein that was cloned into the pGEX-4T-1 vector was a gift from Dr. S. N. Breit, (Centre of Immunology, St. Vincent's hospital and University of New South Wales, Sydney, Australia). cDNA encoding the GST CLIC1-E81M fusion protein cloned into the pGEX-4T-1 vector was a gift from Dr. Stoyan Stoychev (University of the Witwatersrand, Johannesburg, South Africa). The oligonucleotide primers were synthesised by Inqaba Biotechnical Industries (Pty) Ltd (Pretoria, South Africa). All sequencing reactions were done by Inqaba Biotechnical Industries (Pty) Ltd (Pretoria, South Africa). The GeneEditor™ site-directed mutagenesis system and the *Escherichia coli* JM109 and BMH71-18mutS cells were purchased from Promega Corporation (Madison, USA). The QuikChange™ site-directed mutagenesis kit and the *Escherichia coli* BL21 (DE3) competent cells were from Stratagene® (La Jolla, USA). The plasmid DNA FlexiPrep™ kit was purchased from Amersham Biosciences (Buckinghamshire, UK). Dithiothreitol (DTT) was purchased from Melford Laboratories Ltd (Suffolk, UK). Reduced glutathione (GSH), 1-anilino-8-naphthalene-sulfonate (ANS) and thrombin from bovine plasma were purchased from Sigma-Aldrich (St. Louis, MO, USA). Ultrapure urea was purchased from Merck (Darmstadt, Germany). The SDS-PAGE molecular weight markers were purchased from Fermentas (Ontario, Canada). All other reagents were of analytical grade.

2.2. Methods

2.2.1. Oligonucleotide primer design

The oligonucleotide primers used to generate the CLIC1-R29M, E81M, N78A and R29M/E81M mutants were designed using PrimerX (http://www.bioinformatics.org/primerx/cgi-bin/DNA_1.cgi). The computer software package Gene Runner v3.04 was used to analyse the generated primers.

The mutagenic primers designed for use with the GeneEditor™ site-directed mutagenesis system had the following sequences:

- **R29M forward primer:**
  5'-C TGC CCA TTC TCC CAG ATG CTG TTC ATG GTA CTG TGG-3'
- **R29M reverse primer:**
  5'-CCA CAG TAC CAT GAA CAG CAT CTG GGA GAA TGG GCA G-3'

The underlined nucleotides represent the mutation that generates the Arg → Met substitution. The oligonucleotides were 5' phosphorylated.

The mutagenic primers designed for use with the QuikChange™ site-directed mutagenesis kit (Papworth *et al*., 1996) had the following sequences:

- **E81M forward primer:**
  5'–C ACA GAC ACC AAC AAG ATT ATG GAA TTT CTG GAG GCA GTG C-3'
- **E81M reverse primer:**
  5'-CAC TGC CTC CAG AAA TTC CAT AAT CTT GTT GGT GTC TGT G -3'

The underlined nucleotides represent the mutation that generates the Glu → Met substitution.

- **N78A forward primer:**
  5'–CT GAA GTG CAC ACA GAC ACC GCC AAG ATT GAG GAA TTT CTG G-3'
- **N78A reverse primer:**
  5'–C CAG AAA TTC CTC AAT CTT GGC GGT GTC TGT GCA CTT CAG-3'

The underlined nucleotides represent the mutation that generates the Asn → Ala substitution.

In order to generate the CLIC1-R29M/E81M mutant, the plasmid cDNA encoding the CLIC1-R29M mutant was used with the CLIC1-E81M forward and reverse primers.

2.2.2. Site-directed mutagenesis

The CLIC1-R29M mutant was generated using the GeneEditor™ Site-directed Mutagenesis system, using single-stranded plasmid DNA templates as follows:

The plasmid containing the insert coding for CLIC1-WT was used to transform *Escherichia coli* JM109 cells. This was done using a one-step method described by Chung *et al*. (1989). After 50 μl of competent cells had been thawed on ice, 10 ng of CLIC1-WT double-stranded DNA (dsDNA) was added to the reaction mixture and returned to ice for 30 minutes. Subsequently, the cells were heat-shocked for 45 seconds at 42 °C on a heating block and immediately cooled on ice for 2 minutes. SOC media (950 μl containing 2 g tryptone, 0.5 g yeast, 1 ml 1 M NaCl, 0.25 ml 1 M KCl, 1 ml 2 M $MgCl_2$ and 1 ml 2 M glucose per 100 ml dH_2O) was added to the reaction mixture and incubated, shaking at 250 rpm for 60 minutes at 37 °C. The cells were plated on LB-agar plates containing 100 μg/ml ampicillin which were then incubated for 16 hours at 37 °C. Transformants were used to inoculate 100 ml of LB containing 100 μg/ml ampicillin and incubated shaking at 250 rpm for 16 hours at 37 °C. Plasmid DNA was extracted from the LB cultures using the FlexiPrep™ kit from Amersham Biosciences and subsequently alkaline denatured for use with the GeneEditor™ site-directed mutagenesis system. This single-stranded DNA (ssDNA) was then used as the template DNA in the mutagenic sample reactions.

Sample reactions had a total volume of 20 μl containing 0.05 pmol of ssDNA template, 1.25 pmol of mutagenic primer, 0.25 pmol of selection oligonucleotide and 10X annealing buffer (200 mM Tris-HCl, pH 7.5, 100 mM $MgCl_2$ and 500 mM NaCl). The sample reactions were heated at 75 °C for 5 minutes and left to cool slowly to 37 °C. The mutant strand synthesis and ligation sample reactions were performed in a total volume of 30 μl containing T4 DNA polymerase, T4 DNA ligase, 10X synthesis buffer (100 mM Tris-HCl, pH 7.5, 5 mM dNTPs, 10 mM ATP and 20 mM DTT) and 20 μl mutagenic sample reaction. The mutant strand synthesis and ligation reaction samples were incubated at 37 °C for 90 minutes.

Mutant strand synthesis and ligation reaction samples (10 ng) were added to 100 μl *Escherichia coli* BMH71-18 mutS cells and incubated on ice for 30 minutes before being heat-shocked for 45 seconds at 42 °C on a heating block after which they were immediately transferred to ice for 2 minutes. LB (900 μl) was added to the reaction

mixture and incubated by shaking at 250 rpm for 90 minutes at 37 °C. Overnight cultures were prepared by adding 4 ml LB supplemented with 100 μl proprietary mixture of antibiotics (the GeneEditorTM Antibiotic Selection Mix) to the transformation sample reactions. The cultures were incubated by shaking at 250 rpm for 16 hours at 37 °C. Plasmid DNA was then prepared as previously described in section 2.2.2.

The plasmid containing the insert coding for CLIC1-R29M was used to transform *Escherichia coli* JM109 cells. Transformants resistant to the GeneEditor^{TM} antibiotic selection mix were randomly selected and grown in 100 ml 2X YT media supplemented with 100 μg/ml ampicillin and plasmid DNA was prepared as previously described above and in section 2.2.2.

The CLIC1-E81M and N78A mutants were generated using the QuikChange™ site-directed mutagenesis kit by Stratagene® using double-stranded plasmid DNA templates, as follows:
A final volume of 50 μl was used for the sample reactions. The sample reactions consisted of 5 μl (10X) reaction buffer (100 mM KCl, 100 mM $(NH_4)_2SO_4$, 200 mM Tris-HCl, pH 8.8, 20 mM $MgSO_4$, 1% Triton X-100, 1 mg/ml nuclease-free bovine serum albumin), 1 μl (50 ng) dsDNA template, 1 μl (125 ng) forward primer, 1 μl (125 ng) reverse primer, 1 μl dNTP mix, 31 μl sterile distilled water (dH_2O) and 1 µl (2.5 U/µl) *Pfu Turbo* DNA polymerase. The parameters used to generate products were: 16 amplification cycles of 30 seconds at 95 °C to denature the CLIC1-WT dsDNA, 60 seconds at 55 °C to anneal the mutant primers and 60 seconds at 68 °C for DNA extension. A digestion reaction using 1 μl (10 U/μl) *Dpn I* for 1 hour at 37 °C and one hour at 20 °C was conducted in order to digest parental DNA. The reaction products were then used to transform *Escherichia coli* XL1-blue super-competent cells. The cells were plated onto LB-agar plates containing 100 µg/µl ampicillin. The LB-agar plates were incubated for 16 hours at 37 °C. Transformants were randomly selected and plasmid DNA was prepared as previously described in section 2.2.2.

2.2.3. DNA sequencing

CLIC1 cDNA, which encoded the R29M, N78A, E81M and R29M/E81M mutants, were sequenced to confirm the incorporation of the correct mutations into the

pGEX4T-1 plasmid. This also confirmed that no other mutations were generated during the mutagenesis amplification reactions. DNA sequencing was performed by Inqaba Biotechnical Industries (Pty) Ltd (Pretoria, South Africa).

Following the confirmation of the correct incorporation of the mutations into the pGEX4T-1 plasmids, the plasmids containing the inserts coding for CLIC1-R29M, N78A, E81M and R29M/E81M were used to transform *Escherichia coli* BL21 (DE3) cells. This was also done for CLIC1-WT in preparation for the over-expression and purification of the CLIC1 proteins.

2.2.4. Protein over-expression and purification

2.2.4.1. Induction studies

Induction studies for CLIC1-WT and E81M, were conducted as previously described (Fanucchi, PhD thesis, 2006 (http://wiredspace.wits.ac.za/handle/10539/4853) and Stoychev, PhD thesis, 2008 (http://wiredspace.wits.ac.za/handle/10539/5604)). Induction studies were performed in order to determine the optimal induction conditions for CLIC1-R29M. A late-log growth phase culture of *Escherichia coli* BL21 (DE3) cells was used to inoculate LB media, supplemented with 100 μg/ml ampicillin. The cells were grown with shaking at 37 ºC to mid-log growth phase (OD_{600} ~ 0.6). IPTG was added to the cultures to different final concentrations (0.1-1.0 mM) to induce the over-expression of the pGEX4T-1 plasmid containing the cDNA encoding for CLIC1-R29M. From the time of induction, whole cell aliquots were removed from the cultures at 0, 2, 4, 8 and 16 hours. The various samples were diluted down to a cell density equal to that of the two hour sample. This was done by diluting the samples in order to get OD_{600} readings equal to that of the two hour OD_{600} reading. The samples were assessed by sodium dodecyl sulfate-polyacrylamide gel electrophoresis (SDS-PAGE) according to the method of Laemmli (1970) (see section 2.2.6). The SDS-PAGE gels were subsequently analysed with Labworks UVP imaging systems v.4.5 (Cambridge, UK). Also, to reduce the time spent in acquiring purified CLIC1-N78A and R29M/E81M mutant proteins, the over expression conditions used were the same as those used for CLIC1-WT.

2.2.4.2. Over-expression and purification

A cell culture of *Escherichia coli* BL21 *(*DE3) was grown overnight in 100 ml 2X YT LB (1.6 g tryptone, 1 g yeast, 0.5 g NaCl per 100 ml dH_2O) supplemented with 100 μg/ml ampicillin. This overnight culture was used to inoculate fresh 2X YT LB broth (1:20 dilution) containing 100 μg/ml ampicillin. The cells were grown, shaking at 37 ^{o}C (20 ^{o}C for CLIC1-E81M) until mid-log growth phase (OD_{600} ~ 0.6) and protein expression was induced with 1 mM IPTG for CLIC1-WT, R29M, N78A and R29M/E81M and 0.8 mM IPTG for CLIC1-E81M. Protein expression was allowed to continue at 37 ^{o}C for 5 hours for CLIC1-WT, 4 hours for CLIC1-R29M, N78A and R29M/E81M, and at 20 ºC for 16 hours for CLIC1-E81M while shaking at 250 rpm. The cells were harvested by centrifugation for 15 minutes at 5000 rpm at 4 ºC. The pellets were resuspended in 3-4 ml resuspension buffer (10 mM Tris, 200 mM NaCl, 1 mM EDTA, 0.02% NaN_3 and 1 mM DTT, pH 7.5). The resuspended cells were stored in a 50 mL tube at –20 ºC to promote cell lysis. Once thawed on a rotator at 4 ºC, 10 μL of 1 M $MgCl_2$, 1 μl of 100 mg/ml DNAse and 10 μl of 10 mg/ml lysozyme were added to the cells and rotated for a further 15 minutes at 4 ºC. The cells were lysed on ice by pulse sonication for 60 seconds (4 rounds), using a duty cycle of 40% and a power output of 4. This was done using a Sonicator Ultrasonic Processor (Misonix Incorporated). The lysed cells were subsequently centrifuged at 15000 rpm for 30 minutes at 4 ºC in 30 mL tubes.

The CLIC1 proteins were purified according to the method described by Tulk *et al.* (2002). The protein-containing cytosol was diluted 2-fold in resuspension buffer and loaded onto a GSH-Sepharose column pre-equilibrated with equilibration buffer (100 mM Tris, 200 mM NaCl, 1 mM EDTA, 0.02% NaN_3 and 1 mM DTT, pH 8). The GST-CLIC1 fusion protein binds the glutathione of the GSH-Sepharose column which was washed with 10 column volumes of GSH equilibration buffer to elute any unbound GST-CLIC1 fusion protein and contaminating proteins. Thereafter, the GSH-Sepharose column was re-equilibrated with 5 column volumes of thrombin-cleavage buffer (200 mM Tris, 150 mM NaCl, 0.5 mM DTT, 0.02% NaN_3, pH 8.4). A volume of 80 μl (1 U/ml) of thrombin per 1 l of original cell culture, was added to 15 ml of thrombin-cleavage buffer. This thrombin solution was then added to the GSH-Sepharose column and the column rotated for 16 hours at 20 ºC in order to release the CLIC1 proteins from the GST tag bound to the GSH-Sepharose column.

The thrombin solution containing the CLIC1 protein was eluted from the GSH-Sepharose column and applied to a DEAE-anion exchange column that had been pre-equilibrated with 10-column volumes of DEAE equilibration buffer (20 mM Tris, 1 mM DTT, 0.02% NaN_3, pH 6.5) The DEAE-anion exchange column was connected to an Äktaprime system (Amersham Biosciences). The theoretical pI values for thrombin and CLIC1-WT, R29M, E81M, N78A and R29M/E81M calculated by the ExPASy server program ProtParam (Gasteiger *et al.*, 2005) are 8, 5.02, 4.94, 5.09, 5.02 and 5, respectively. Therefore, at pH 6.5, thrombin is positively charged and does not bind the DEAE-column. However, CLIC1 is negatively charged at pH 6.5 and should bind the DEAE-column. DEAE elution buffer (20 mM Tris, 300 mM NaCl, 0.02% NaN_3, pH 6.5) was used to elute the CLIC1 protein from the DEAE-anion exchange column. Fractions (2 ml) were collected and assessed for purity using a 15% acrylamide SDS-PAGE gel (see section 2.2.6). Fractions containing pure protein were pooled and dialysed against 2 l of CLIC1 storage buffer (50 mM $NaHPO_4$, 1 mM DTT, 0.02% NaN_3, pH 7.0).

The GSH-Sepharose column was regenerated by washing the GSH-Sepharose column with 5-column volumes of GSH-Sepharose elution buffer (50 mM Tris, 10 mM GSH, 0.02% NaN_3, pH 8.0) to elute any column-bound GST as well as any uncleaved GST-CLIC1.

For all experiments, the CLIC1 proteins were dialysed weekly against CLIC1 storage buffer containing fresh DTT. Unless otherwise stated, all experiments described hereafter were performed in this buffer.

2.2.5. Protein concentration determination

The behaviour of proteins under a variety of solvent conditions may be examined by spectroscopy which also permits comparisons between related proteins, such as mutated forms and homologous proteins (Schmid, 1997). Advantages of this methodology are that spectroscopic measurements usually take place in solution and only tiny amounts of sample are needed for investigation and since it is non-destructive, it allows for the recovery of sample. Within the UV range of an absorbance spectrum, proteins absorb and emit radiation. It is the peptide groups, aromatic amino acids and to a smaller degree the disulfide bonds that are responsible for the absorption

(Schmid, 1997). Absorbance spectroscopy is most ordinarily used to determine the concentration of biological macromolecules in solution. The absorbance of each of the protein stock solutions was measured spectroscopically. The concentrations were then calculated using the Beer-Lambert law:

$$A_{280} = \varepsilon cl \qquad (1)$$

where A_{280} is absorbance at 280 nm, ε is the molar absorption coefficient of the protein, c is the concentration of the protein and l is the cuvette path length (1 cm).

The molar extinction coefficient (ε) of the CLIC1 proteins at 280 nm was calculated by using the extinction coefficients of the tryptophan, tyrosine and cysteine residues as described by Perkins, (1986):

$$\begin{aligned} \varepsilon_{280}\,(M^{-1}cm^{-1}) &= 5550\ \Sigma\ Trp + 1340\ \Sigma\ Tyr + 150\ \Sigma\ Cys \qquad (2) \\ &= 5550(1) + 1340(8) + 150(6) \\ &= 17170\ M^{-1}cm^{-1} \end{aligned}$$

2.2.6. Purification analysis

SDS-PAGE is extensively used to analyse protein mixtures qualitatively. SDS-PAGE is often used to examine protein purification and because the method is founded on the separation of proteins by size, the technique can also be employed to determine the relative molecular masses of proteins (Simpkins, 2000).

Discontinuous SDS-PAGE was used to assess protein over-expression, as well as the purity of the purified CLIC1 protein samples (Laemmli, 1970). SDS-polyacrylamide separating gels consisting of 15% acrylamide and stacking gels consisting of 4% acrylamide were used. Protein samples were prepared by a 1:1 dilution with sample buffer. The samples were boiled prior to being loaded on the SDS-polyacrylamide gel. Separation was achieved at 140 volts for approximately 2 hours.

The protein molecular mass markers contained a mixture of seven proteins namely: β-galactosidase (116 kDa), bovine serum albumin (66.2 kDa), ovalbumin (45 kDa),

lactate dehydrogenase (35 kDa), restriction endonuclease Bsp98I (25 kDa), β-lactoglobulin (18.4 kDa) and lysozyme (14.4 kDa). After completion of electrophoresis, the gels were stained overnight with Coomassie Brilliant Blue and were destained with destaining solution (25% ethanol and 10% acetic acid) for 6 hours prior to visualisation (Laemmli, 1970).

2.2.7. Structural characterisation

2.2.7.1. Circular dichroism spectroscopy

Circular dichroism (CD) spectroscopy is a method that relies on the fact that when molecules are exposed to left and right circularly polarised light they interact with the light in different ways. Circularly polarised light is chiral, i.e. it has two non superimposable forms that are mirror images of one another (Woody, 1995). As most biological molecules display chirality, they are able to differentiate between the two chiral forms of light. CD spectroscopy measures the difference in the absorbance of left and right circularly polarised light by optically active molecules (Schmid, 1997). Thus, CD spectroscopy is used to analyse the relative amounts of the different secondary structural elements of polypeptide chains as well as provide information about the environments of the chromophores of the aromatic amino acids, and the contributions from disulfide bonds and non-protein cofactors in solution (Kelly and Price, 1997). CD spectroscopy obeys the Beer-Lambert law in that, the CD spectrum of each constituent in a solution is directly proportional to its concentration, and the entire spectrum corresponds to the sum of all the contributing spectra (Greenfield, 1999). Therefore, any change in the CD spectrum of a protein when perturbants such as ligands, denaturants or heat are applied, are directly proportional to the amount of protein altered by the perturbation (Greenfield, 1999).

Far-UV CD spectra (250-170 nm) are sensitive to the secondary structural conformation in which the backbone and amide bond chromophores are arranged in a structured arrangement such as α-helices and β-sheets (Woody, 1995; Kelly and Price, 1997). Secondary structure conformations present distinct spectral features in the far-UV CD spectrum. Proteins with a high α-helical content display characteristic double minima, with broad ellipticities at 208 and 222 nm (associated with the low-energy electronic transition $n \rightarrow \pi^*$), as well as an intense positive ellipticity near 190 nm

(associated with the $\pi \rightarrow \pi^*$ electronic transition) (Woody, 1995; Kelly and Price, 2000).

Far-UV CD spectra were recorded using 2 μM CLIC1-WT and mutant proteins at pH 7 and pH 5.5. CLIC1 storage buffer was diluted 10X to reduce the noise-to-signal ratio at the lower end of the spectrum owing to the buffer signal. Data were obtained using a Jasco J-810 spectropolarimeter using a cell length of 2 mm, data pitch 0.5 nm, 0.5 second response, 1 nm band width, standard sensitivity and a scan speed of 200 nm/min at 20 ºC. The data obtained from the far-UV CD analyses were an average of 5 accumulations from 250 nm to 190 nm. The negative exponential smoothing technique (SigmaPlot® v11.0) was used to smooth the data. This technique smoothes the data using polynomial regression and weights computed from the Gaussian density function with a sampling proportion of 0.1.

Near-UV CD spectra (340-250 nm) are dictated by absorption bands from the side chains of the aromatic residues, Phe, Tyr and Trp (Woody, 1995). These aromatic residues have characteristic $\pi \rightarrow \pi^*$ absorbance bands in the near-UV and far-UV (Woody, 1995). Other contributions may arise due to the presence of disulfides or prosthetic groups (Woody, 1995). The aromatic amino acids Phe, Tyr and Trp have characteristic wavelength contours: Phe displays sharp, fine structures between 255 and 270 nm, Tyr has a peak between 275 and 283 nm and Trp has a peak near to 290 nm with fine structures between 290 and 305 nm (Strickland, 1974). Since near-UV CD is sensitive to the environment of the aromatic amino acid side chains, it provides information about the tertiary structure of proteins (Woody, 1995).

Strickland (1974) also showed that useful information can be obtained by recording CD spectra at low temperatures since these greatly improve the CD spectral resolution. In light of this, low temperature CD makes it possible to look at the structures of individual “frozen” conformational states of proteins that may be speedily inter-changing at higher temperatures (Strickland, 1974).

Near-UV CD spectra were recorded using 40 μM CLIC1-WT and mutant proteins at pH 7 and pH 5.5 at 5 ^{o}C. Data were obtained using a Jasco J-810 spectropolarimeter using a cell length of 1 cm, data pitch 0.5 nm, 1 second response, 0.5 nm band width,

high sensitivity and a scan speed of 200 nm/min. The temperature was maintained at 5 ^{o}C by a Jasco PTC-423S Peltier-type temperature control system. The data obtained from the near-UV CD analyses were an average of 5 accumulations from 310 nm to 260 nm.

The mean residue ellipticities [θ] of the spectra were calculated from the equation:

$$[\theta] = 100(\theta)/cnl \qquad (3)$$

where, θ is the observed ellipticity signal in millidegrees, c is the protein concentration in mM, n is the number of amino acid residues in the protein chain and l is the path length in cm (Schmid, 1997).

2.2.7.2. Fluorescence spectroscopy

Fluorescence spectroscopy can be used in many ways to analyse proteins since it fundamentally analyses changes in the local environment of fluorophores in proteins (Lakowicz, 1999). Fluorescence emission occurs when an electron is excited from a ground state and then returns from the excited state back to the ground state (Schmid, 1997). During the excited state, energy is lost through vibrational, rotational and conformational non-radiative processes, which means that the energy of the emitted light will be less than the absorbed light, and the fluorescence of the fluorophore occurs at a greater wavelength than its absorbance (Schmid, 1997).

The fluorescence of proteins originates from Phe, Tyr and Trp amino acid residues (Schmid, 1997). Fluorescence is usually governed by the contribution of tryptophan residues because both their absorbance at the wavelength of excitation and their quantum yield of emission are much greater than the values for Tyr and Phe (Schmid, 1997). Trp residues are roughly five times more sensitive than Tyr, mainly because Trp has a molar extinction coefficient of 5.5 x 10^3 $M^{-1}cm^{-1}$ at 280 nm which is greater than the extinction coefficient for Tyr at 274 nm (Eftink, 1995). Also, the indole ring of tryptophan is highly sensitive to solvent polarity (Lakowicz, 1999). Emission spectra of this residue reflect the polarity of its surrounding environment and therefore, Trp fluorescence is used to monitor local tertiary structural changes in proteins. CLIC1-WT and mutant proteins contain one Trp (Trp35), located on the C-terminal end of helix 1

within the N-terminal domain (Figure 1). This helix has been proposed to transverse the membrane (Harrop *et al.*, 2001; Berry and Hobert, 2006; Singh and Ashley, 2006) and therefore, Trp35 is an excellent probe to report on local structural changes. CLIC1 also consists of eight Tyr residues, mainly located within the C-terminal domain. Low quantum yields are produced when selectively exciting the single Trp residue (Fanucchi, PhD thesis, 2006 (http://wiredspace.wits.ac.za/handle/10539/4853)) and, therefore, excitation at 280 nm will be used to improve the signal. In so doing so, not only will the eight Tyr residues become excited but so too will the lone Trp residue. Since the Tyr residues are within close range to the Trp residue, fluorescence resonance energy transfer from the Tyr residues to the Trp residue will occur (Lakowicz, 1999).

A PerkinElmer LS-50B luminescence spectrophotometer was used to measure the fluorescence spectra of 2 μM concentrations of CLIC1-WT and mutant proteins. This was carried out at pH 7 and pH 5.5 at 20 ºC. A path length of 1 cm was used and the slit widths used were 5 nm for both excitation and emission. The proteins were excited at 280 nm and emission spectra obtained for the wavelength range 280 nm to 450 nm at a scan speed of 350 nm/min. The spectra were an average of 3 accumulations. The negative exponential smoothing technique (SigmaPlot® v11.0), mentioned in section 2.2.7.1 was used to smooth the data.

ANS is one of the most commonly used extrinsic fluorescent probes for the analysis of the structural properties of protein molecules (Uversky *et al.*, 1998). ANS was originally used to investigate the hydrophobicity of native proteins by Stryer in 1965 who found that an interaction of ANS with solvent-exposed hydrophobic clusters of apomyoglobin and apohaemoglobin resulted in an increase of the ANS fluorescence intensity (Stryer, 1965). This increased ANS fluorescence intensity was accompanied by a considerable blue shift of the fluorescence spectrum of this probe (Stryer, 1965).

ANS is least fluorescent in polar environments such as aqueous solutions due to quenching by water but, its fluorescence emission increases substantially in non-polar environments (Stryer, 1965). The hydrophobic interaction of ANS with proteins is also a commonly used method for characterising and/or distinguishing partially folded states of proteins (Semisotnov *et al.*, 1991). Partially folded states of proteins consist of groups of hydrophobic side chains that are not yet completely buried in the native core

structure and make available binding sites for ANS. ANS fluorescence has also been applied to protein folding in that it has been shown that there is a preference for ANS to interact with equilibrium and kinetic molten globule states in relation to native and totally unfolded proteins (Rodionova *et al*., 1989, Semisotnov *et al*., 1991).

Free ANS excited at 390 nm emits at 540 nm. However, when ANS binds to exposed hydrophobic sites on a protein, the emission is lowered to around 470 nm. The change in emission wavelength is reliant on the hydrophobicity of the ANS binding sites available on the protein and the quantum yield of ANS (Stryer, 1965).

Stock solutions of ANS (2 mM) were prepared by weight and made-up with CLIC1 storage buffer at pH 7 and 5.5. The concentration of ANS was checked using an extinction coefficient of 4950 $M^{-1}cm^{-1}$ at 350 nm (Weber and Young, 1964). ANS was added to each sample to a final concentration of 200 μM and incubated for a further hour at 20 ^{o}C. This allowed the ANS to bind to exposed hydrophobic sites on the proteins.

A PerkinElmer LS-50B luminescence spectrophotometer was used to measure each of the CLIC1-WT and mutant protein samples at pH 7 and pH 5.5 at 20 ºC. A path length of 1 cm was used and the slit widths used were 5 nm for excitation and emission, respectively. ANS was excited at 390 nm and emission spectra obtained from 390 nm to 600 nm at a scan speed of 350 nm/min. The spectra were an average of 3 accumulations. Each unfolding curve was done in triplicate and averaged. Spectra were corrected for free ANS by measuring an additional set of samples but in the absence of protein.

To check that ANS binding was not a result of protein aggregation, Rayleigh scatter was monitored by fluorescence using slit widths of 5 nm and excitation and emission wavelengths of 390 nm.

Employing fluorescence quenching to provide knowledge about the dynamic character of proteins was first established by Lacowicz and Weber in 1973 (Lacowicz and Weber, 1973). Proteins are not inflexible structures, but constantly undergo stochastic structural oscillations that assist the inward diffusion of quenchers such as iodide,

oxygen and acrylamide. Consequently, acrylamide can be used to quench fluorescence of exposed and buried tryptophan residues such as that shown in ribonuclease T1 and aldolase (Eftink and Ghirion, 1975; Eftink and Ghirion, 1976; Eftink and Ghirion, 1977). Acrylamide can be described as an extremely efficient quencher that is neutral, however, more polar than oxygen in character. A striking attribute of acrylamide as a quencher is that is does not significantly interact with proteins (Eftink and Ghirion, 1976).

The conventional Stern-Volmer equation relates the decrease in fluorescence intensity to the concentration of collisional quencher Q, as follows:

$$F_0 / F = 1 + K_{sv} [Q] \quad (4)$$

where F_0 and F are the fluorescence intensities in the absence and presence of quencher, respectively, and K_{sv} is the Stern-Volmer constant for the collisional quenching processes. The K_{sv} value supplies information regarding the extent of exposure of tryptophan residues (Eftink and Ghirion, 1981)

A PerkinElmer LS-50B luminescence spectrophotometer was used to measure the quenching of the CLIC1-WT and mutant proteins intrinsic tryptophan fluorescence by acrylamide at pH 7 and pH 5.5 at 20 ºC. This information was used to determine the exposure of Trp35. Acrylamide (0-0.3 M) was added to 2 μM protein after which Trp35 was selectively excited at 295 nm and the fluorescence maximum was monitored at 345 nm, in the presence and absence of acrylamide. The scan speed used was 350 nm/min. A pathlength of 1 cm and a slit width of 5 nm for both excitation and emission were used. The spectra were an average of 3 accumulations and each sample was measured in triplicate. The data were plotted using SigmaPlot® v11.0 and analysed according to equation 4.

2.2.8. Conformational stability studies

Measuring the unfolding of a protein is a useful way of estimating the conformational stability of that protein. The effect of a mutation on the stability of a protein can be studied by comparing the equilibrium unfolding data of the wild type and mutant

proteins. The unfolding of proteins can be induced in several ways including increasing or decreasing temperature, adding chaotropic chemical denaturants such as urea or guanidine hydrochloride, exposing the protein to extremes of pH, and increased hydrostatic pressure (Eftink, 1995).

Measuring the conformational stability of a protein necessitates the establishment of equilibrium and, therefore, it is most important to assess the degree of recovery of the native state. This will establish that equilibrium exists between the folded and unfolded state of the protein, thus allowing the thermodynamic parameters of unfolding to be established (Pace, 1986).

$$\text{Folded protein (N)} \leftrightarrow \text{Unfolded protein (U)} \qquad (5)$$

Recovery of the native state of the CLIC1-WT and mutant proteins at pH 7 and pH 5.5 were determined using the method described by Pace and Scholtz, 1996. A solution of 10 μM protein in 7.5 M urea was incubated at 20 ºC for 1-2 hours, allowing the protein to completely unfold. A 10-fold dilution of the solution was made and left for 1-2 hours at 20 ºC, this allowed the protein to recover its native structure and was monitored using fluorescence spectroscopy as described in section 2.2.7.2. Far-UV CD was not used as a probe to establish reversibility as the signal-to-noise ratio was very poor. A sample consisting of 1 μM protein in 0.75 M urea, representing the final conditions used for refolding, was used as a control. The percentage recovery was calculated for each protein unfolded and refolded at pH 7 and pH 5.5.

Equilibrium unfolding studies were performed at pH 7 and pH 5.5 at 20 ^{o}C. Fresh 10 M urea stock solutions were prepared using CLIC1 storage buffer and used as the denaturant. The molarities of the urea stock solutions were checked by refractometry (Pace, 1986).

CLIC1-WT and mutant proteins (2 μM) were incubated in 0 to 8 M urea at pH 7 and pH 5.5 at 20 °C and left to establish equilibrium. The conformational stabilities of the CLIC1-WT and mutant proteins were monitored using far-UV CD and tryptophan fluorescence spectroscopy as structural probes (previously described in sections 2.2.7.1 and 2.2.7.2).

The equilibrium unfolding data are an average of three replicates. Any major outliers were removed from the data sets.

The extent of Rayleigh scatter due to protein aggregation throughout the unfolding process was monitored for each protein at pH 7 and pH 5.5. This was achieved by setting the excitation and emission wavelengths at 340 nm and then measuring the fluorescence intensity. The excitation and emission slit widths were 2.5 nm.

2.2.8.1. Equilibrium-unfolding data fitting

The thermodynamic parameters of equilibrium unfolding, $\Delta G(H_2O)$ (free energy change in the absence of denaturant) and the *m*-value (dependence of free energy on denaturant concentration), were determined using global fitting analysis (Beecham, 1992). This was accomplished by use of the program Savuka v. 6.2.26 (Zitzewitz *et al.*, 1995; Bilsel *et al.*, 1999) and a Poisson probability distribution. The program uses a Marquardt-Levenberg type 87 non-linear least-squares routine to analyse simultaneously multiple sets of data from different experiments in terms of internally consistent sets of fitting parameters (Beecham, 1992). This fitting procedure minimises error and better resolves the model.

Global analysis involves simple modifications of current non-linear least-square packages. The main change in the algorithm is an additional procedure whereby the model-dependent summation of the normal non-linear least-squares equations can be performed (Beechman, 1992). Simply put, non-linear optimisation of a model for sets of data entails an iterative search in parameter space to reduce differences between theory and experimental data. A succession of error-reducing procedures is selected where the best new direction is reassessed at each procedure. During non-linear least-squares, the change of the search direction is done in the same way as normal non-linear least-squares. The only difference is that the global comparison of the theory data is controlled by many data sets. This is accomplished with global mapping vectors that connect a specific subset of the total parameters to a local (single curve) fitting function (Knutson *et al*., 1983).

2.2.8.1.1. Two-state fitting model (N ↔ U)

For a two-state monomer unfolding transition, a protein may exist only in the native (N) or unfolded (U) state, with the absence of any intermediates (I). This is characterised by the reaction:

$$N \overset{K_U}{\leftrightarrow} U \tag{6}$$

where K_U represents the equilibrium constant.

As the native and unfolded conformations in a two-state unfolding transition are the only species present,

$$F_N + F_U = 1 \tag{7}$$

where F_N and F_U are the fractions of protein in the native and unfolded states, respectively. Therefore, the y-value (signal obtained for the respective spectroscopic probe) at any point in the equilibrium unfolding transition is represented by:

$$y = Y_N F_N + Y_U F_U \tag{8}$$

where Y_N and Y_U represent the y-values (signal obtained for the respective spectroscopic probe) of the native and unfolded states, respectively. Y_N and Y_U are estimated from the linear extrapolation of the pre- and post-transition baselines, respectively. When equations (7) and (8) are combined, the fraction of unfolded protein is:

$$F_N = (Y_N - y) / (Y_N - Y_U) \tag{9}$$

Similarly, the fraction of unfolded protein can be obtained:

$$F_U = (y - Y_U)/(Y_N - Y_U) \tag{10}$$

The equilibrium constant for the unfolding reaction (K_{eq}) is:

$$K_{eq} = F_U / F_N \tag{11}$$

So, therefore, if equations 9 and 10 are substituted into equation 11:

$$K_{eq} = (Y_N - y) / (y - Y_U) \quad (12)$$

Given that:

$$\Delta G = - RT \ln K_{eq} \quad (13)$$

where ΔG is the change in free energy of unfolding, R is the gas constant, T is temperature in kelvin and K_{eq} is the equilibrium constant for the reaction. Then, in order to determine $\Delta G(H_2O)$ it is assumed that ΔG has a linear dependence on denaturant concentration [denaturant] for all urea concentrations (Tanford, 1970).

Then,

$$\Delta G = \Delta G(H_2O) – m[\text{denaturant}] \quad (14)$$

where $\Delta G(H_2O)$ represents the free energy difference between the folded and unfolded states in the absence of denaturant. The m-value is determined from the slope of the ΔG versus denaturant concentration plot and is indicative of the difference of the solvent accessible surface area between native and unfolded states of proteins (Green and Pace, 1973).

It should be noted that the two-state monomeric transition model can only be used if the data appears monophasic and that the data monitored by different probes are superimposable. Any deviations from these criteria could lead to the assumption that the transition from the folded to unfolded state is no longer monophasic owing to the incorporation of some form of intermediate specie(s) and should rather be fitted to a three-state transition model. Also, if the probes used to observe the unfolding events do not make a distinction between the intermediate and unfolded states, the presence of intermediate states can be assumed if the unfolding curves shift to a lower concentration of denaturant and if there is a concomitant decrease in the gradient of the transition region of the unfolding curve (Soulages, 1998).

2.2.8.1.2. Three-state fitting model (N ↔ I ↔ U)

For a three-state monomer unfolding transition, a protein may exist in the native (N), intermediate (I) and unfolded (U) states:

$$\begin{matrix} & K_1 & K_2 & \\ \mathrm{N} & \leftrightarrow & \mathrm{I} & \leftrightarrow \mathrm{U} \end{matrix} \qquad (15)$$

where K_1 represents the equilibrium constant for the N ↔ I transition and K_2 represents the equilibrium constant for the I ↔ U transition.

As the native, unfolded and intermediate conformations in the three-state unfolding transitions are the only species present,

$$F_N + F_I + F_U = 1 \qquad (16)$$

$$K_1 = F_I/F_N \qquad K_2 = F_U/F_I \qquad K_U = F_U/F_N = K_1K_2 \qquad (17)$$

where F_I is the fraction of intermediate present. The equilibrium constant for N ↔ U is represented by K_1K_2. y (signal obtained for the respective spectroscopic probe) can be represented as:

$$y = Y_NF_N + Y_IF_I + Y_UF_U \qquad (18)$$

where Y_I depicts the measured signal of the intermediate. Y_N and Y_U are estimated from the linear extrapolation of the pre- and post-transition baselines, respectively. Now, by solving F_U in terms of K_1 and K_2 and by combining equations (16) and (17)

$$F_U = (K_1K_2)/(K_1K_2 + 1 + K_1) \qquad (19)$$

Rearranging and substituting equation (17) into equation (18) and solving for F_N and F_I in terms of K_1 and K_2:

$$F_N = F_U/K_1K_2$$

therefore,

$$F_N = 1/[(K_1K_2 + 1 + K_1)/K_1K_2] \quad (20)$$

Similarly

$$F_I = K_1/[(K_1K_2 + 1 + K_1)/K_1K_2] \quad (21)$$

Substituting equations (19), (20) and (21) into equation (18) gives:

$$y = (Y_N + Y_IK_1 + Y_U(K_1K_2))/(1 + K_1 + K_1K_2) \quad (22)$$

We know that:

$$\Delta G_1 = -RT\ln K_1 \text{ hence } K_1 = e^{-\Delta G1/RT} \quad (23)$$

and

$$\Delta G_1 = \Delta G_2(H_2O) - m_1[\text{denaturant}] \quad (24)$$

By combining equations (23) and (24):

$$K_1 = e^{[-\Delta G1(H2O)-m1[\text{denaturant}]]/RT} \quad (25)$$

Similarly,

$$K_2 = e^{[-\Delta G2(H2O)-m2[\text{denaturant}]]/RT} \quad (26)$$

Substituting equations (25) and (26) into (22) the final equation to fit the data is achieved:

$$y = [Y_N + Y_I(e^{[-\Delta G1(H2O)-m1[\text{denaturant}]]/RT}) + Y_U(e^{[-\Delta G1(H2O)m1[\text{denaturant}]]/RT})(e^{[-\Delta G2(H2O)-m2[\text{denaturant}]]/RT})]/[1 + (e^{[-\Delta G1(H2O)-m1[\text{denaturant}]]/RT}) + (e^{[-\Delta G1(H2O)-m1[\text{denaturant}]]/RT})(e^{[-\Delta G2(H2O)-m2[\text{denaturant}]]/RT})] \quad (27)$$

2.2.9. Software for structural, sequence and protein property analysis

CLIC1-WT and mutant protein graphics were generated using Swiss-PDB Viewer v3.7 (Guex and Peitsch, 1997). The CLIC1-WT and mutant DNA sequences obtained were viewed using the program Chromas version 1.45 (32 bit) (http://www.technelysium.com.au/chromas.html; Technelysium Pty. Ltd., Helensvale, Australia). The theoretical p*I* values for CLIC1-WT, mutant proteins and thrombin were obtained using the ExPASY tool ProtParam (Gasteiger *et al*., 2005). Assessing the SDS-PAGE gels for optimum induction conditions was done using the Labworks UVP BioImaging System. Unless otherwise stated, data were plotted using SigmaPlot version 11.0 (SPSS Science, Chicago, Illinois USA).

CHAPTER 3

RESULTS

3.1. Verification of the CLIC1 mutations

The sequencing confirmed that the desired mutations in the cDNA encoding CLIC1-R29M, E81M, N78A and R29M/E81M mutant proteins had been correctly incorporated and verified the absence of any other mutations. Portions of the cDNA sequences containing the codon change of interest for the CLIC1-R29M, E81M, N78A and R29M/E81M mutants are shown in Figure 7.

3.2. Protein over-expression and purification

The over-expression conditions for CLIC1-WT and E81M had been previously determined (see section 2.2.4). Therefore, the over-expression of CLIC1-WT, E81M, N78A and R29M/E81M was conducted as described in section 2.2.4. However, prior to over-expression of CLIC1-R29M, induction studies were carried out in order to determine the optimal induction time and IPTG concentration. The results of the CLIC1-R29M induction study showed that the optimum induction conditions were a four hour growth time and 1 mM IPTG (Figure 8).

The solubility of CLIC1-R29M was assessed by SDS-PAGE of the cytosol and the pellet fractions. The mutant protein was found to be soluble, with no visible band appearing at 27 kDa in the insoluble pellet fraction. This result was the same for CLIC1-WT, E81M (induced at 20 ^{o}C), N78A and R29M/E81M. Therefore, all the expressed CLIC1 proteins were soluble.

The CLIC1-WT and mutant proteins were purified as described in section 2.2.4 and the purity was assessed by SDS-PAGE (Figure 9A). The CLIC1-WT and mutant proteins were found to have a molecular mass of approximately 27 kDa (Figure 9B), corresponding to that previously reported (Littler *et al*., 2004). In the absence of other protein bands in the SDS-PAGE gels, and since only a single band corresponding to a

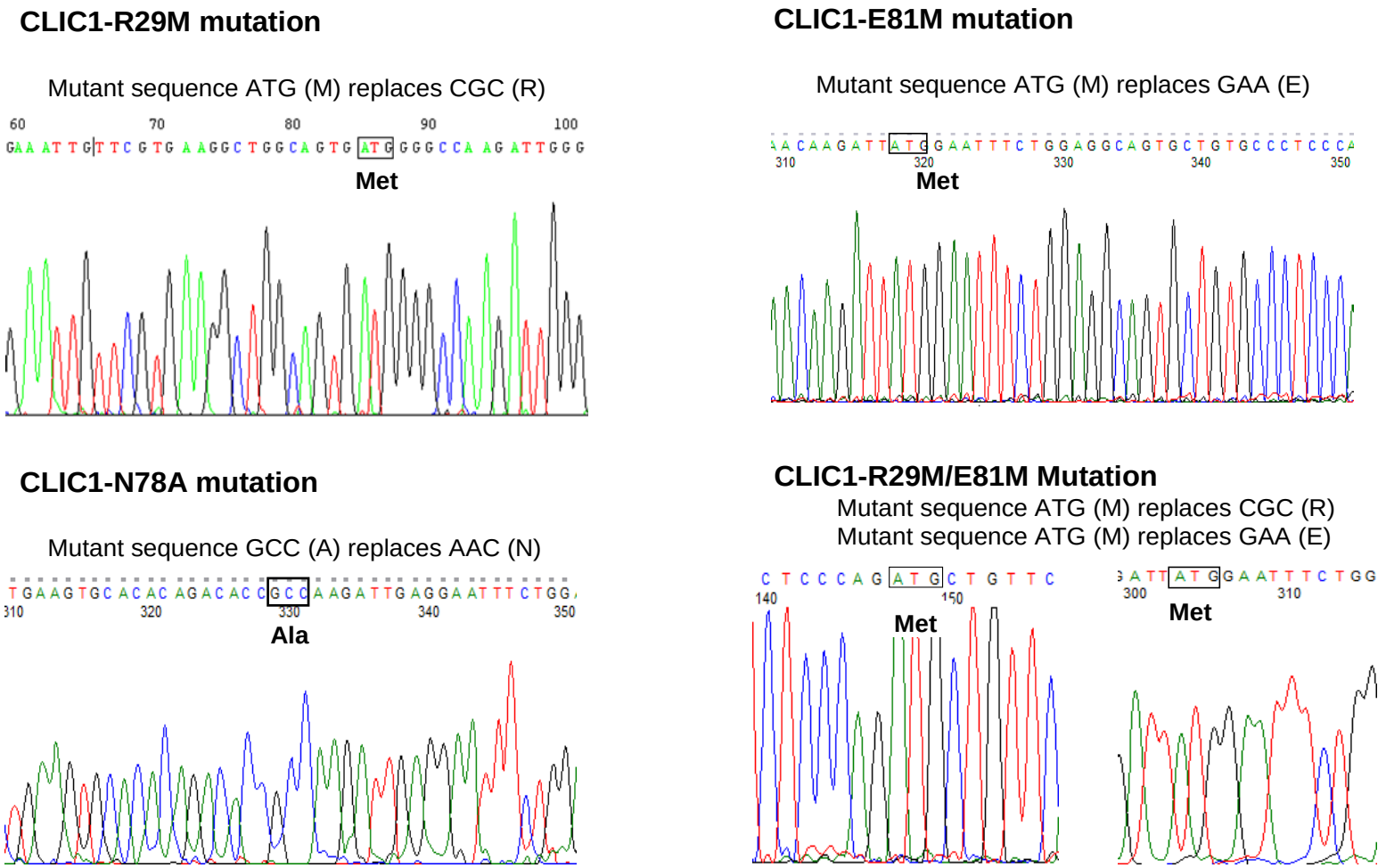
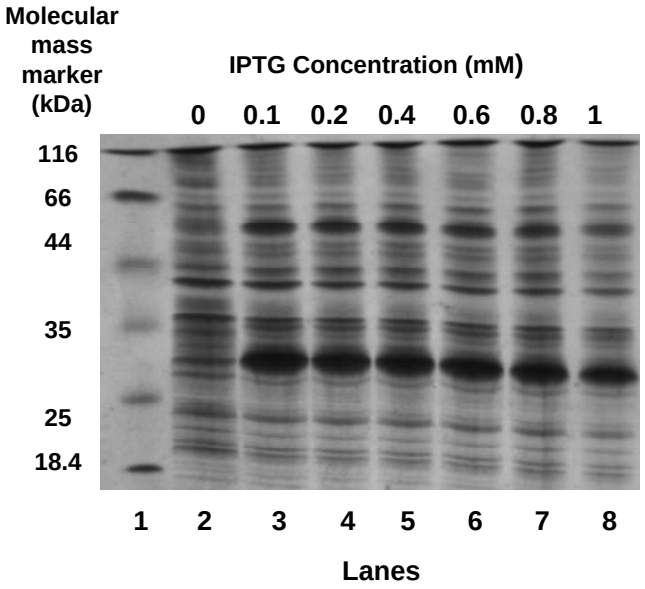


Figure 7: **Verification of the CLIC1-R29M, E81M, N78A and R29M/E81M mutations**

The sequences obtained from sequencing were viewed using the program Chromas version 1.45 (http://www.technelysium.com.au/chromas.html; Technelysium Pty. Ltd., Helensvale, Australia). Shown here are segments of the sequences. The boxed regions indicate the CLIC-1 R29M codon (ATG), CLIC1-E81M codon (ATG), CLIC1-N78A codon (GCC) and CLIC1-R29M/E81M codons (ATG/ATG).

(A)



(B)

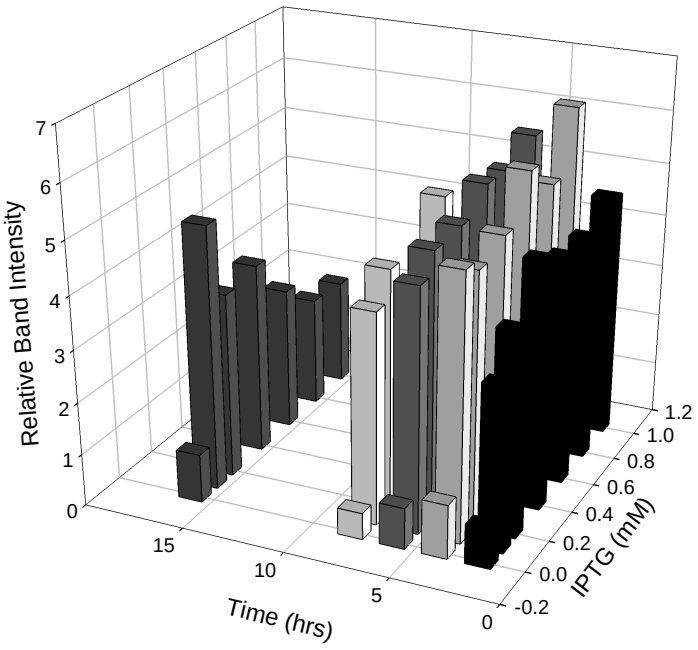
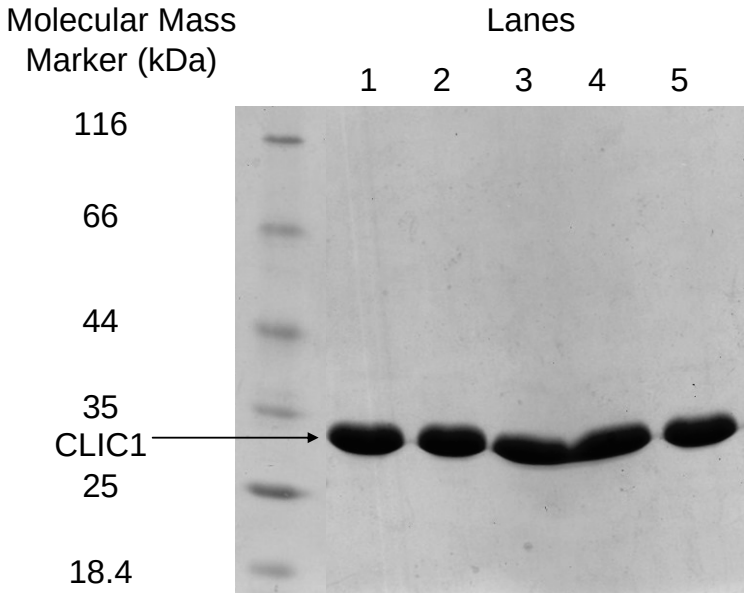


Figure 8: Over-expression and induction study of CLIC1-R29M

(A) SDS-PAGE gel (15% acrylamide) showing the samples induced for 4 hours at various IPTG concentrations. Lane 1: SDS molecular mass markers. Lanes 2 to 8: the samples at various IPTG concentrations. **(B)** Three-dimensional bar-chart showing the band intensity corresponding to that of CLIC1-R29M at various times and IPTG concentrations. The greatest band intensity occurred at 4 hrs at an IPTG concentration of 1 mM.

(A)



(B)

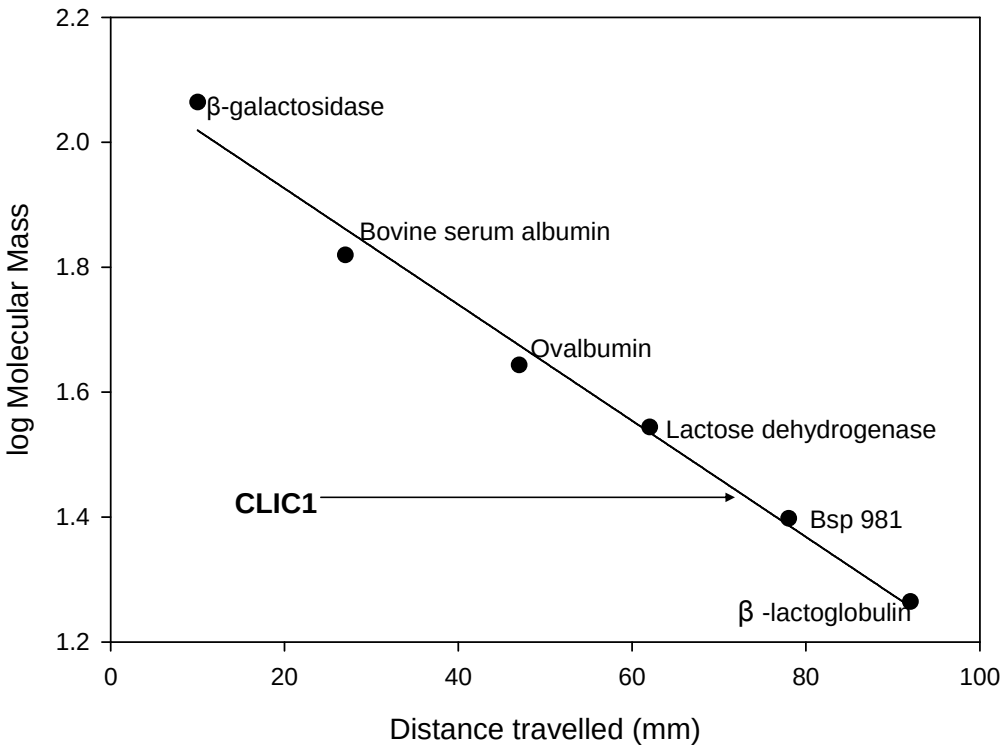


Figure 9: **SDS-PAGE and calibration curve**

(A) SDS-PAGE gel (15% acrylamide) showing the molecular mass of the purified CLIC1-R29M protein (27 kDa). Lane 1: SDS molecular mass markers. Lanes 2-5: purified CLIC1-WT, R29M, E81M, N78A and R29M/E81M proteins. (**B**) Calibration curve indicating the molecular mass of the CLIC1 proteins relative to the molecular mass markers ($R^2 = 0.98$).

molecular mass of 27 kDa was present, one can conclude that the CLIC1-WT and mutant proteins had been purified successfully.

3.3. Protein concentration determination

CLIC1-WT and mutant protein concentrations were determined after purifications as described in section 2.2.5. It is important to mention that all CLIC1-WT and mutant protein stocks were maintained at lower concentrations (20-30 μM) when dialysed into pH 5.5 compared to pH 7. This was done since CLIC1 tends to aggregate at low pH when the protein concentration is high (40-100 μM). Concentration determinations were consistently reliable, with R^2 values ranging between 0.98 and 1.

3.4. Structural integrity of the CLIC1 mutant proteins

3.4.1. Far-UV and near-UV CD spectroscopy

The far-UV CD spectra for native CLIC1-WT and mutant proteins were determined between 250 nm and 190 nm at 20 ºC and plotted as mean residue ellipticity versus wavelength (Figure 10). The spectra of CLIC1-WT and mutant proteins displayed troughs at 208 nm and 222 nm and a peak at 190 nm, at pH 7 and pH 5.5. This is indicative of proteins with a predominantly α-helical content and conforms to the CLIC1 crystal structure (Harrop *et al.*, 2001).

This result indicates that the mutations have not caused significant global secondary structural changes to the CLIC1 protein. This was later confirmed by the crystal structure of the R29M/E81M mutant (see Appendix).

As mentioned in section 2.2.7.1, some buffers produce poor signal-to-noise ratios and, therefore, readings below 210 nm are often not reliable. The signal-to-noise ratio was best at a wavelength of 222 nm and, therefore, the ellipticity values at 222 nm were used for comparative purposes. The secondary structural content of CLIC1-WT decreased by approximately 13.5%, when subjected to a pH of 5.5. This value is comparable to values previously reported (Fanucchi *et al.*, 2008). The CLIC1-R29M mutant also shows a decreased secondary structural content at pH 5.5 compared to that at pH 7. Interestingly, CLIC1-R29M/E81M appears to have increased secondary structural content at pH 5.5

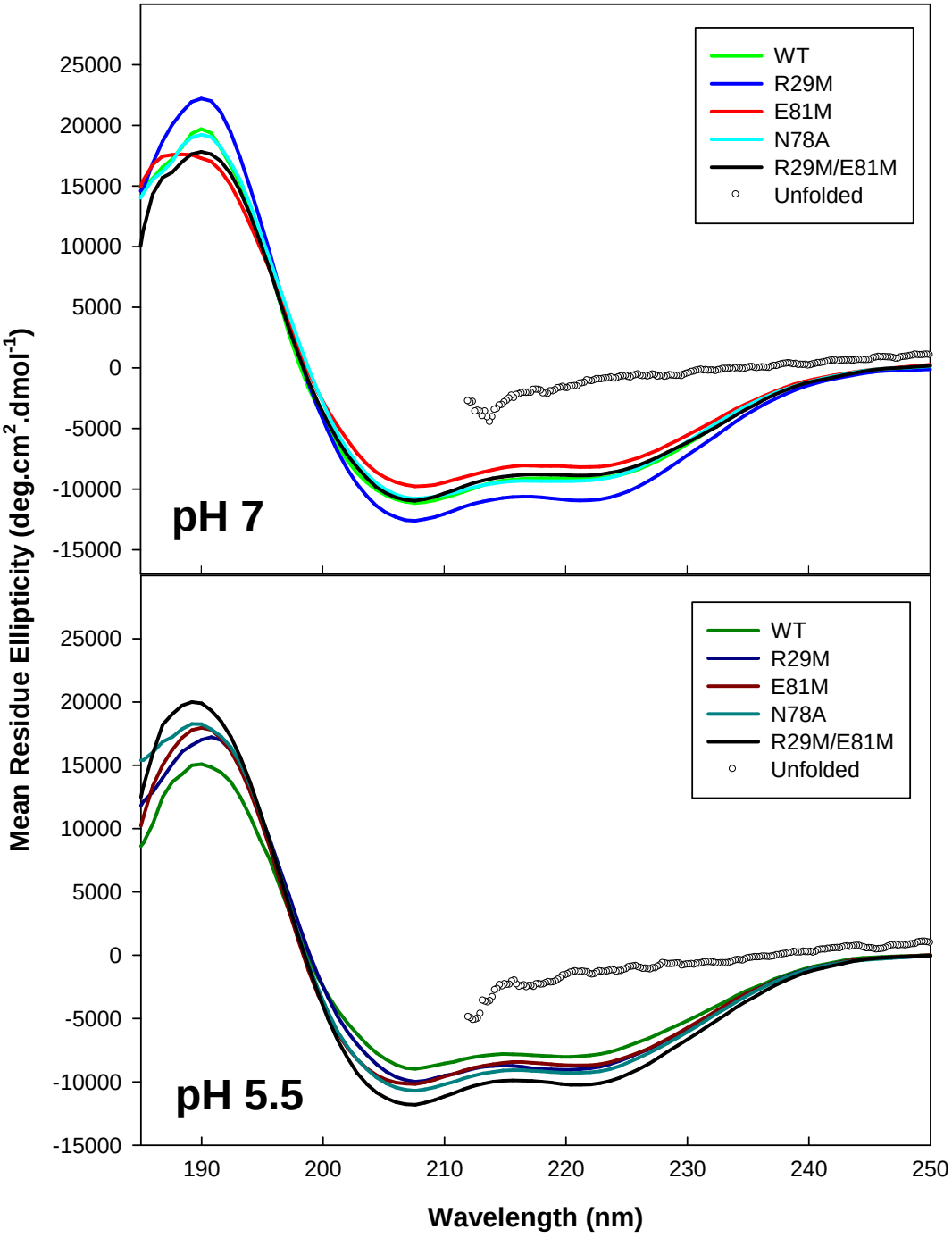


Figure 10: **Far-UV CD spectra of the native CLIC1-WT and mutant proteins at pH 7 and 5.5.**

Spectra of the CLIC1-WT, R29M, E81M, N78A and R29M/E81M proteins are represented by green, blue, red, cyan and black, respectively. A representative of the unfolded proteins in 8 M urea is shown (◦). The spectral analyses were performed at 20 ^{o}C using 2 μM protein at pH 7 (top panel) and 5.5 (bottom panel).

compared to that at pH 7. The CLIC1-E81M and N78A mutants do not show significant changes in secondary structural content. Despite small changes in ellipticity, the crystal structure of the R29M/E81M mutant confirms that there were no significant changes in the secondary structural content owing to the mutations (Appendix).

The secondary structures of the CLIC1-WT and mutant proteins were found to be completely disrupted once unfolded in 8 M urea as shown in Figure 10. The distinctive double minima initially observed for the native conformations were no longer evident.

Close packing of the aromatic functional groups in native protein cores produce near-UV CD spectra which are reliant on the solvent and the immediacy of the other functional groups (Towell and Manning, 1994; Kahn, 1979; Strickland, 1974). The near-UV CD spectra of CLIC1-WT and mutant proteins at pH 7 and pH 5.5 displayed bands at 264 nm, 267 nm and 270 nm (Phe bands), 274 nm and 284 nm (Tyr bands) and a large predominant band at 287 nm, as well as broad band at 297 nm, due to Trp (Figure 11), indicating that each protein has a tightly packed core. The overall similarities of the near-UV CD between the wild type and the mutant CLIC1 proteins indicate that the mutations do not considerably disturb the packing of the proteins.

3.4.2. Fluorescence spectroscopy

CLIC1's single Trp35, within the TMR region, was used as a fluorescence probe to monitor tertiary structural changes at the domain interface. The fluorescence spectra for CLIC1-WT and mutant proteins at pH 7 and pH 5.5 were determined by excitation at 280 nm (Figure 12). The emission maxima of native CLIC1-WT and mutant proteins occur at about 345 nm (Figure 12). This result is consistent with the crystal structure of CLIC1, in that Trp35 is partially exposed to the solvent in its native state (Harrop *et al.*, 2001). The CLIC1- R29M, E81M and R29M/E81M mutants have red wavelength shifts of approximately 2 nm at pH 7. However, this small shift does not appear to be significant suggesting that there were no significant changes in the environment of the Trp35 residue. This result was later confirmed by the crystal structure of R29M/E81M (see Appendix).

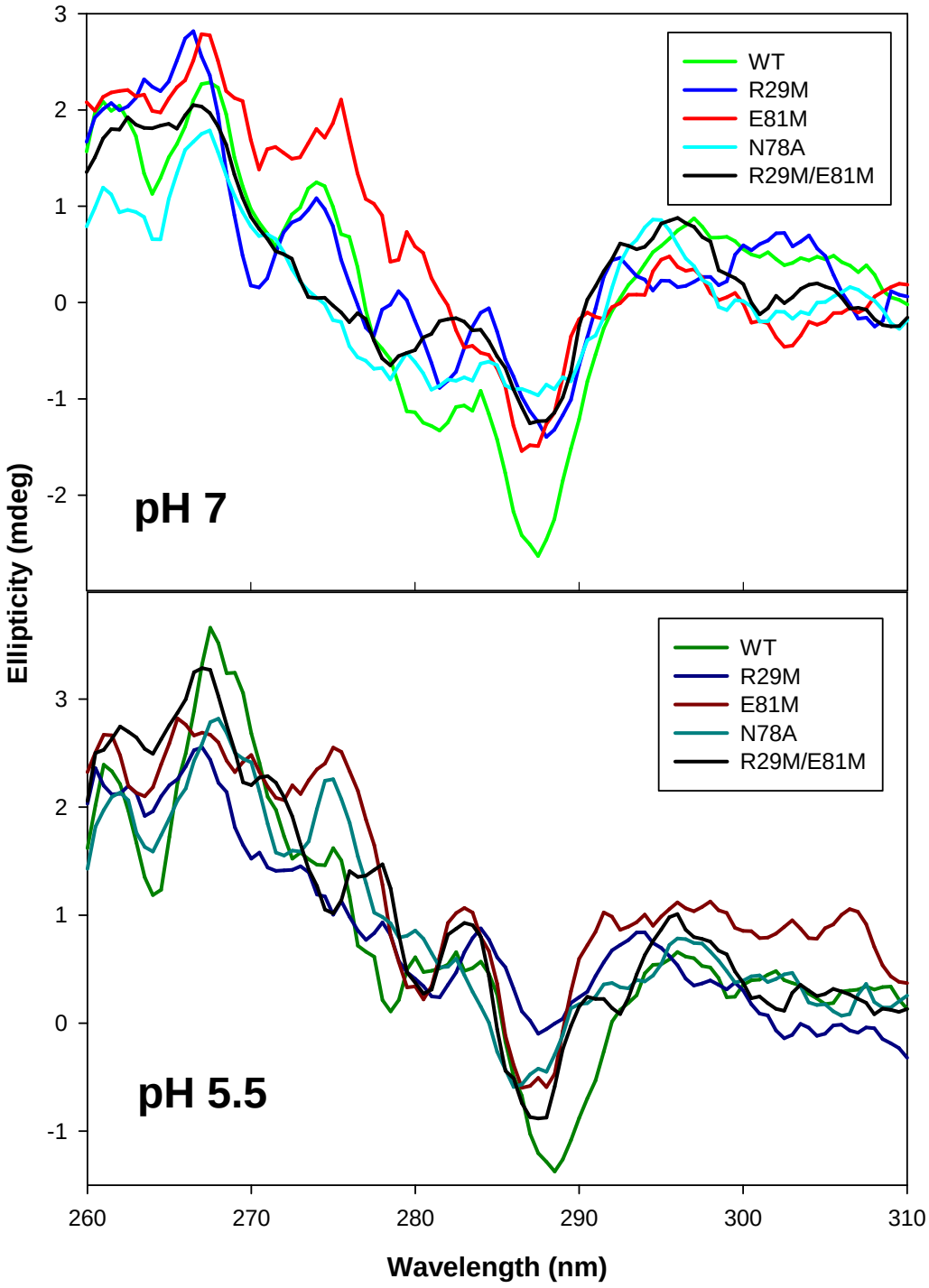


Figure 11: **Near-UV CD spectra of the native CLIC1-WT and mutant proteins at pH 7 and 5.5.**

Spectra of the CLIC1-WT, R29M, E81M, N78A and R29M/E81M proteins represented by green, blue, red, cyan and black, respectively. The spectral analyses were performed at 5 ^{o}C using 40 μM protein at pH 7 (top panel) and 5.5 (bottom panel).

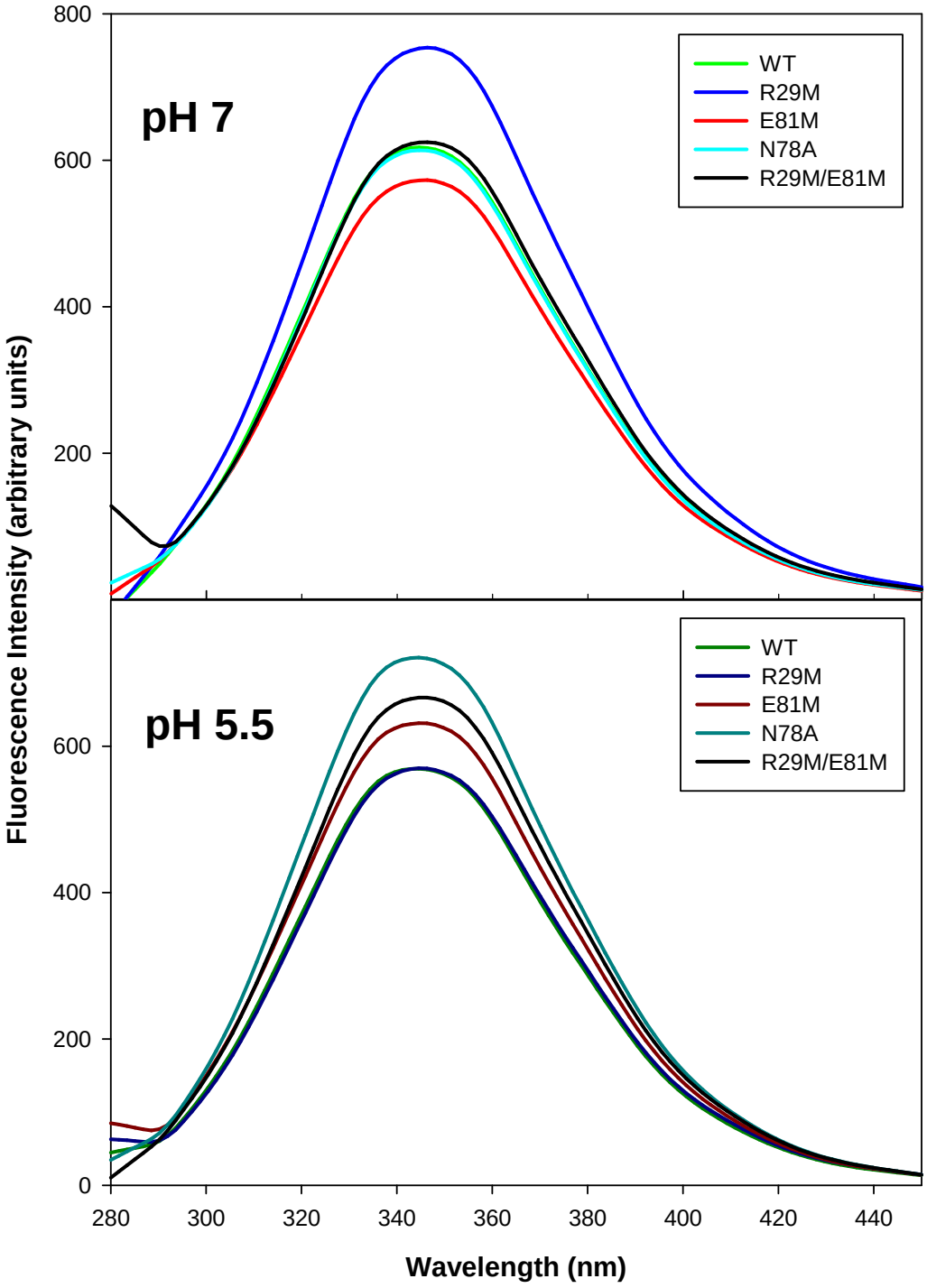


Figure 12: Fluorescence spectra of the native CLIC1-WT and mutant proteins.
The tyrosine and the tryptophan residues were excited at 280 nm. Spectra of the CLIC1-WT, R29M, E81M, N78A and R29M/E81M proteins are represented by green, blue, red, cyan and black, respectively. Maximum emission for all the proteins occurred at 345 nm. The spectral analyses were performed at 20 ^{o}C using 2 μM protein at pH 7 (top panel) and 5.5 (bottom panel).

The fluorescence intensities of the native CLIC1-WT and mutant proteins were also similar. However, at pH 7, a slight increase in fluorescence intensity (approximately 18%) was observed in the emission spectrum of the CLIC1-R29M mutant when compared to that of CLIC1-WT. Changes in the intensity of the other CLIC1 mutants at pH 7 were not considered to be significant as the values were within the range of error of the fluorescence spectrophotometer.

Also, at pH 5.5, slight increases in fluorescence intensities were observed in the emission spectra of all the CLIC1 mutants when compared to CLIC1-WT, but increases above that owing to error were only observed for the CLIC1-R29M and CLIC1-N78A (approximately 21% and 15%, respectively).

Once unfolded in 8 M urea, fluorescence spectra of the CLIC1-WT and mutant proteins at pH 7 and pH 5.5 showed that the emission maximum wavelengths of the proteins were red-shifted from approximately 345 nm to 356 nm (Figure 13). This is indicative of the Trp35 residue becoming exposed to solvent. When the denatured states of the proteins were excited at 280 nm, a small peak appeared at around 310 nm due to Tyr fluorescence. This can be explained by the fluorescence resonance energy transfer from Tyr to Trp becoming disrupted as the Tyr and Trp residues move further apart during the unfolding process (Edelhoch, 1967).

Furthermore, the fluorescence intensity of the denatured CLIC1-WT and mutant proteins decreased substantially, about 60%, compared to the native proteins (Figure 13). This is indicative of the Trp35 residue having moved into a quenching environment as the proteins unfold. Also, during the denaturation process, charged residues such as Arg and Lys may be positioned closer to the Tyr residues and the Trp35 residue than they are in the native folded state of CLIC1. For example, in the native state of CLIC1, Lys37 is positioned away from Trp35. However, once the protein unfolds, Lys37 is positioned adjacent to Trp35, which means that it is able to quench Trp35 fluorescence.

The ability of acrylamide to quench Trp35 fluorescence is a useful way of determining the exposure of Trp35 to the solvent (Figure 14). The K_{sv} values (Table 2) for the CLIC1-WT

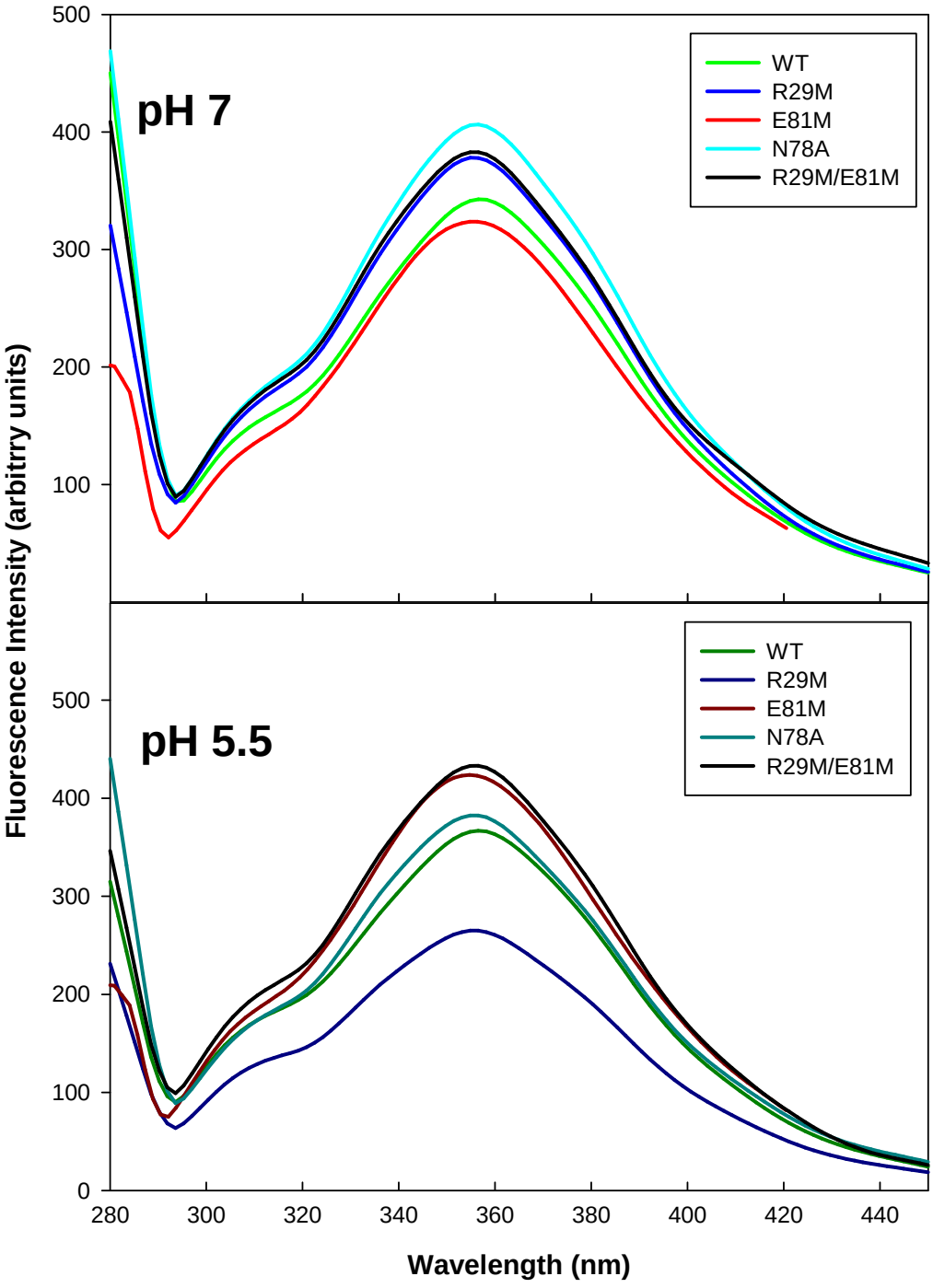


Figure 13: Fluorescence spectra of the unfolded CLIC1-WT and mutant proteins in the presence of 8 M urea.

The tyrosine and the tryptophan residues were excited at 280 nm. Spectra of the CLIC1-WT, R29M, E81M, N78A and R29M/E81M proteins are represented by green, blue, red, cyan and black, respectively. Maximum emission occurred at approximately 356 nm. The spectral analyses were performed at 20 ^{o}C using 2 μM protein at pH 7 (top panel) and 5.5 (bottom panel).

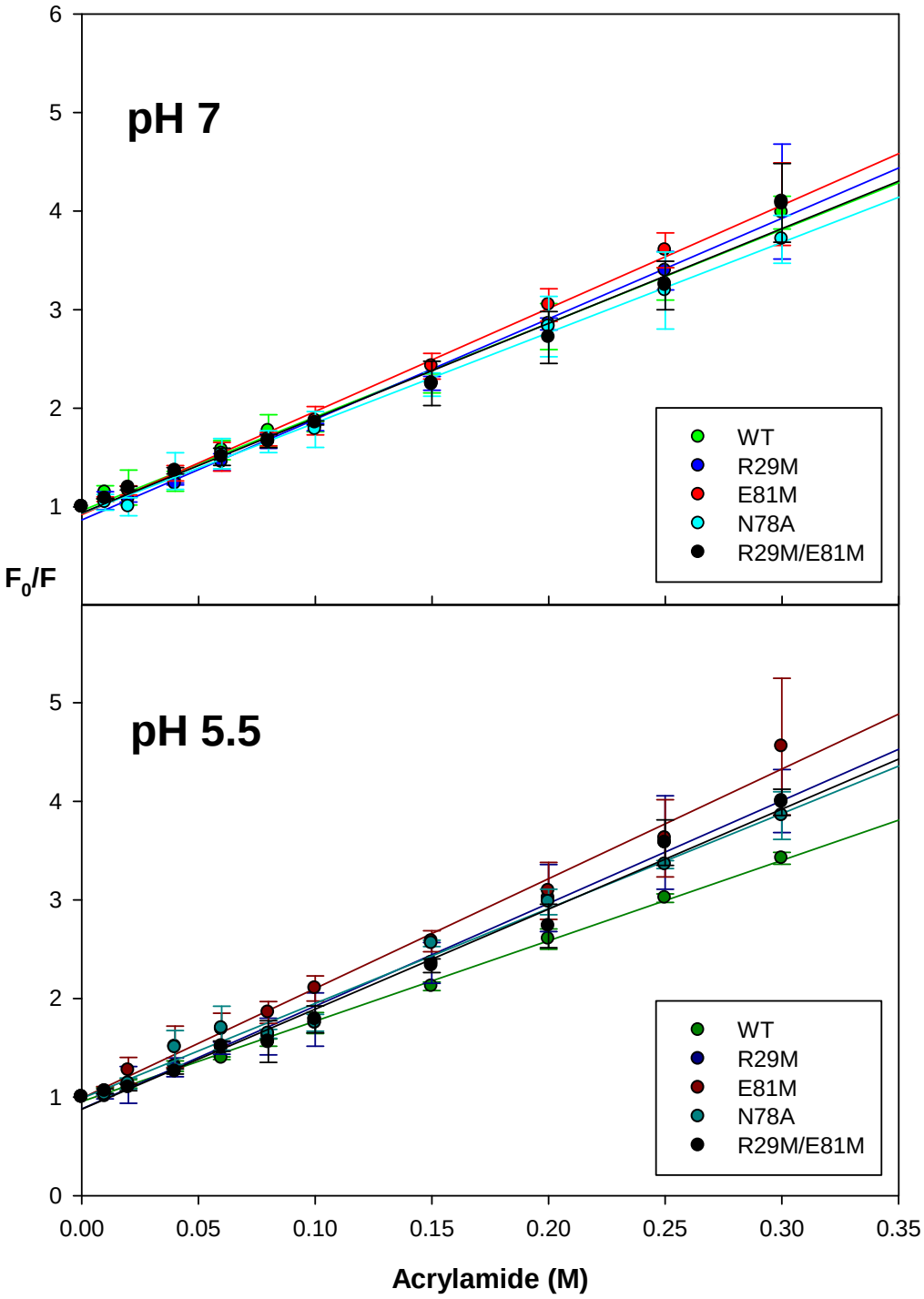


Figure 14: Stern-Volmer plots of the native CLIC1-WT and mutant proteins
F_o and F are the fluorescence intensities in the absence and the presence of acrylamide, respectively. Data for the CLIC1-WT, R29M, E81M, N78A and R29M/E81M proteins are represented by green, blue, red, cyan and black symbols, respectively. The experimental conditions were 20 ^oC and 2 μM protein. pH 7 (top panel) and 5.5 (bottom panel).

Table 2: K_{sv} values for the quenching of fluorescence by acrylamide

pH 7		
CLIC1	**K_{sv}**	**R^2**
WT	9.5 +/- 0.3	0.98
R29M	10.2 +/- 0.3	0.97
E81M	10.5 +/- 0.3	0.98
N78A	9.2 +/- 0.3	0.96
R29M/E81M	9.6 +/- 0.3	0.96

pH 5.5		
CLIC1	**K_{sv}**	**R^2**
WT	8.2 +/- 0.1	0.99
R29M	10.4 +/- 0.4	0.96
E81M	11.1 +/- 0.5	0.95
N78A	9.6 +/- 0.3	0.98
R29M/E81M	10.1 +/- 0.3	0.98

and mutant proteins were relatively high, which is consistent with a protein with a partially exposed Trp residue(s) (Eftink and Ghiron, 1976**)**. The K_{sv} values were similar to each other at both experimental pH values. Also, the values for the CLIC1 mutant proteins were similar to that of CLIC1-WT at both experimental pH values (Table 2). Therefore, it can be said that the acrylamide quenching of the CLIC1-WT and mutant proteins shows that the mutations do not appear to significantly alter the exposure of the Trp35 residue to the solvent.

3.5. Conformational stability of the CLIC1-WT and mutant proteins

3.5.1. Recovery

To define the thermodynamic parameters ($\Delta G(H_2O)$ and the *m*-value) of equilibrium unfolding, the unfolding process must be shown to attain equilibrium (Pace, 1986). This requires one to show that the native state is able to be recovered once the protein has been unfolded. CLIC1-WT and mutant proteins were unfolded in the presence of 8 M urea. The protein solutions were then diluted 10 fold with CLIC1 storage buffer. This was necessary to allow recovery of the native state. Far-UV CD spectroscopy produced poor signal-to-noise ratios, owing to the low concentrations of protein used, and therefore, only fluorescence spectroscopy could be used as a probe to reliably measure the recovery of the native state of the proteins.

The percentage recoveries reported in Table 3 show that the unfolding events of the CLIC1-WT and mutant proteins are reversible. In light of this, equilibrium unfolding studies were undertaken in order to establish the thermodynamic parameters of equilibrium unfolding.

3.5.2. Urea-induced equilibrium unfolding

Intrinsic fluorescence and far-UV CD spectroscopy were used to monitor the unfolding of the CLIC1-WT and mutant proteins (section 2.2.7 and 2.2.8). Proteins at a concentration of 2 μM were unfolded in 0-8 M urea at 20 ºC and allowed to achieve equilibrium over a period of 16 hours. This was done at both pH 7 and pH 5.5.

The unfolding data were plotted by overlaying the curves obtained by far-UV CD and fluorescence spectroscopy. The unfolding curves for each protein are shown in Figure 15. It

Table 3: **Percentage recoveries of the native folds of the CLIC1-WT and mutant proteins**

CLIC1	Fluorescence Intensity at 345 nm (native)	Fluorescence Intensity at 345 nm (refolded)	% Recovery
WT pH 7	248.7	248.3	99.8
WT pH 5.5	270.3	290.5	107.4
R29M pH 7	266.7	264.6	99.2
R29M pH 5.5	245.9	284.9	115.9
E81M pH 7	251.8	281.8	111.9
E81M pH 5.5	289	261.3	90.4
N78A pH 7	292.6	295.9	101.2
N78A pH 5.5	258.6	301.8	116.7
R29M/E81M pH 7	254.5	260.4	102.3
R29M/E81M pH 5.5	327.1	308.4	94.3

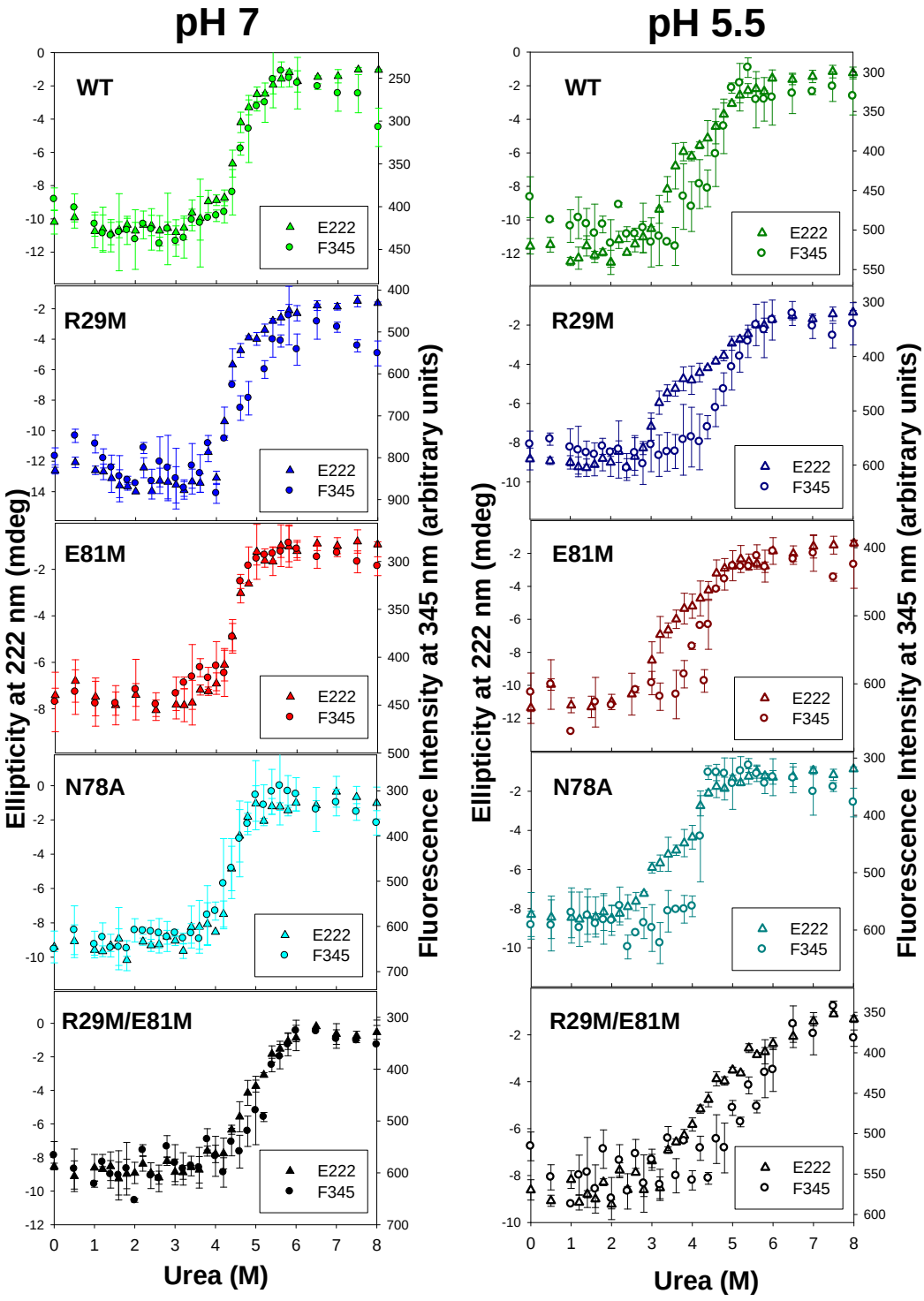


Figure 15: **Urea-induced equilibrium unfolding of CLIC1-WT and mutant proteins monitored by far-UV CD and fluorescence spectroscopy.**

The unfolding curves for the CLIC1-WT, R29M, E81M, N78A and R29M/E81M proteins are represented by green, blue, red, cyan and black symbols, respectively. Studies conducted at pH 7 (light, full symbols) and pH 5.5 (dark, open symbols) are represented on the left and right hand side of the page, respectively. Experiments were conducted at 20 ^{o}C using 2 μM protein.

is evident that the unfolding curves of CLIC1-WT, E81M and N78A mutants, at pH 7, are single sigmoidal curves. The far-UV CD and fluorescence data superimpose throughout the transition and the slopes of the curves show that the loss of secondary structure and the tertiary environment of Trp35 occur simultaneously. However, the unfolding data monitored by far UV-CD and fluorescence spectroscopy for CLIC1-R29M and CLIC1-R29M/E81M at pH 7 are not superimposable (Figure 15). The two individual data sets for CLIC1-R29M and CLIC1-R29M/E81M separate within the transition region between 3 and 6 M urea, suggesting the formation of intermediate species during unfolding.

The far-UV CD and fluorescence unfolding data of the individual proteins, monitored at pH 5.5, are not single sigmoidals. The far-UV CD and fluorescence unfolding data of the individual proteins were also not superimposable. The transition regions of the pH 5.5 unfolding data are broader compared to the transition regions of the unfolding data at pH 7. Also, the transition regions, at pH 5.5, are shifted to lower urea concentrations compared to the transition regions at pH 7. The slopes of the transition curves at pH 5.5 show that the loss of secondary structure and the environment of Trp35 have reduced cooperativity when compared to the slopes of the transition curves at pH 7. The results obtained for the urea-induced equilibrium unfolding at pH 5.5, therefore, suggests that significant populations of intermediate species are present at pH 5.5 (Soulages, 1998).

Furthermore, using intrinsic fluorescence as a probe, plots of the maximum emission wavelength were constructed as a function of the urea concentration (Figure 16). Representing the fluorescence data in this way is independent of the fluorescence intensity, but may be used to identify wavelength shifts associated with the presence of an intermediate species. During urea-induced unfolding the CLIC1-WT, E81M, and N78A proteins at pH 7 undergo red wavelength shifts. This is consistent with the proteins undergoing a transition from the native folded state to a denatured unfolded state that is, N ↔ U. However, it is evident from the maximum emission wavelength plots at pH 7, that blue wavelength shifts occur for the CLIC1-R29M and R29M/E81M mutants between 3.5 and 5.75 M urea (Figure 16). This shows that intermediate species are significantly populated between 3.5 and 5.75 M urea for the CLIC1-R29M and R29M/E81M mutant proteins. This is consistent with the proteins undergoing a transition from the native folded state to an intermediate state (blue

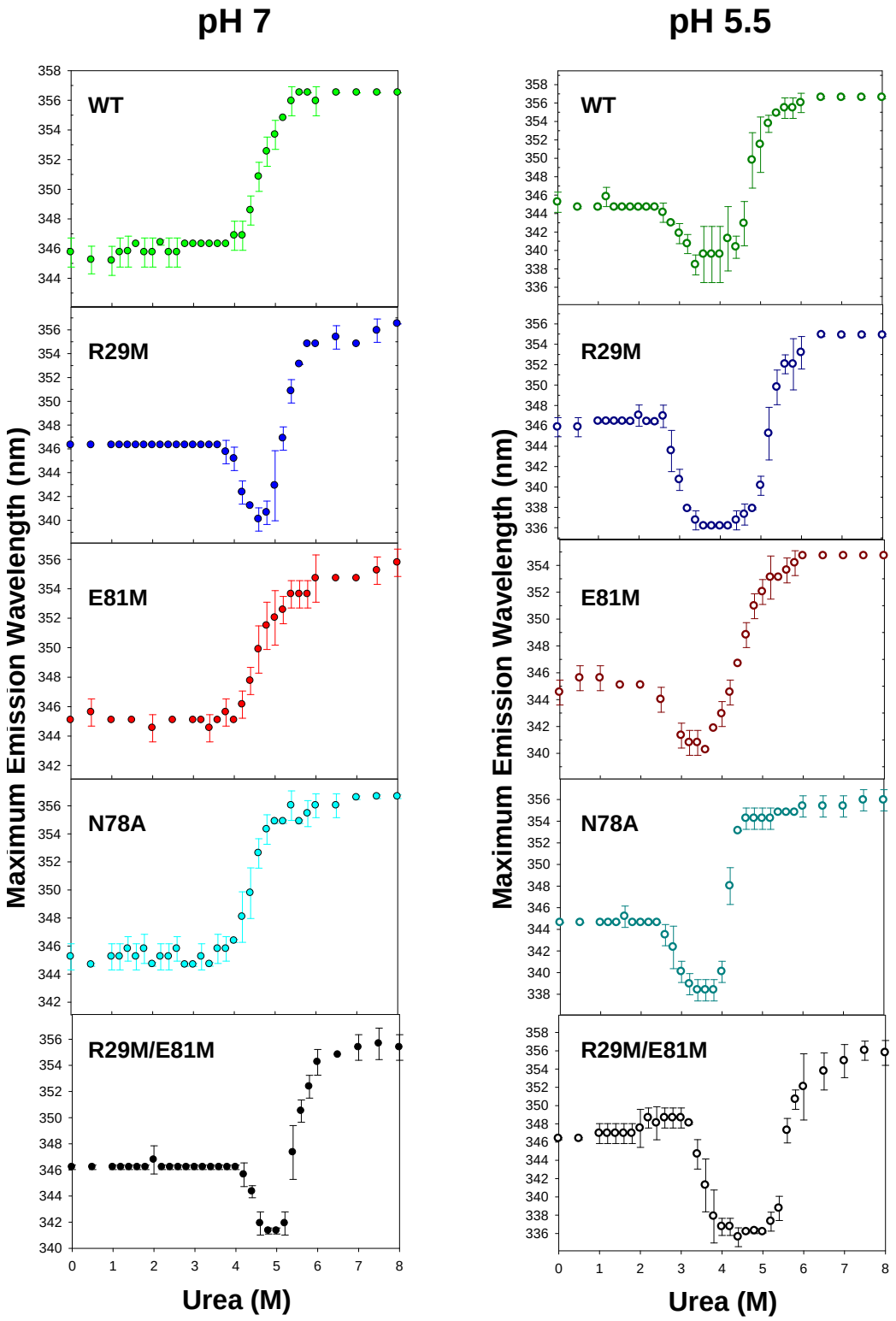


Figure 16: Maximum emission wavelengths of CLIC1-WT and mutant proteins.
The data points for the CLIC1-WT, R29M, E81M, N78A and R29M/E81M proteins are represented by green, blue, red, cyan and black symbols, respectively. Studies conducted at pH 7 (closed symbols) and pH 5.5 (open symbols) are represented on the left and right hand side of the page, respectively. Experiments were conducted at 20 ^{o}C with 2 μM protein at pH 7 and pH 5.5.

wavelength shift) and finally to a denatured unfolded state (red wavelength shift) that is, N ↔ I ↔ U. When the maximum emission wavelengths for the CLIC1-WT and mutant proteins unfolding curves at pH 5.5 were plotted all the proteins displayed blue wavelength shifts from 2.75 to 6 M urea (Figure 16). Blue wavelength shifts are also indicative of Trp35 moving into a more hydrophobic environment. The CLIC1-WT and mutant proteins spectra did not show any significant increase in the Rayleigh scatter along the entire unfolding transition at both pH values (Figure 17) indicating the absence of protein aggregation.

3.5.3. Fitting of equilibrium unfolding data

Criteria have been established in order for a protein to be considered to undergo a two-state unfolding transition (Whitten and Garcia-Moreno, 2000). Namely: (1) the proteins must have identical $\Delta G(H_2O)$ values when monitored by different probes, (2) the quality of the two-state fits to the data must be good, (3) the far-UV CD and fluorescence unfolding curves for the proteins must be superimposable, and (4) the shape of the unfolding curves must be single sigmoidal. Furthermore, as mentioned in section 2.2.8.1.1, if the probes used to observe the unfolding events fail to differentiate between the intermediate and unfolded states, the presence of intermediate states can be assumed if the unfolding curves shift to a lower concentration of denaturant and if there is a concomitant decrease in the gradient of the transition region of the unfolding curve (Soulages, 1998).

In addition to the criteria set out by Whitten and Garcia-Moreno (2000) and Soulages (1998), it should be mentioned that the fluorescence spectra of proteins that undergo two-state unfolding transitions display only red fluorescence wavelength shifts when they go from the folded to the unfolded state (N ↔ U).

3.5.3.1. Two-state unfolding model

Since the pH 7 data for CLIC1-WT, E81M and N78A comply with the conditions outlined for a two-state model (section 3.5.3) and the proteins displayed only red wavelength shifts during unfolding (Figure 16), the intrinsic fluorescence intensities at 310 nm (F310), 320 nm (F320), 330 nm (F330) and 345 nm (F345), as well as the ellipticity at 222 nm (E222) were globally fit to a two-state monomer model (N ↔ U) (Beecham, 1992), as described in

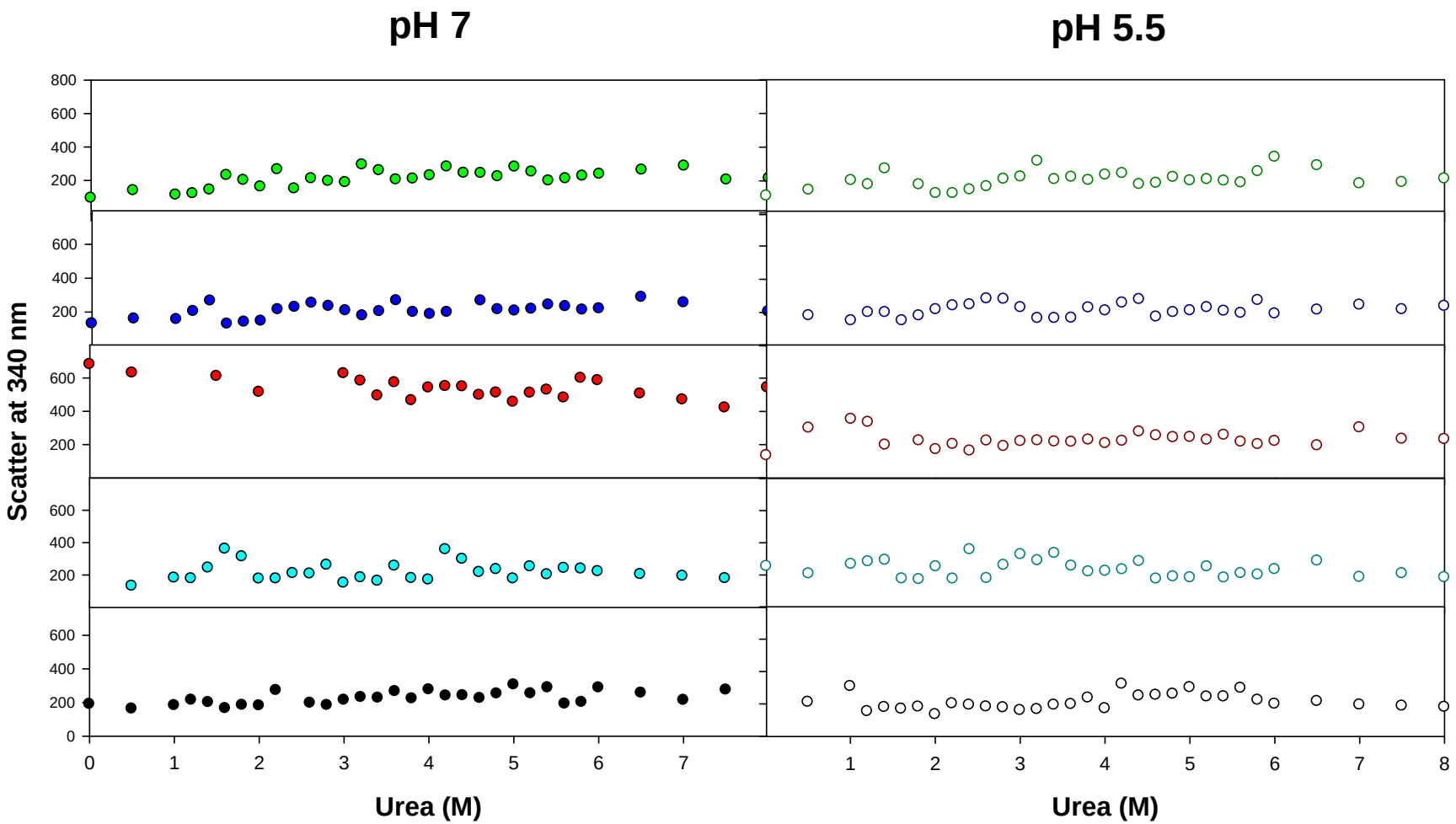


Figure 17: Rayleigh scatter measured during urea-induced equilibrium unfolding.
The data points for the CLIC1-WT, R29M, E81M, N78A and R29M/E81M proteins are represented by green, blue, red, cyan and black symbols, respectively. Studies conducted at pH 7 (light, closed symbols) and pH 5.5 (dark, open symbols) are represented on the left and right hand side of the page, respectively. Experiments were conducted at 20 ^{o}C. The excitation and emission wavelengths used were 340 nm.

2.2.8.1.1 and 2.2.8.1.2 (Figure 18). By combining together multiple sets of data using different probes the resolution of the model used to fit the data is better resolved (Beechem, 1992). Residual plots for the fits of the data are shown in Figure 19. The χ^2 statistic is a function that advances to unity when the data is correctly weighted and the fits are good. This statistic will increase in value as the data fit becomes poorer (Beechem, 1992). The $\Delta G(H_2O)$ and *m*-value for CLIC1-WT obtained from the global fitting procedure were similar to those previously reported by Fanucchi *et al.* (2008), that is a $\Delta G(H_2O)$ value of 9.5 +/- 0.6 kcal.mol^{-1} and an *m*-value of 2.0 +/- 0.1 kcal.mol^{-1}(M urea)$^{-1}$.

The CLIC1-N78A mutants' $\Delta G(H_2O)$ and *m*-value are similar to that of CLIC1-WT at pH 7 (Table 4). Therefore, it appears that this mutation does not appear to impact upon the conformational stability and cooperativity of CLIC1 at pH 7.

The thermodynamic parameters ΔG_{nu} and m_{nu}, generated by the global fitting of the E81M mutants unfolding data at pH 7 were increased relative to those of CLIC1-WT (Table 4). This indicates that the CLIC1-E81M mutation appears to have caused an increase in the conformational stability of CLIC1 as well as its cooperativity. The increase in the m_{nu} value is consistent with an increase in the accessibility to denaturant that may be caused by an expansion of the denatured state of the mutant protein.

3.5.3.2. Three-state unfolding model

CLIC1-WT has been previously shown to follow a three-state unfolding transition at pH 5.5 (Fanucchi *et al.*, 2008). CLIC1-WT and mutant proteins at pH 5.5, and the R29M and R29M/E81M mutants at pH 7 do not conform to the criteria stipulated for a two-state unfolding transition (Whitten and Garcia-Moreno, 2000). For example, the proteins do not have identical $\Delta G(H_2O)$ values when monitored by different probes, the quality of the two-state fits to the data were not good, the far-UV CD and fluorescence unfolding curves for the individual proteins were not superimposable (Figure 15), and lastly, the shape of the unfolding curves were not single sigmoidal. Also, blue fluorescence wavelength shifts were observed during unfolding (Figure 16). In light of these findings, a three-state unfolding transition model was used for global analyses of the unfolding events of CLIC1-WT and mutant proteins at pH 5.5 and for the CLIC1-R29M and CLIC1-R29M/E81M mutants at

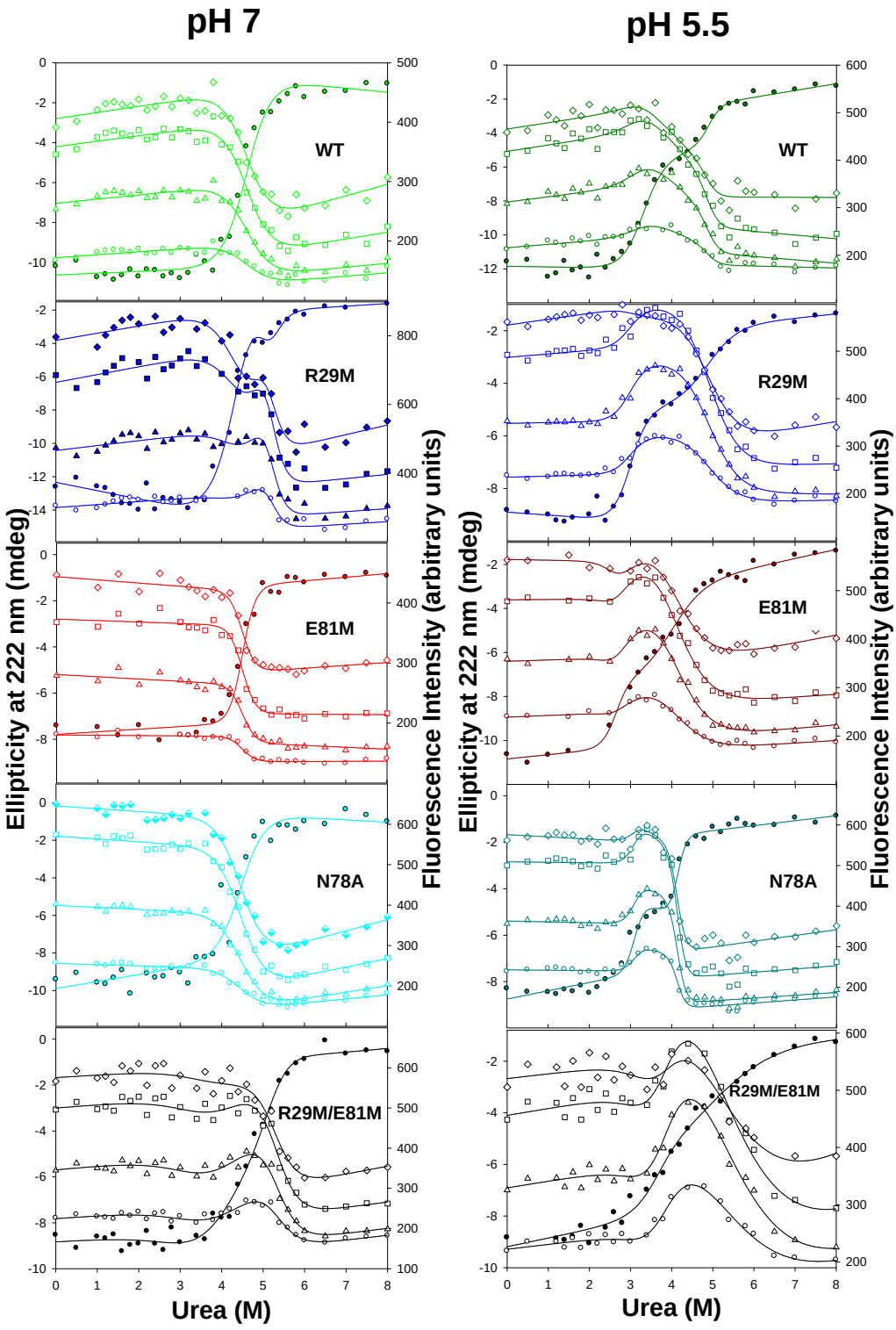


Figure 18: Global fitting of unfolding data obtained at pH 7 and pH 5.5

The data points for the CLIC1-WT, R29M, E81M, N78A and R29M/E81M proteins are represented by green, blue, red, cyan and black symbols, respectively. The ellipticity at 222 nm is represented by ● and the fluorescence intensities F310 ○, F320 Δ, F330 □ and F345 ◊. Lines through the data represent the global fits.

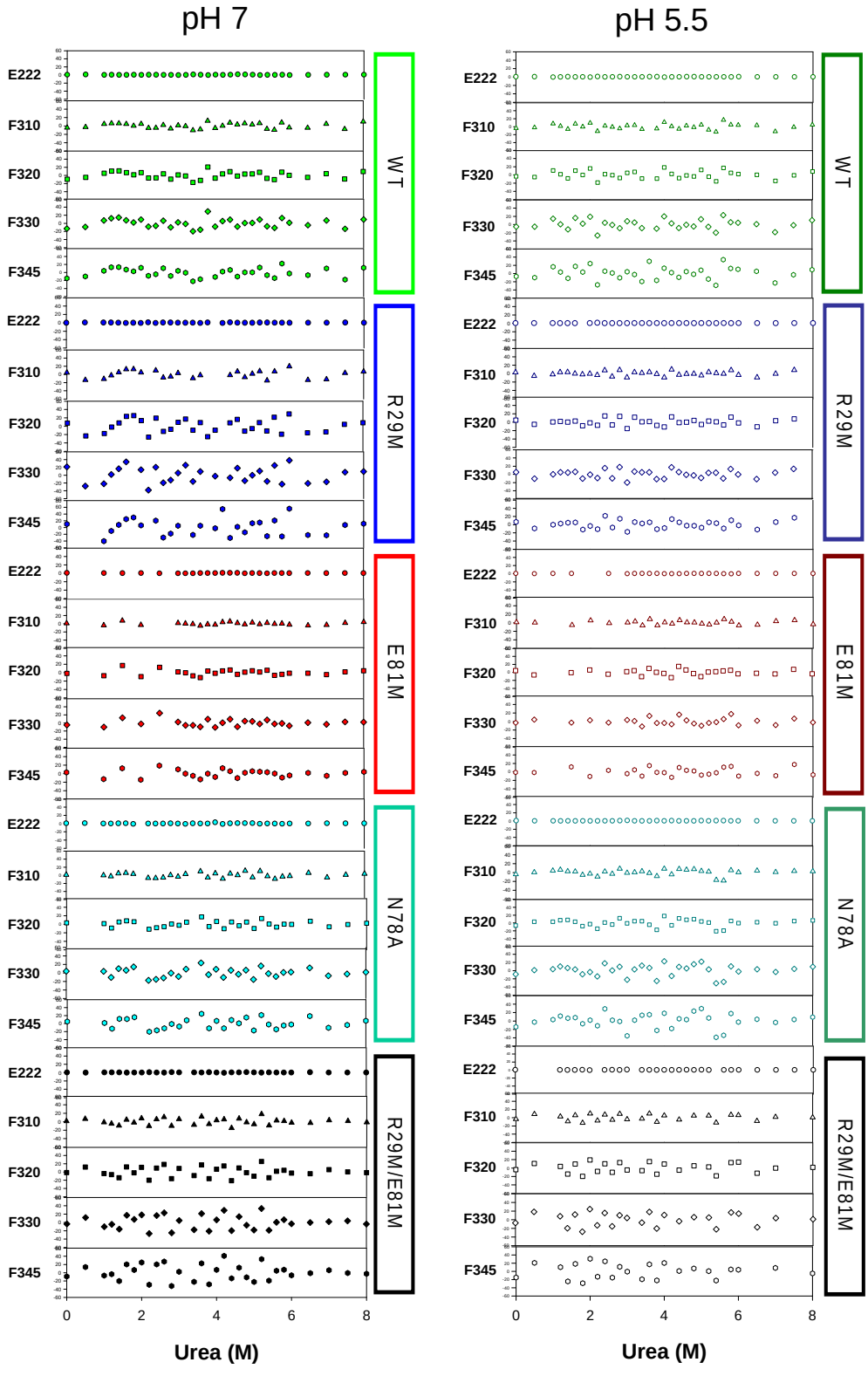


Figure 19: Residual plots of the globally-fitted data.

The CLIC1-WT, R29M, E81M, N78A and R29M/E81M fluorescence and CD residuals measured at pH 7 (left panel) and pH 5.5 (right panel) are represented by green, blue, red, cyan and black symbols, respectively.

Table 4: Thermodynamic parameters and statistical data from global fitting

CLIC1 pH 7 (2-state)	ΔG_{nu} (kcal.mol^{-1})	m_{nu} (kcal.mol^{-1}(M urea)$^{-1}$)	Reduced χ^2	Goodness of Fit
WT	9.2 +/- 0.7	2.0 +/- 0.1	0.35	1
E81M	16.8 +/- 1.5	3.7 +/- 0.3	0.17	1
N78A	9.0 +/- 0.5	2.0 +/- 0.1	0.34	1

CLIC1 pH 7 (3-state)	ΔG_{ni} (kcal.mol^{-1})	m_{ni} (kcal.mol^{-1}(M urea)$^{-1}$)	ΔG_{iu} (kcal.mol^{-1})	m_{iu} (kcal.mol^{-1}(M urea)$^{-1}$)	Reduced χ^2	Goodness of Fit
R29M	9.1 +/- 1.5	2.0 +/- 0.4	19.6 +/- 3.6	3.7 +/- 0.7	0.7	1
R29M/E81M	4.3 +/- 1.6	1.2 +/- 0.5	11.6 +/- 1.6	2.2 +/- 0.3	0.49	1

CLIC1 pH 5.5 (3-state)	ΔG_{ni} (kcal.mol^{-1})	m_{ni} (kcal.mol^{-1}(M urea)$^{-1}$)	ΔG_{iu} (kcal.mol^{-1})	m_{iu} (kcal.mol^{-1}(M urea)$^{-1}$)	Reduced χ^2	Goodness of Fit
WT	7.5 +/- 2.2	2.3 +/- 0.7	18.8 +/- 5.5	3.8 +/- 1.1	0.41	1
R29M	8.3 +/- 1.4	2.8 +/- 0.5	7.8 +/- 0.7	1.6 +/- 0.1	0.18	1
E81M	8.9 +/- 4.9	3.3 +/- 1.9	5.8 +/- 0.5	1.5 +/- 0.1	0.16	1
N78A	14.6 +/- 5.4	4.7 +/- 1.8	23.2 +/- 3.1	5.6 +/- 0.7	0.51	1
R29M/E81M	7.0 +/- 1.9	1.8 +/- 0.6	3.2 +/- 2.1	0.7 +/- 0.3	0.44	1

The subscripts nu, ni and iu refer to native-to-unfolded, native-to-intermediate and intermediate-to-unfolded transitions of the proteins, respectively.

pH 7. The intrinsic fluorescence intensity data at various wavelengths as well as the ellipticity at 222 nm data were thus fitted accordingly (Figure 18). Residual plots for the fits of the data are shown in Figure 19.

The CLIC1-R29M and R29M/E81M mutants at pH 7 seem to mimic the behaviour of CLIC1-WT at pH 5.5 in that they unfold via a three-state transition with a highly populated and energetically favourable intermediate species (Figures 16 and 18). The impact of these mutations on the CLIC1 protein at pH 7 is a loss in the cooperativity of unfolding of the proteins, that is, the proteins no longer follow a two-state unfolding transition from N ↔ U at pH 7.

The $\Delta G(H_2O)$ and *m*-value of N78A mutant for the N ↔ I and I ↔ U transitions are comparable to those of CLIC1-WT at pH 5.5 (considering the standard error). Once again, as also observed at pH 7, Asn78 does not seem to be essential for the maintenance of the conformational stability of soluble CLIC1 as it does not appear to perturb the thermodynamic parameters of equilibrium unfolding.

The $\Delta G(H_2O)$ and *m*-values of the R29M, E81M and R29M/E81M mutants for the N ↔ I transition are similar to those of CLIC1-WT at pH 5.5. However, diminished $\Delta G(H_2O)$ and *m*-values for the I ↔ U transitions for the R29M, E81M and R29M/E81M mutants indicate that their intermediate species at pH 5.5 are energetically less stable than that for the WT at pH 5.5 (Table 4). Reduced *m*-values indicate a loss of cooperativity (slope of unfolding transitions). Therefore, the CLIC1-R29M, E81M and R29M/E81M mutations appear to negatively impact upon the conformational stability of the CLIC1 intermediate at pH 5.5.

3.6. ANS binding

ANS is an anionic dye that binds to hydrophobic surfaces of proteins through its hydrophobic aniline naphthalene group (Figure 20) (Semisotnov *et al.*, 1991). Thus, ANS was used as a

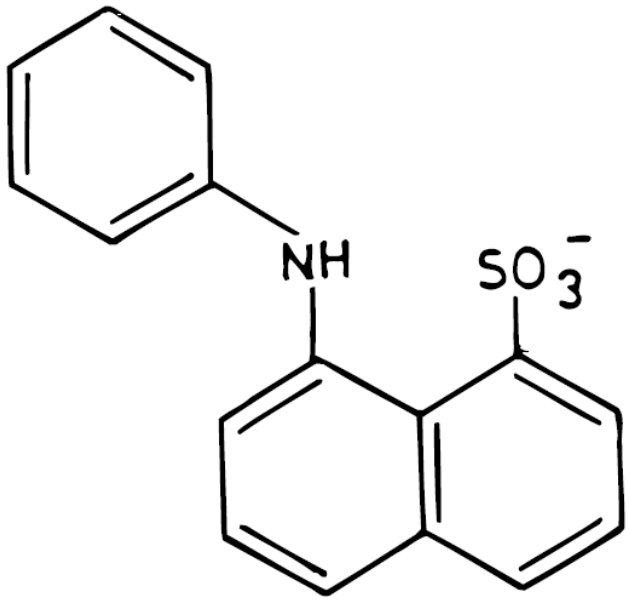


Figure 20: Chemical structure of 1-anilinonaphthalene-8-sulfonate (ANS).

probe to detect the intermediate species that become populated during the urea-induced equilibrium unfolding of CLIC1-WT and mutant proteins. In the absence of protein, free ANS in water was observed to have an emission maximum at 530 nm. Upon binding of the ANS to the intermediate species of CLIC1-WT and mutant proteins, blue wavelength shifts in the emission maximum to 470 nm were observed. The emission at 470 nm was plotted as a function of urea concentration. The fits through the data were done using a 4 parameter Gaussian fit in SigmaPlot® v11.0. This was done in order to more easily define the ANS binding peaks.

No significant binding of ANS was observed along the unfolding curves for the CLIC1-WT, CLIC1-E81M and CLIC1-N78A mutants (Figure 21). However, the R29M and R29M/E81M mutants displayed ANS binding peaks that were not due to protein aggregation (Figure 22).

The ANS binding observed in the transition region of urea-induced unfolding for CLIC1-R29M and R29M/E81M at pH 7 compared well with the data shown in Figure 16 in that ANS was observed to bind at urea concentrations ranging from 2-6.25 M and these regions of unfolding displayed blue fluorescence wavelength shifts. CLIC1-R29M showed ANS binding between 3.5 and 5.75 M urea and CLIC1-R29M/E81M bound ANS between 3.75 M and 6 M urea. This data strongly supported the blue-shifted fluorescence wavelengths observed for the two mutant proteins at pH 7 (Figure 16).

Fanucchi *et al*. (2008) reported that ANS binds to CLIC1-WT at pH 5.5 between 3 M and 4.8 M urea. In this study, CLIC1-WT, R29M, E81M, N78A and R29M/E81M mutant proteins bind ANS between 2-5.5 M, 2-5.5 M, 1.5-6 M, 2.5-4.75 M and 2.5-6.25 M urea, respectively. The blue fluorescence wavelength shifts observed during urea-induced unfolding at pH 5.5, represented in Figure 16 compare well with the ANS binding observed during urea-induced unfolding at pH 5.5. Fluorescence properties of ANS do not change in the pH range 2-11 (Freedom and Radda, 1969). This is because the pK of the sulfonate group of ANS lies between 0 and 1 (Flanagan and Hesketh, 1973). Therefore, the results obtained here are not likely due to any effect of pH on ANS itself. ANS binding during unfolding suggests the formation of an intermediate which is consistent with a three-state model. Therefore, it can be

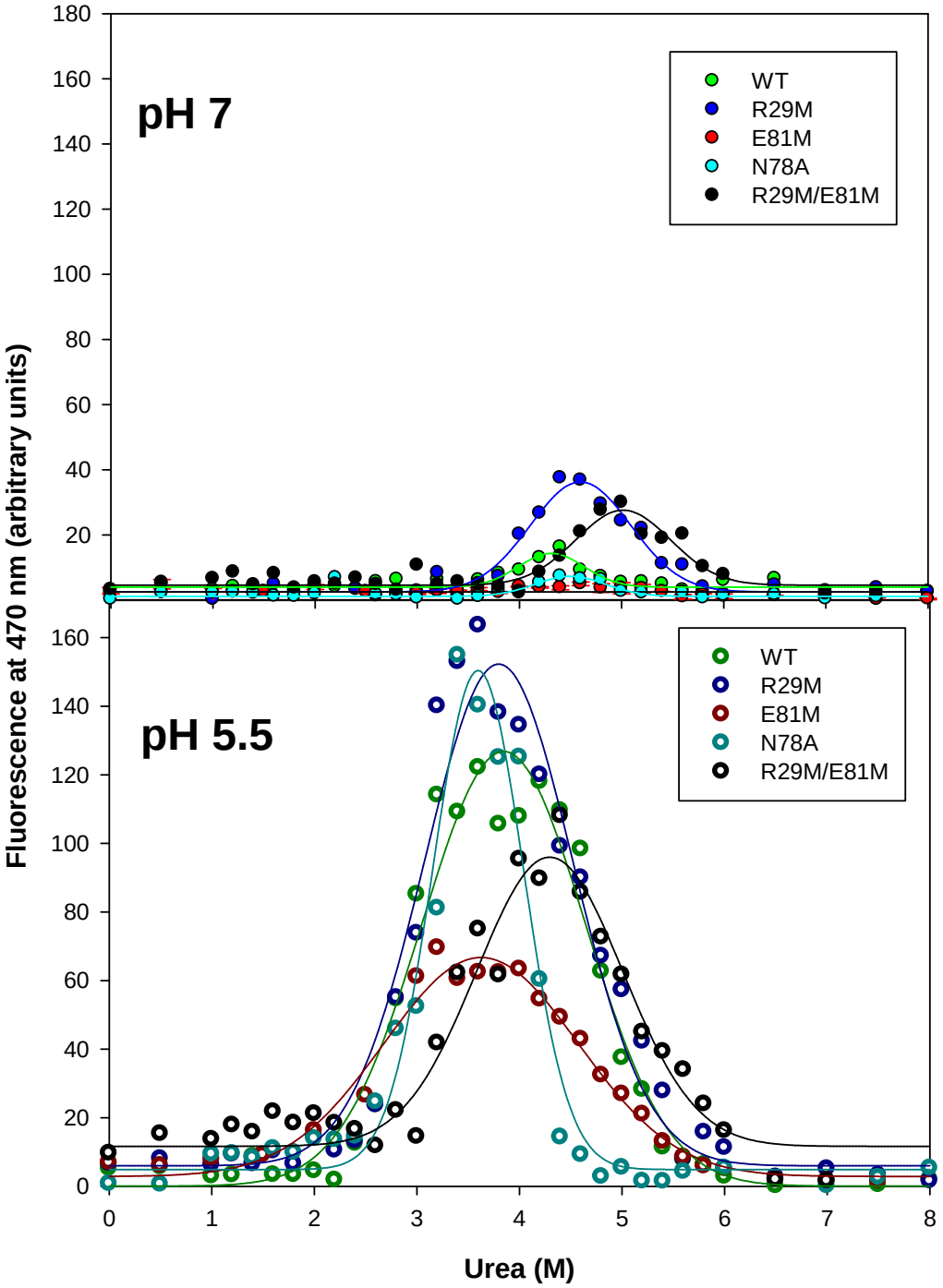


Figure 21: ANS binding during unfolding.

Binding of 200 μM ANS (closed and open spheres) are represented as a function of urea. The lines through the data provide an easy means to distinguish each of the ANS binding profiles. The data are an average of three separate experiments and were corrected for the contribution due to free ANS in buffer. The experimental conditions were 20 ^{o}C and 2 μM protein. pH 7 (top panel) and 5.5 (bottom panel).

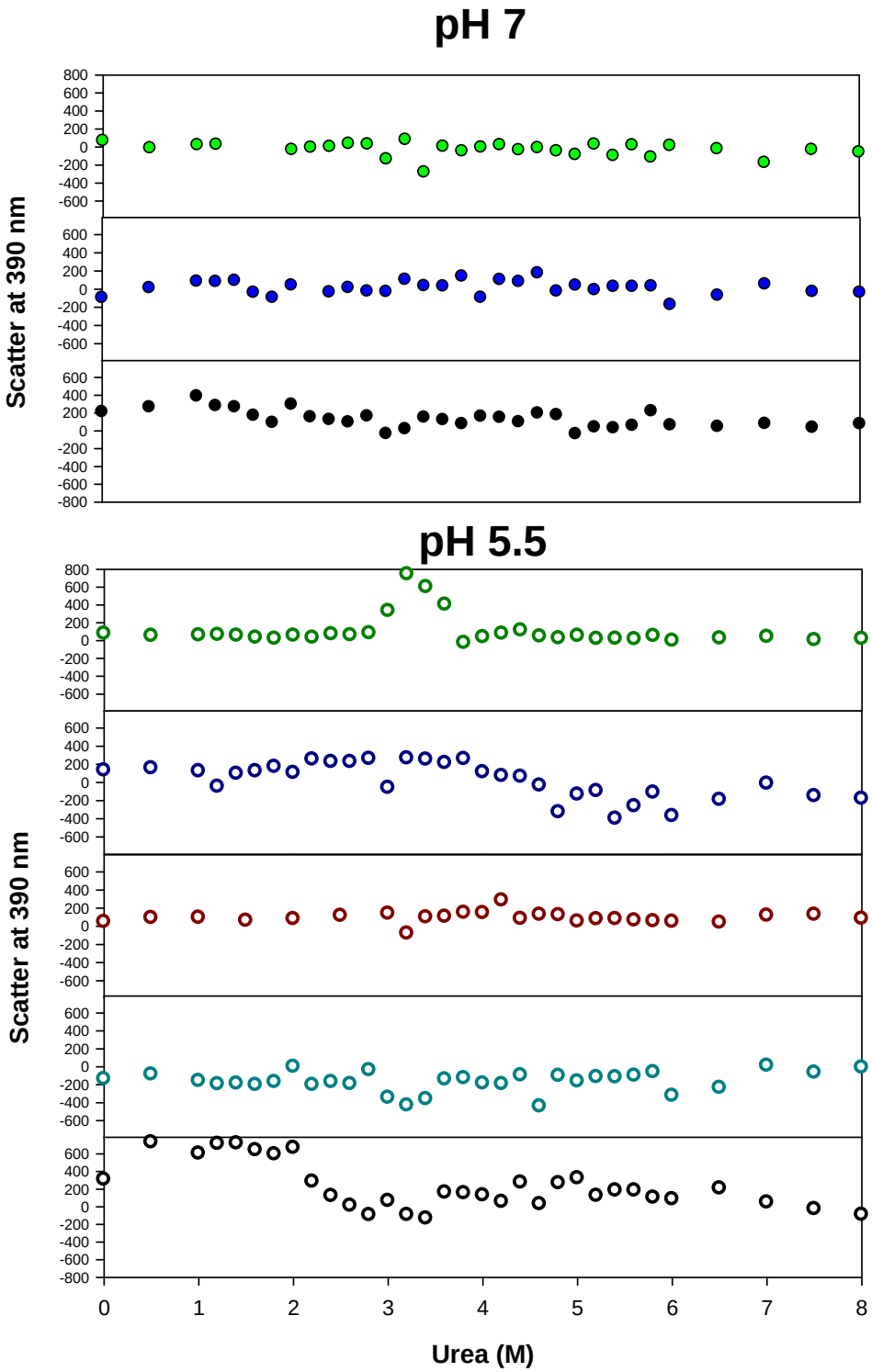


Figure 22: Rayleigh scatter plots for unfolding in the presence of ANS.

The data points of the CLIC1-WT, R29M, E81M, N78A and R29M/E81M mutant proteins are represented by green, blue, red, cyan and black symbols, respectively. Studies were conducted at pH 7 (light, full symbols) and pH 5.5 (dark, hollow symbols), respectively. Experiments were conducted at 20 ^{o}C using 2 μM. The excitation and emission wavelength used was 390 nm.

concluded that all the CLIC1 mutants at pH 5.5 and the CLIC1-R29M and R29M/E81M mutants at pH 7 unfold via a three-state transition with a well populated intermediate species.

Rayleigh scatter was used to monitor protein aggregation during urea-induced unfolding (Figure 22). No significant increase in the Rayleigh scatter measured was observed during unfolding of either CLIC1-WT or mutant proteins.

3.7. Properties of unfolding intermediate

The intermediate species of the CLIC1-WT and mutant proteins are most populated between 3.2 and 5.2 M urea (Figure 23). Under these urea conditions, the intermediate is more populated than the native and unfolded states. Although the secondary structure of the intermediate species differs to that of the native CLIC1-WT (Figure 24), the intermediate species do maintain a certain amount of structure as shown by their fluorescence spectra (Figure 25) and indicate that Trp35 has moved into a more hydrophobic environment. This is consistent with the blue wavelength shifts in fluorescence observed during the formation of the intermediate (Figure 16). Furthermore, the intermediate species of CLIC1-WT and mutant proteins bind ANS through their exposed hydrophobic patches (Figure 21). The hydrophobic character of the ANS binding patches of the intermediates are shown by the blue wavelength shifts in fluorescence as well as the enhanced fluorescence intensities of the intermediate-bound ANS (Figures 16 and 21).

The intermediates unfold cooperatively at high concentrations of urea from I ↔ U. This is consistent with the presence of significant tertiary interactions. Together, the properties of the intermediate species of the CLIC1 proteins are inconsistent with that of a molten globule-like state. Molten globule proteins typically display poorly defined tertiary structure, bind to ANS weakly (millimolar range) and unfold in a non-cooperative manner at low urea concentrations (Ptitsyn, 1995; Fink, 1995; Kuwajima, 1989; Chamberlain and Marqusee, 1998; Jamin *et al*., 2000; Bailey *et al*., 2001 and Banerjee and Kishore, 2005). Therefore, the intermediate species of CLIC1-WT and mutant proteins appear to be the same although they may differ in stability.

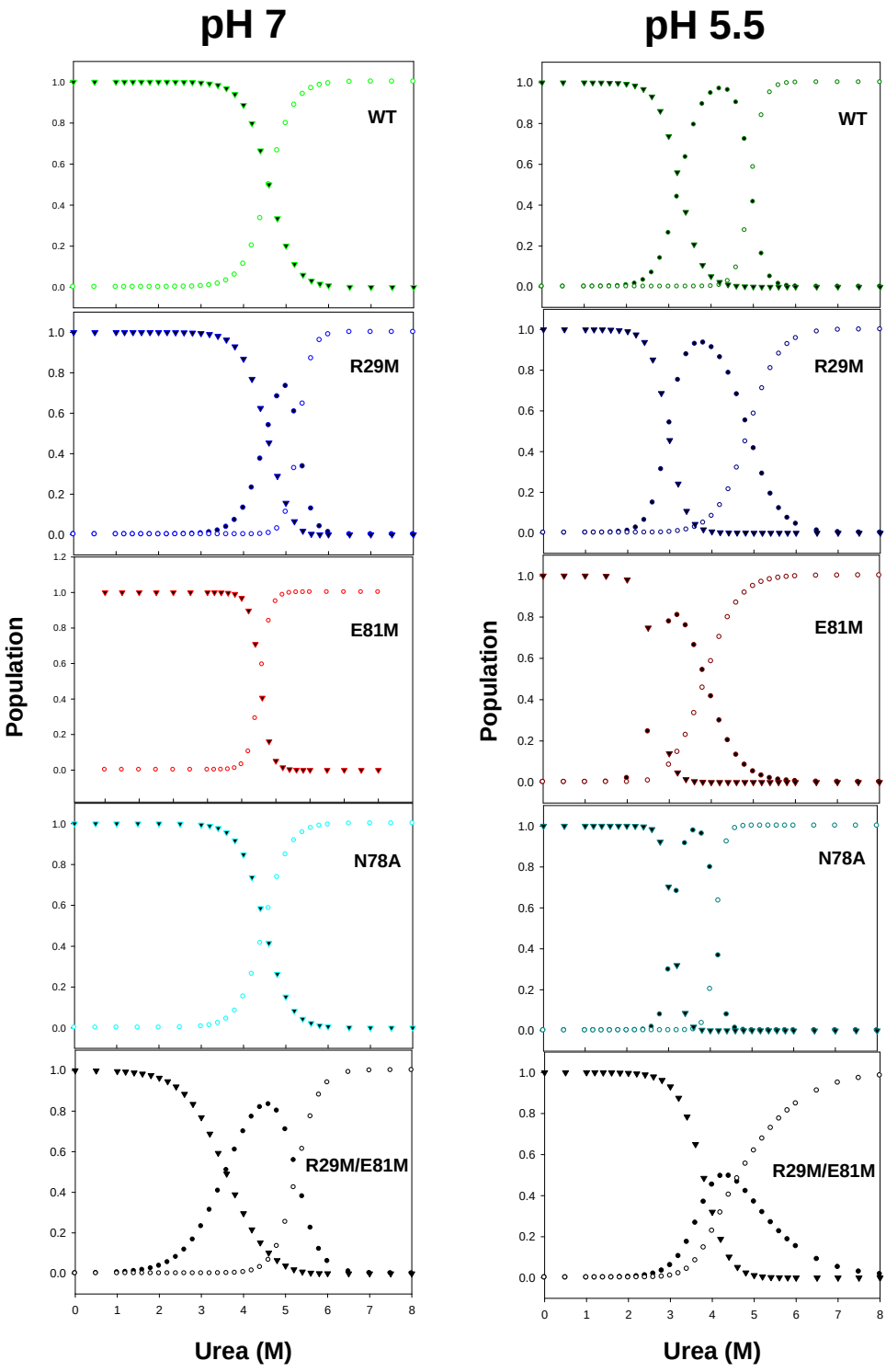


Figure 23: Fractional populations of N, U and I states of CLIC1-WT and mutant proteins

Fractional populations of the native (○), unfolded (▼) and intermediate states (●) of the CLIC1 proteins as a function of urea concentration. The populations were calculated using the thermodynamic parameters obtained from globally fitting the data to a two-state model at pH 7 (left panel) and to a three-state model at pH 5.5 (right panel). Experiments were conducted at 20 ^{o}C with 2 μM protein at pH 7 and pH 5.5.

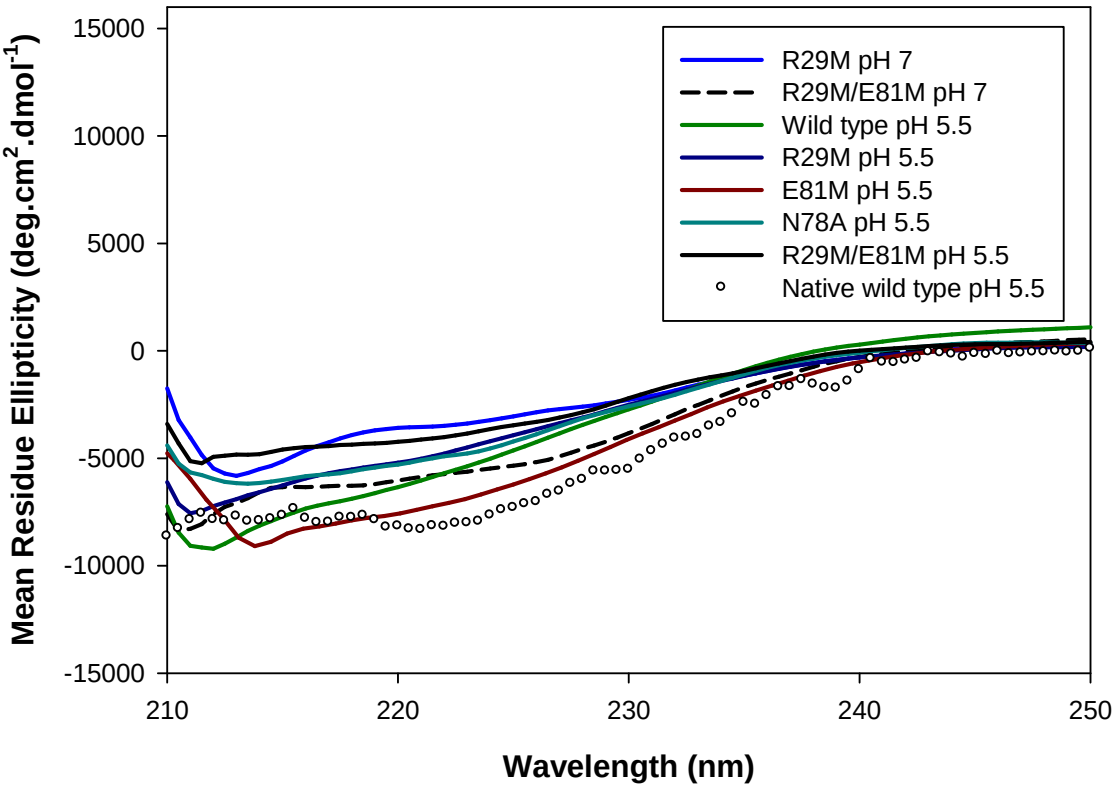


Figure 24: Far-UV CD spectra of the intermediate species of CLIC1-WT and mutant proteins

The far-UV CD spectra of the CLIC1-WT and mutant intermediate species (see insert). Also shown is the spectrum of native CLIC1-WT at pH 5.5 (o). The intermediate species maintain a degree of secondary structure. The spectral analyses were performed at 20 ^{o}C using 2 μM protein.

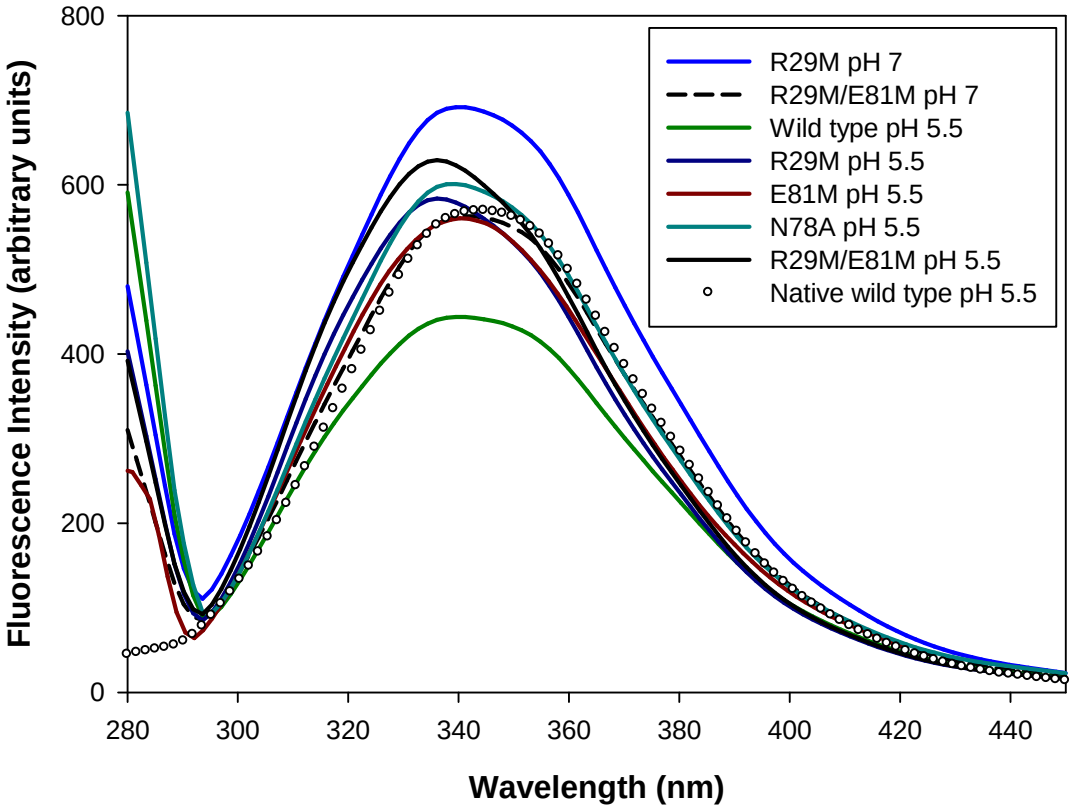


Figure 25: Fluorescence spectra of the intermediate species of CLIC1-WT and mutant proteins

The fluorescence spectra of the CLIC1-WT and mutant intermediate species are shown (see insert). Also shown is the spectrum of native CLIC1-WT at pH 5.5 (o). The tyrosine residues and the tryptophan residue were excited at 280 nm. The intermediate species display blue fluorescence wavelength shifts when compared to native wild type. The spectral analyses were performed at 20 ^{o}C using 2 μM protein at various urea concentrations.

CHAPTER 4

DISCUSSION

CLIC proteins exist in two forms, namely; a cytosolic soluble form with a GST topology and an insoluble membrane-bound form with an unknown topology (Harrop *et al*., 2001; Tulk *et al*., 2002; Warton *et al*., 2002; Berryman *et al*., 2004; Littler *et al*., 2004; Littler *et al*., 2005; Singh and Ashley, 2006; Cromer, 2007; Singh and Ashley, 2007; Singh *et al*., 2007). Triggers such as redox conditions (Harrop *et al*., 2001; Littler *et al*., 2004; Littler *et al*., 2005; Singh and Ashley, 2007 and Goodchild *et al*., 2009) and pH (Tulk *et al*., 2002; Warton *et al*., 2002; Cromer *et al*., 2007; Littler *et al*., 2007), have been shown to play a role in the ability of CLIC proteins to bind to and transverse membranes in order to function as ion transporters, with maximal binding and insertion occurring at low pH (5.5) and under oxidising conditions (Tulk *et al*., 2000; Warton *et al*., 2002; Littler *et al*., 2004; Littler *et al*., 2005; Cromer *et al*., 2007; Littler *et al*., 2008; Goodchild *et al*., 2009). However, the mechanism by which CLIC proteins change from their soluble to membrane-bound form is still unknown. Recent studies have shown that in order for CLIC proteins to bind to and transverse membranes and form functional ion selective pores, large scale rearrangements of the N-terminal domain (consisting of the TMR (helix 1 and β-sheet 2)) are required (Littler *et al*., 2004; Goodchild *et al*., 2009). These structural rearrangements require a certain amount of flexibility in the structure of CLIC proteins and result in the exposure of hydrophobic surfaces that can bind and insert into membranes (Goodchild *et al*., 2009).

Littler *et al*. (2001) were the first to hypothesise that the N-terminal domain of CLIC1 could provide the flexibility required for CLIC1 to undergo large scale structural rearrangements in order to form its membrane-bound topology. Recent studies supporting this hypothesis have been reported. HXMS data showed that the N-terminal domain of CLIC1 is less stable than the all α-helical C-terminal domain and although the structural integrity of CLIC1 is unchanged at pH 5.5 (low pH conditions present at the membrane surface), its conformational flexibility increases (Stoychev *et al*., 2009). Urea-induced equilibrium unfolding studies on CLIC1 also revealed that its conformational stability is reduced at low pH (5.5) (Fanucchi *et al*., 2008). It was proposed that the acid-induced destabilisation and partial unfolding of

CLIC1 involve helix 1 (Fanucchi *et al*., 2008) since it provides most of the domain-domain interactions. They also proposed that the acidic environment found at the membrane surface (van der Goot *et al*., 1991) may prime the CLIC1 TMR of the N-terminal domain by protonating certain amino acids and thereby lowering the energy barrier required for CLIC1 to change from its soluble to membrane-bound topology.

It appears as though the membrane-bound topology of CLIC proteins is “trapped” or “hidden” within the soluble N-terminal domain. Therefore, understanding what determines the conformational stability of the soluble GST-like topology of CLIC proteins, in particular the N-terminal domain (TMR) is important since the N-terminal domain is involved in membrane insertion and is required to undergo large structural rearrangements in order to insert into membranes. This information may provide insight into how the topology of soluble CLIC1 is primed or changed to reveal its membrane-bound topology.

An inspection of the N-terminal domain using structural and sequence alignments of the CLIC proteins (see Figures 4 and 6) revealed a conserved salt-bridge (Figure 5). The topologically equivalent residues in CLIC1 are Arg29 and Glu81 (Figure 5). Residues Arg29 and Glu81 also form hydrogen bonds with Asn78 (Figure 5). Since these residues and the salt-bridge between them are conserved in the CLIC proteins (Figures 4, 5 and 6) they may play an important role in maintaining the structural integrity and conformational stability of the soluble form of CLIC proteins. This hypothesis was investigated by mutating residues Arg29 and Glu81 to methionine (bulk maintained but charge altered) and mutating Asn78 to alanine (polar, uncharged to non-polar) and assessing the effect of the mutations on the structure and stability of CLIC1.

This was done by spectroscopically analysing the structures of the mutant proteins using CD and fluorescence spectroscopy, acrylamide quenching and ANS binding. The stabilities of the mutant proteins were assessed by urea-induced equilibrium unfolding studies. The crystal structure of the double mutant protein, R29M/E81M (PDB code: 3P8W) was used to verify and interpret the spectroscopic structural and stability data. All the data were compared to that of the wild type protein.

4.1. Impact of the mutations on the structural integrity of CLIC1

The residues selected for mutagenesis namely, Arg29, Glu81 and Asn78 are positioned on helices 1 and 3 of the N-terminal domain at the domain interface. Here, they form hydrogen bonds and a salt-bridging interaction (Figure 5). The role these residues play in maintaining the structural integrity of CLIC1 was investigated spectroscopically for the solution structures of the mutant proteins. The far-UV CD spectral properties of the native mutant proteins when compared to those of CLIC1-WT showed that the proteins displayed minima at 208 nm and 222 nm at both pH 7 and pH 5.5 (Figure 10). This result is typical for proteins with a high α-helical content (Woody, 1995) and agrees with the crystal structure of CLIC1 (Figure 1).

Fluorescence spectroscopy revealed a maximum emission at 345 nm for all the mutant proteins at both pH 7 and pH 5.5 (Figure 12). This result is consistent with the partial exposure of Trp35 to solvent in native CLIC1 (Harrop *et al*., 2001). Acrylamide quenching studies show similar results to near-UV CD and fluorescence spectroscopy in that Trp35 is partially solvent exposed for all mutant proteins and that no major secondary or tertiary structural changes have taken place due to the incorporation of the mutations (Figures 11, 12 and 14).

The crystal structure of R29M/E81M (PDB code: 3P8W) was used to verify the spectroscopic data. The crystal structure of R29M/E81M showed that the mutations did not cause significant global structural changes and that the R29M/E81M structure compared well with that of the CLIC1-WT structure (see Figure A in Appendix). Since Trp35 was used as a local structural probe, it is important to look at its position and interactions in the R29M/E81M structure and make comparisons with the WT protein. It can be seen in Figure 26 that no significant change has occurred in the position of Trp35 in the mutant protein compared to the WT. Therefore, it was concluded that the mutations are structurally non-disruptive and that residues Arg29, Glu81 and Asn78 do not play a role in maintaining the structural integrity of CLIC1.

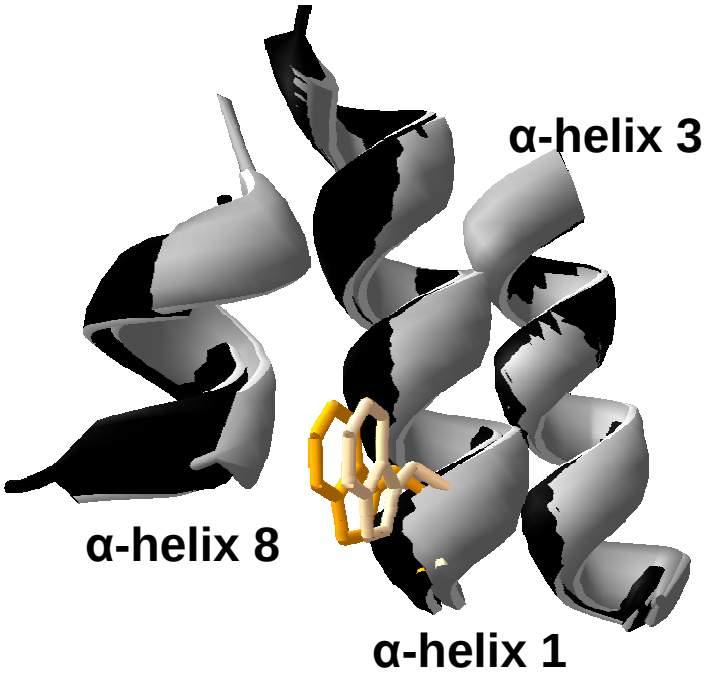


Figure 26: **Ribbon representations of the tertiary environment around Trp35 of CLIC1-WT and CLIC1-R29M/E81M**
Superimposed helices 1, 3 and 8 of CLIC1-WT (black) and CLIC1-R29M/E81M (grey) showing the position of Trp35 (WT (dark amber) and R29M/E81M (light amber)). This image was generated using Swiss PDB Viewer (Guex and Peitsch, 1997) using PDB codes 1K0M (Harrop *et al*., 2001) and 3P8W (http://www.rcsb.org/pdb/explore/explore.do ?structureId=3P8W).

4.2. Impact of the mutations on the stability of CLIC1

Urea-induced equilibrium unfolding of CLIC1-WT and mutant proteins showed that the native states of the proteins were recovered after unfolding in urea (Table 3). Fanucchi *et al*. (2008) have shown that CLIC1-WT unfolds via a two-state unfolding transition at pH 7. At pH 5.5, however, CLIC1-WT is destabilised resulting in the formation of a highly populated intermediate species that has a solvent-exposed hydrophobic surface (Fanucchi *et al.*, 2008). This destabilisation may be due to the protonation of certain amino acids at pH 5.5 (Fanucchi *et al.*, 2008). Therefore, at pH 5.5 CLIC1-WT unfolds via a three-state transition with an intermediate state that compares to that of the oxidised form of CLIC1 in that it resembles a membrane insertion 'intermediate state'. This is because both the CLIC1-WT intermediate and the oxidised form of CLIC1 contain a large exposed hydrophobic surface (Goodchild *et al*., 2009).

Trends in the thermodynamic stability of the WT and mutant proteins are summarised and illustrated in Figure 27. The urea-induced equilibrium unfolding at pH 7 of N78A and E81M mimics that of the WT protein in that unfolding takes place via a two-state transition (Figure 16). Also, N78A and E81M do not bind ANS and do not display blue fluorescence wavelength shifts during unfolding (Figures 16 and 21). The thermodynamic parameters, ΔG_{nu} and m_{nu}, for N78A at pH 7 are almost identical to that of the WT protein (Table 4). This indicates that the N78A mutation does not impact upon the stability of CLIC1 at pH 7. Residue Asn78 is solvent exposed as indicated by its accessible surface area calculated by GET AREA (Fraczkiewicz and Braun, 1998). The N78A mutation does not appear to impact upon the packing density of the core of CLIC1. Also, Asn78 is not conserved amongst the CLIC proteins, as shown by the sequence and structural alignments (Figures 4 and 6) and, therefore, appears not to be critical for the stability of CLIC1 at pH 7.

The increased ΔG_{nu} and m_{nu} values of E81M at pH 7 compared to that of the WT (Table 4) are rather unexpected since its unfolding behaviour mimics that of the WT. Also, Arg29 is likely to remain positively charged at pH 7 and substituting the charged Glu81 with an uncharged methionine would leave the partially buried and charged Arg29 electrostatically unsatisfied. It is expected that this would cause the protein to become destabilised. However, this is not the case. It is interesting to speculate as to why the E81M mutant does not show

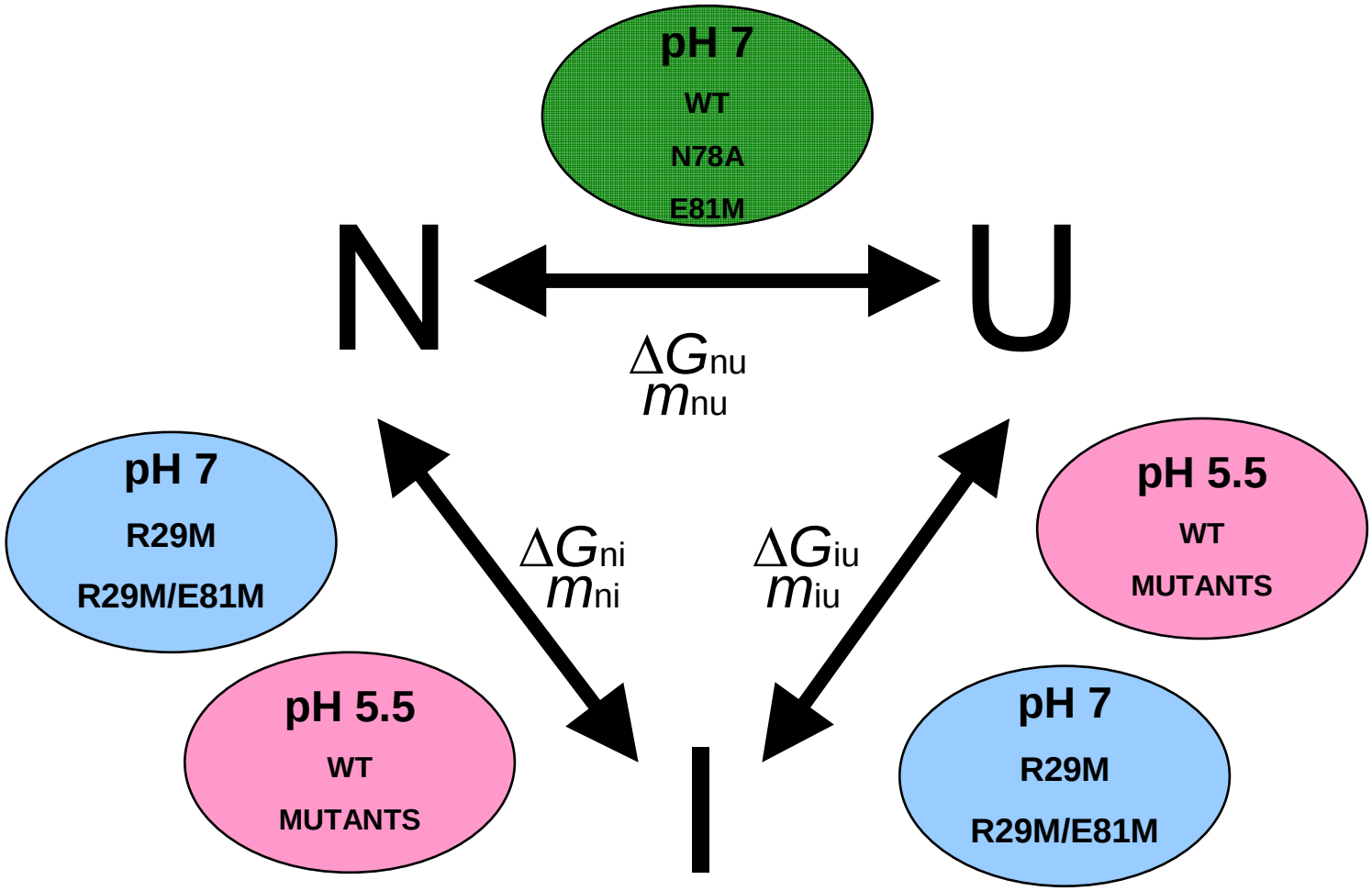


Figure 27: Schematic of the thermodynamic unfolding pathways of the CLIC1-WT and mutant proteins.

The subscripts nu, ni and iu refer to native-to-unfolded, native-to-intermediate and intermediate-to-unfolded transitions of the proteins, respectively. N ↔ U represents a two-state unfolding transition whereas, N ↔ I ↔ U represents a three-state unfolding transition.

decreased thermodynamic stability at pH 7. A possible explanation for the increased stability of E81M is that the charge-charge pair Arg(+)-Glu(-) is less stabilising than the Arg(+)-Glu(neutral) pair. Consequently, substituting a charged Glu81 with a neutral methionine would stabilise the protein. An example of this was reported by Bosshard *et al*. (2004) who calculated free energy contributions of salt-bridges by measuring changes in pK_a values. In an interhelical salt-bridge (Glu22-Arg27) in a leucine zipper, the negatively charged side chain of Glu22 was shown to destabilise the native protein while the positively charged side chain Arg27 stabilised the native protein (Bosshard *et al*., 2004). Others have also reported increased protein stabilities by removing one of the charges within a charge(+)-charge(-) pair (Anderson *et al*., 1990; Sanchez-Ruiz and Makhatadze, 2001). This leads one to believe that Glu81 may be destabilising in its charged form at pH 7, while charged Arg29 is stabilising and therefore, by removing Glu81 the stability of the protein is enhanced. This hypothesis could be tested by measuring the pK values for Arg29 and Glu81 and then using these values to calculate the stability contributions to the salt-bridging interaction. However, the stability of the E81M mutant at pH 7 does not provide evidence against the salt-bridge as only the net free energy of a salt-bridge (net energetic contributions of Arg29 and Glu81 together) can distinguish between a stabilising or destabilising interaction (Bosshard *et al*., 2004). Furthermore, if two charged residues are interacting, the change in stability of the double mutant will not equal the sum of the changes in stability of the single mutants, as is the case for R29M, E81M and R29M/E81M. This shows that although charged Glu81 may be destabilising at pH 7, it does form interactions with Arg29 in the wild type protein.

The Arg29-Glu81 salt-bridge is partially buried in the protein interior and to bury a salt-bridge in the protein interior is energetically unfavourable and costly. This implies that replacing a residue that forms part of a buried salt-bridge with a hydrophobic residue (preferably isosteric), is favourable (Hendsch and Tidor, 1994; Waldburger *et al*., 1995). In fact, this was exactly the finding of a study by Walburger *et al*. (1995) with the Arc repressor homodimer. The Arc repressor comprises two partially buried salt-bridge triads, the most stabilising type of salt-bridge interaction (Kumar and Nussinov, 1999). Walburger *et al*. (1995) replaced each of the salt-bridge residues with isoteric, non-polar groups. The result was that the Arc repressor protein was stabilised by ~4.5 $kcal.mol^{-1}$. Therefore, it is possible that the E81M mutant has an increased stability compared to that of the WT protein due to

the formation of stabilising hydrophobic interactions with the surrounding hydrophobic residues namely, Val33, Ile80, Leu84 and Leu175. The hydrophobic residues may pack tightly against each other and thereby stabilise the protein. This hypothesis may be verified by obtaining the crystal structure of CLIC1-E81M.

Furthermore, Arg29 may form cation-π interactions with Phe26 and Phe31 (both of which are conserved in CLICs 1-4). Cation-π interactions are becoming accepted as significant noncovalent binding interactions that are related to structural biology (Dougherty, 1996; Ma and Dougherty, 1997; Scrutton and Raine, 1996). A study by Piromjitpong *et al*. (2007) on *Anopheles dirius* GSTD4-4 investigated the role of a conserved electrostatic region at the dimer interface comprising Arg96 in helix 4 and Glu75 in helix 3. They created two single mutants namely R96A and E75A to assess the role of the conserved interaction in maintaining stability and folding of GSTD4-4. What they found was that both mutants reduced the stability of GSTD4-4 but far more so for the R96A mutant. A possible explanation for this is that Arg96 forms interactions with Glu75 and it also forms cation- π interactions with the aromatic ring of Tyr89. These cation-π interactions may compensate for the loss of interaction with Glu75 in the E75A mutant. Consequently, it is feasible that a similar stabilisation of Arg29 in CLIC1 occurs due to cation-π interactions with Phe26 and Phe31 and thereby compensates for the loss of interactions with Glu81 in the E81M mutant.

Therefore, it appears as though other interactions compensate for the loss of electrostatic contacts that are normally provided by Glu81 in the wild type protein, or that charged Glu81 at pH 7 is destabilising and therefore its removal enhances stability. These compensatory interactions and/or the removal of a destabilising Glu81 enable E81M to retain a two-state unfolding transition at pH 7 much like that of CLIC1-WT.

Unlike the WT, N78A and E81M proteins, the R29M and R29M/E81M mutants do not follow a two-state unfolding transitions from N ↔ U at pH 7. This indicates that the R29M and R29M/E81M mutants no longer unfold in a cooperative manner from N ↔ U. This loss in cooperativity from N ↔ U was concomitant with the formation of an intermediate species. Therefore, the R29M and R29M/E81M mutations at pH 7 mimic the effects of low pH (5.5) that are exhibited by the WT protein. Ultimately, the R29M mutation removes all the

hydrogen bonding interactions between Glu81 and residue 29, leaving the negative charge on Glu81 electrostatically unsatisfied and thus causes destabilisation.

The R29M/E81M mutants loss in cooperativity from N ↔ U at pH 7 compared to wild type is probably due to the replacement of Arg29 and Glu81 with methionine. This has removed van der Waals interactions that are normally present in the wild type protein namely; the hydrogen bonding interaction Arg29 makes with Asn78 and the van der Waals interactions Glu81 makes with Val33 and Leu175 (Table 5). This causes changes in the packing of the protein that reduce van der Waals contacts and thereby alters the cooperativity of unfolding from N ↔ U of the protein. Furthermore, a number of hydrogen bonding interactions that Arg29 and Glu81 make with surrounding water molecules are also lost due to the incorporation of the mutations, thereby reducing the van der Waals contacts. This can be verified by looking at the crystal structure of the CLIC1-R29M/E81M mutant (Figure 28) as well as schematic representations that highlight the network of interactions between Arg29, Glu81 and other interacting residues and water molecules (Figure 29). Figure 29 also illustrates how the R29M/E81M mutation reduces the number of interactions within this network.

At pH 5.5 CLIC1-WT, R29M, N78A, E81M and R29M/E81M all follow a three-state unfolding transition. The ΔG_{ni} and m_{ni} values of all the mutant proteins were not significantly different to that of the WT when including the standard error (Table 4). However, the ΔG_{iu} and m_{iu} values at pH 5.5 are reduced for the mutant proteins compared to WT, except for N78A (Table 4). This shows that the mutations have caused changes in the stability of the intermediate species of CLIC1. Also, one should note that the reduced m_{iu} values of the mutants compared to the WT implies that the intermediate species unfold less cooperatively compared to the wild type intermediate species. The m_{iu} value for N78A may appear to be greater than the wild type value. However, when the standard error is taken in to count, there is no significant difference between the N78A mutant and the wild type protein. It is also interesting to note that the ΔG_{iu} and m_{iu} values of R29M at pH 5.5 are reduced compared to those at pH 7. This further reduction in stability of the intermediate specie may be due to an increase in the pK_a of Glu81 such that Glu81 becomes uncharged, since buried non-charged polar groups that are unable to hydrogen bond are destabilising and sustain energy costs of up

Table 5: Residues interacting with residues 29 and 81 in CLIC1-WT and CLIC1-R29M/E81M

Residues within 4 Å of R29 in CLIC1-WT	Residues within 4 Å of M29 in CLIC1-R29M/E81M	Residues within 4 Å of E81 in CLIC1-WT	Residues within 4 Å of M81 in CLIC1-R29M/E81M
Pro25	Pro25	Arg29	Met29
Phe26	Phe26	Val33	No Interaction
Ser27	Ser27	No Interaction	Leu 30
Gln28	Gln28	Thr77	Thr77
Leu30	Leu30	Asn78	Asn78
Phe31	Phe31	Lys79	Lys79
Met32	Met32	Ile80	Ile80
Val33	Val33	Glu82	Glu82
Thr77	Thr77	Phe83	Phe83
Asn78	No Interaction	Leu84	Leu84
Glu81	Met81	Glu85	Glu85
Cys178	Cys178	Leu175	No Interaction
Asn179	Asn179	HOH607	No Interaction
No Interaction	HOH309	HOH608	No Interaction
No Interaction	HOH426	HOH631	No Interaction
No Interaction	HOH427		
HOH565	No Interaction		
HOH566	No Interaction		
HOH608	No Interaction		
HOH631	No Interaction		

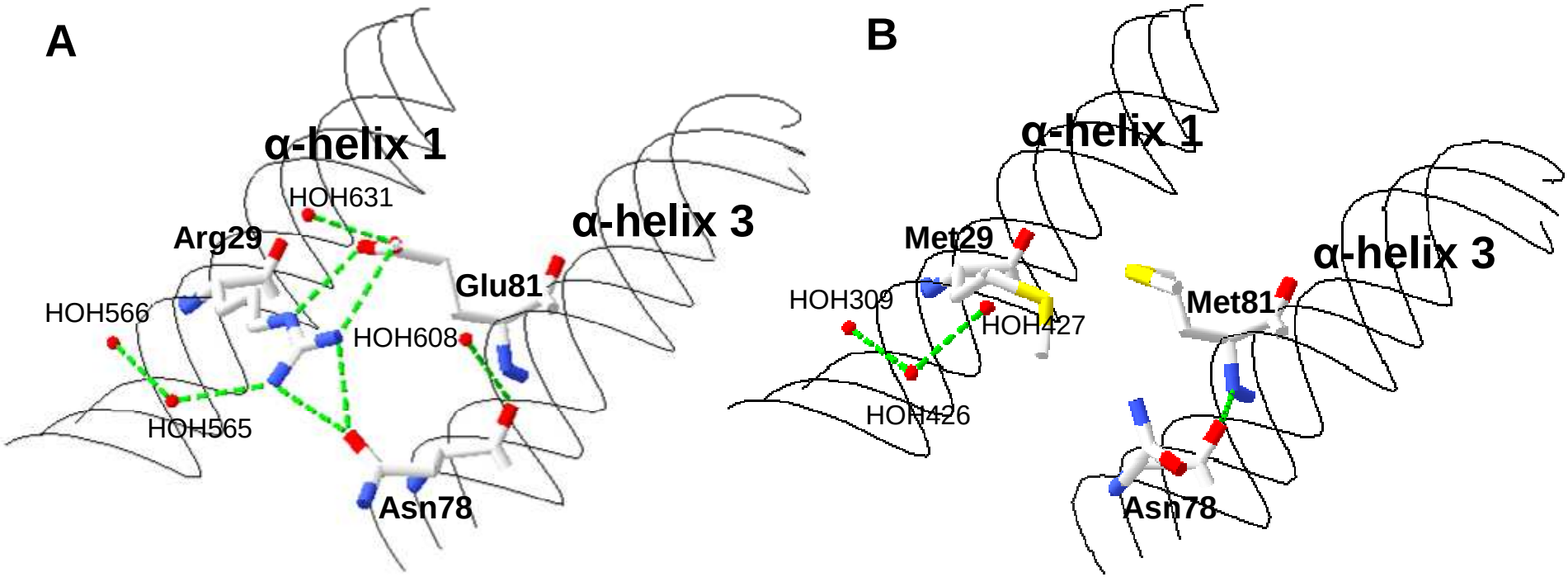


Figure 28: Hydrogen bonds between residues 29, 78, 81 and water in CLIC1-WT and R29M/E81M
The hydrogen-bond interactions between the residues of CLIC1-WT (A) and CLIC1-R29M/E81M (B) are indicated by green dashed lines. The water molecules are represented by red spheres and are numbered accordingly. This image was generated using Swiss PDB Viewer (Guex and Peitsch, 1997) using PDB codes 1K0M (Harrop *et al*., 2001) and 3P8W (http://www.rcsb.org/pdb/explore/explore.do? structure Id=3P8W).

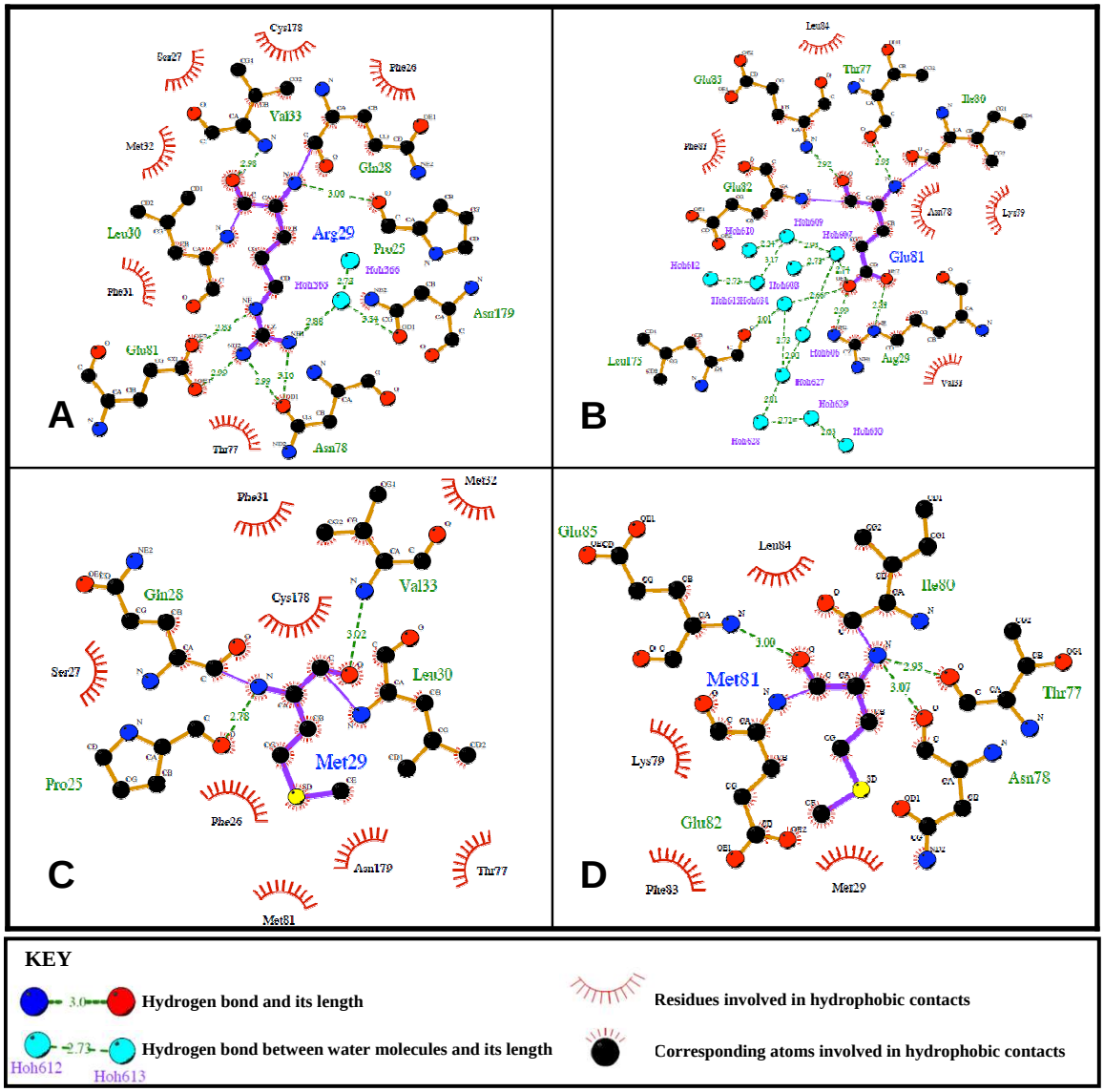


Figure 29: A schematic representation of the electrostatic network of CLIC1-WT and CLIC1-R29M/E81M with reference to residues 29 and 81.

The electrostatic network in CLIC1 with reference to Arg29 (A) and Glu81 (B) and Met29 (C) and Met81 (D). The LIGPLOTS were generated by Dr M Soliman from the Computational Chemistry & Modelling Department of Chemistry, University of Bath, using the program, LIGPLOT (Wallace *et al*., 1995).

to 2.99 kcal.mol^{-1} (Blaber *et al.*, 1993). Environmental factors have been shown to alter the pK's of ionisable groups whereby they are markedly increased or decreased compared to their intrinsic pK value (Pace *et al.*, 2009). Furthermore, hydrogen bonds provide up to 2 kcal.mol^{-1} to protein stability (Takano *et al.*, 2003) and when hydrogen bonds are made to ionisable groups, as is the case for the Arg29 and Glu81 residues, the hydrogen bonds can increase or decrease the pK by several pK units (Li *et al.*, 2005). An example of this was provided by Thurkill *et al.* (2006) who measured the pK_a of the carboxyl group of Asp76 in RNase T1. The Asp76 residue is a buried charged residue with a pK value of 0.6. It forms three intramolecular hydrogen bonds to the side chains of Asn9, Tyr11 and Thr91. These hydrogen bonds were removed and the pK of Asp76 measured. As a single hydrogen bond was removed the average pK increased to 3.3, when two hydrogen bonds were removed the pK increased to 5.1 and when the third hydrogen bond was removed the pK increased to 6.4. So it is possible that the pK_a of Glu81 increases such that Glu becomes uncharged. The further reduction in the ΔG_{iu} and m_{iu} values of R29M at pH 5.5 compared to pH 7 may also be due to the side chains of Arg29 and Glu81 interacting with other charges apart from their reciprocal partner residues. Therefore, other back-round interactions may be forming and/or breaking and thereby altering the stability of the intermediate species of R29M at pH 5.5. Since both Arg29 and Glu81 are partly buried in the native state of the protein there may also be contributions from solvation or desolvation during unfolding. Therefore, the major changes in the stability of CLIC1 that lead to a three-state unfolding transition and the simultaneous formation of an intermediate species seem to be "triggered" by either a change in pH from 7 to 5.5 or when the hydrogen bonding interactions (including the salt-bridge) between residues 29 and 81 are removed from the N-terminal domain.

In CLIC1-WT, it is possible that at pH 5.5 the electrostatic interactions between the salt-bridge residues Arg29 and Glu81 are altered and this triggers a conformational stability change in CLIC1 that destabilises the N-terminal domain (specifically helix 1) to such an extent that it forms an intermediate species that has a solvent exposed hydrophobic surface that may interact with membranes.

Therefore, it can be hypothesised that the Arg29-Glu81 salt-bridge may function as a pH-induced switch. A proposed mechanism is that in the cytosol (pH 7) the polar charged amino

acids are either positively or negatively charged and, therefore, the salt-bridge between Arg29 and Glu81 will form. However, when CLIC1 moves near the surface of the membrane, where the environment has a low pH (pH 5.5), the Glu81 residue may become protonated and may, therefore, no longer be able to form a salt-bridge with Arg29. This salt-bridge destabilisation would reduce the stability of the protein's domain interface and thereby enable the protein's domain interface to become more flexible thereby priming the protein to undergo the conformational change required for membrane insertion.

In order to assess the feasibility of the above hypothesised role of the Arg29-Glu81 salt-bridge, one needs to look at what others have discovered regarding the roles of salt-bridges in maintaining the structural integrities and thermodynamic stabilities of proteins.

Salt-bridges are important in maintaining the structures and functions of proteins. This has been illustrated in oligomerisation, molecular recognition, allosteric regulation, domain motions, thermostability and α-helix capping (Perutz, 1970; Fersht, 1972; Barlow and Thornton, 1983; Musafia *et al*., 1995; Xu *et al.*, 1997; Xu *et al*., 1997a; Kumar *et al*., 2000). Theoretical and experimental approximations of the electrostatic free energy contribution of salt-bridges vary from stabilising (Anderson *et al*., 1990; Horovitz and Fersht, 1992, Marqusee and Sauer 1994; Lounnas and Wade, 1997; Hendsch and Tidor, 1994, Kumar and Nussinov, 1999) to being insignificant (Perutz *et al*., 1985; Singh 1988; Serrano *et al*., 1990) and to being destabilising (Sun *et al*., 1991; Hendsch and Tidor, 1994). The stabilisation or destabilisation of salt-bridges depends on a number of factors such as whether or not the salt-bridge is buried or exposed with respect to the protein structure, the position of the side-chain groups of the residues forming the salt-bridge with respect to each other and the interaction of charged groups of the salt-bridge with other charged groups in the protein structure (Kumar and Nussinov, 1999). Amino acid residues that form surface exposed salt-bridges ordinarily have lower desolvation energy costs when compared to those that form buried salt-bridges (Hendsch and Tudor, 1994). Interestingly, buried salt-bridges have frequently been shown to be destabilising (Honig and Hubell, 1984; Dao-pin *et al*., 1991; Hendsch and Tudor, 1994; Waldburger *et al*., 1995). However, exceptions have been reported by Lounas and Wade (1997) and Anderson *et al*. (1990) amongst others. Furthermore, it has been stated that there are no major differences between surface-located and buried salt-bridges insofar as both can

be stabilising or destabilising (Hendsch and Tudor, 1994; Kumar and Nussinov, 1999; Kajander *et al*., 2000) and consequently the influence of salt-bridges on protein structures and stabilities seems to be strongly context dependent.

There are many studies that demonstrate that buried salt-bridges have numerous functions. This can be highlighted by looking at the work on cytochrome P450cam by Lounnas and Wade (1997). Cytochrome P450cam contains four remarkably stable salt-bridges, two of which are buried. These salt-bridges have evolved functional roles. Firstly, these salt-bridges bind the heme cofactor and secondly they control the access of substrate to the buried active site (Lounnas and Wade, 1997). They have proposed to do this by regulating protein motions that are essential for substrate access channel formation. Other examples of salt-bridges are the salt-bridges at the interface of bovine β-lactoglobulin that function to manipulate its monomer-dimer equilibrium in a pH-dependent manner (Kazumasa and Goto, 2002) and the Arg75-Glu81 buried salt-bridge in parvalbumins that play a role in adjusting calcium and magnesium affinity as well as conformational changes of its AB loop (Hoh *et al*., 2009).

However, a major finding in this study was that the role of the buried salt-bridge formed between Arg29 and Glu81 appears to be stabilisation of the N-terminal domain of soluble CLIC1 and more particularly stabilising the interaction between helices 1 and 3. In fact, many studies have illustrated the significance of buried salt-bridges in maintaining the stabilities of helices. Many of these studies show that the ability of buried salt-bridges to stabilise helices occurs in a pH-dependent manner. An example where helix stability has been shown to rely greatly on pH is that of the isolated C-peptide of ribonuclease A (Bierzynski *et al*., 1982). It was revealed that the protonation or deprotonation state of residues Glu9 and His12 determined helical stability of the C-peptide (Bierzynski *et al*., 1982). pH titration data indicated that stable helix formation required both a negatively charged Glu9 residue and a positively charged His12 residue. Other work on the C-peptide of ribonuclease A also illustrated that pH-dependent side-chain interactions are imperative in stabilising the C-peptide helix (Rico *et al*., 1983; Shoemaker *et al*., 1985). The role of the Glu2(-) - Arg10(+) side chain interaction, also in the C-peptide of Ribonuclase A, was assessed using pH titration, substitution testing and ion screening. Fairman *et al*. (1990) reported that the Glu2(-)

- Arg10(+) salt-bridge is linked to helix formation and contributes to the stability of the C-peptide helix.

T4 lysozyme comprises a salt-bridge between residues His31 and Asp70 that has been demonstrated to be stabilising (Anderson *et al*., 1990). His31, as reported by Bosshard *et al*. (2004), needs to be positively charged and Asp70 needs to be negatively charged in order to contribute to stabilising T4 lysozyme. At low or high pH the salt-bridge is broken due to protonation of the side chain of Asp70 and deprotonation of the His31 side chain. Therefore, the His31-Asp70 salt-bridge in T4 lysozyme provides another example of a stabilising pH-dependent buried salt-bridge.

In 1996, Pervushin and co-workers explained that the 63 residue N-terminal DNA-binding domain of the 434 repressor includes a buried salt-bridge Arg10-Glu35 that has demonstrated stabilisation. The NMR solution structures of the 434 repressor (residues 1-63) and mutant 434 repressor R10M (residue 1-63) were determined in order to assess the structural role of the Arg10-Glu35 salt-bridge (Pevushin *et al*., 1996). Both protein structures comprised the global fold of five helices and a helix-turn-helix motif that is formed by helices 2 and 3. The most important difference between the structures was translation of helix 1 along its axis relative to the helix 2- turn-helix 3 motif. A change in the stability of the mutant protein 434 repressor R10M was also reported as being decreased at pH 4.8 (Pevushin *et al*., 1996).

Therefore, based on the fact that a number of studies on buried salt-bridges illustrate their ability to provide stabilisation in proteins and helices, it is reasonable to state that the role of the Arg29-Glu81 salt-bridge in soluble CLIC1 is to stabilise the N-terminal domain. Two other salt-bridges are also present at the domain interface namely, the Lys20-Asp225 salt-bridge between β-strand 1 and helix 9 and the salt-bridge Lys37-Glu85 between helices 1 and 3 (Figure 30). There are a number of polar residues charged and uncharged that appear to form an intricate electrostatic and hydrogen bonding network along the domain interface of CLIC1. These bonding interactions indirectly join the three salt-bridges together (Figure 31). Consequently, the Arg29-Glu81 salt-bridge may not act in isolation and is likely to form part of an electrostatic and hydrogen bonding network that acts in a cooperative manner to stabilise the domain interface of CLIC1.

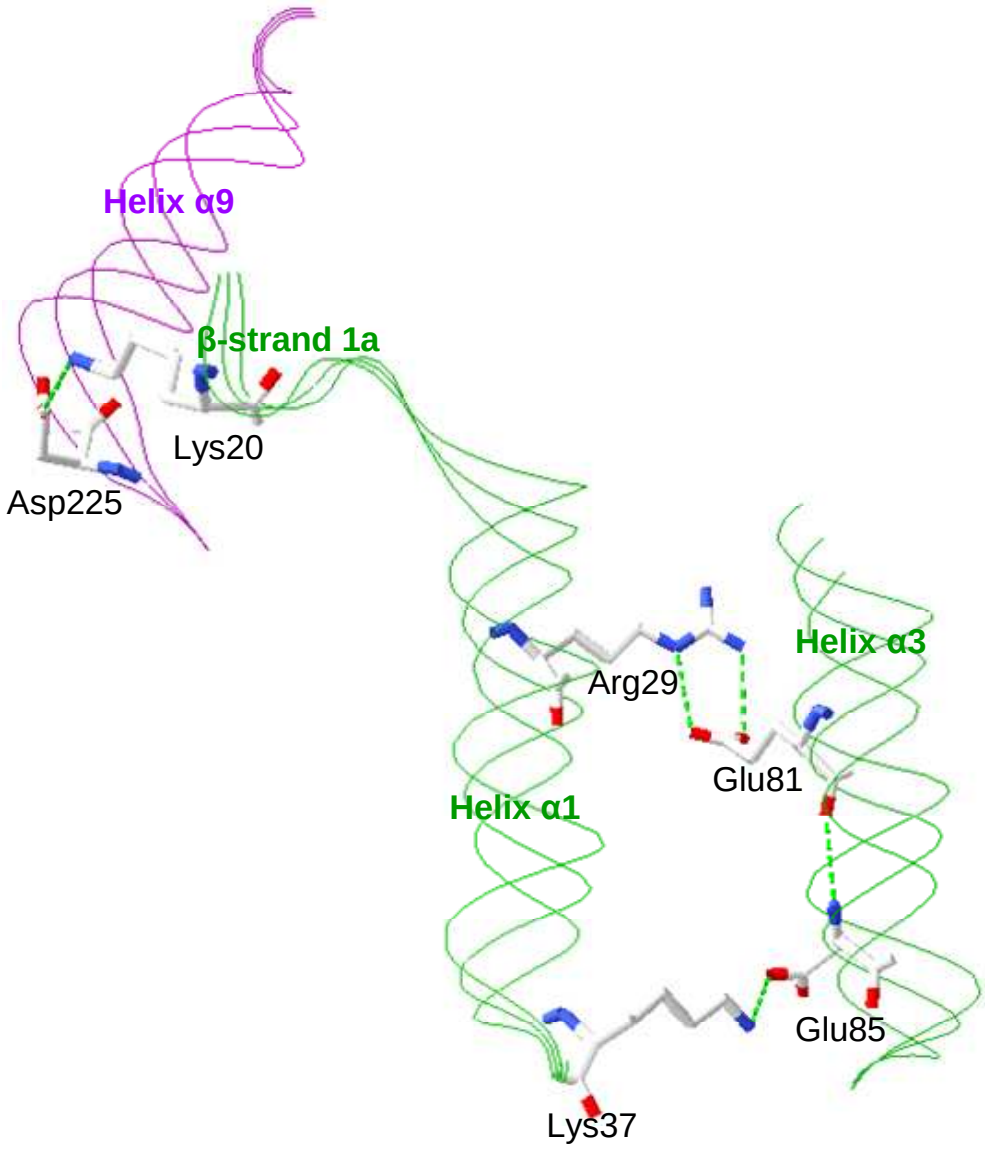


Figure 30: Salt-bridges at the domain interface of CLIC1

The salt-bridging residues, and secondary structures at the domain interface are labelled accordingly. The hydrogen bonding interactions are represented by green dashed lines.

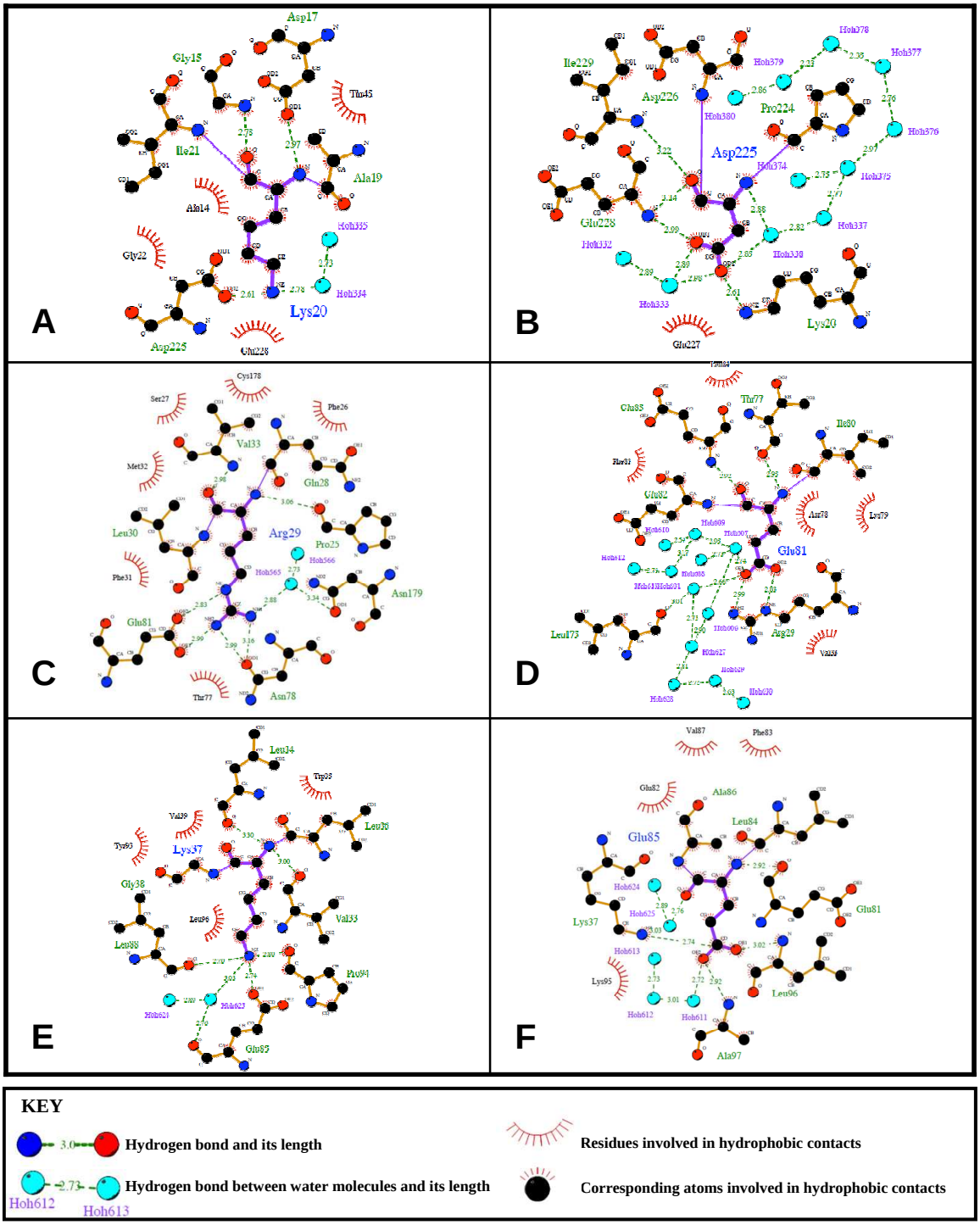


Figure 31: A schematic representation of the electrostatic and hydrogen bonding network at the domain interface of CLIC1.

AB, CD and EF show the electrostatic interactions involving salt-bridges Asp225-Lys20, Arg29-Glu81 and Arg37-Glu85, respectively. This network of interactions "runs" along the domain interface of CLIC1. The LIGPLOTS were generated by Dr M Soliman from the Computational Chemistry & Modelling Department of Chemistry, University of Bath, using the program, LIGPLOT (Wallace *et al*., 1995).

At pH 5.5, acidic residues Glu81, Glu85 and Asp225 are likely to be protonated and neutral due to shifts in their pK_a values (described previously) and so would no longer form salt-bridges with Arg29, Lys37 and Lys20 respectively. This would also impact upon other hydrogen bonds these residues make with other nearby residues as well as water mediated hydrogen bonds.

Therefore, under acidic conditions, such as those at the membrane surface, the salt-bridges and electrostatic and hydrogen bond network of CLIC1 would be destabilised resulting in decreased protein stability at the domain interface. This would increase the flexibility of the domain interface and thus allow the protein to be primed to undergo conformational changes required for membrane insertion.

A number of proteins utilise hydrogen bonding networks or electron sharing networks to perform certain functions. For example, *Anopheles dirius* GSTD3-3 contains an electron sharing network that consists of a salt-bridge between the negatively charged α-carboxylate group of GSH and the positively charged Arg66 and negatively Asp100 (Winayanuwattikun and Ketterman, 2005). These functional groups produce a motif that is stabilised by a network of hydrogen bonds provided by Ser65, Thr158, and Thr162 and a conserved water-mediated contact. Residues Arg66 and Asp100 were mutated to alanine and this resulted in the disturbance of the electron sharing in the network (Winayanuwattikun and Ketterman, 2005). The study revealed that the electron sharing network aids in the ionisation of the thiol group of GSH through the base-assisted deprotonation model. Interestingly, this network in other GST proteins has not yet been characterised and is not conserved in the primary amino acid sequence. However, structural comparisons of GST crystal structures propose that the electron sharing network is located within in the same region in all GST proteins (Winayanuwattikun and Ketterman, 2005).

A network of hydrogen bonds that fastens helix 1 of the N-terminal domain to the last helix of the C-terminal domain is present in *Ochrobactrum anthropi* beta-class GST (Federici *et al*., 2009). The network is formed by Ser11 and Glu198 that interact indirectly through a water molecule that is hydrogen bonded to both residues. Also, His15 forms hydrogen bonds with Glu198 - these residues are conserved throughout the beta-class GSTs (Federici *et al*.,

2009). When Ser11 was mutated to an alanine residue, the catalytic efficiency of the protein was reduced due to loss of global structural stability (Federici *et al*., 2007). Also, when His15 and Glu198 were mutated to alanine the enzyme lost its activity and had reduced stability. The loss in stability of the hydrogen bond network was due to His15 deprotonation and loss of its interaction with Glu198 (Federici *et al*., 2009).

Electrostatic mechanisms have also been shown to play crucial roles in protein systems that cycle between being soluble and membrane-bound. One such example is the myristoyl-electrostatic switch of the myristoylated alanine rich protein kinase C substrate protein (McLaughlin and Aderem, 1995; Arbuzova *et al*., 2000; Seykora *et al*., 1996). The myristoylated alanine rich protein kinase C substrate protein is attached to the membrane by a myristoyl tail but this attachment is not sufficient to maintain attachment to the membrane. Full membrane attachment necessitates favourable electrostatic interactions between the effector domain of the protein and the negatively charged inner portion of the plasma membrane (Thuddappathy *et al*., 2006a). The electrostatic interaction is reversible when the effector domain is phosphorylated. This phosphorylation alters the net charge of the protein thus driving localisation to the cytosol (Kim *et al*., 1994).

There is also evidence that electrostatic networks play a role in the membrane insertion of Bcl-$_{XL}$ (Thudappathy *et al*., 2006a). The *in vivo* signal for Bcl-$_{XL}$ to undergo the conformational change that is necessary for its membrane insertion remains unknown. However, low cytosolic pH during apoptosis has been reported (Matsuyama *et al*., 2000). Thudappathy *et al*. (2006a) suggested that an electrostatic mechanism of only a few kcal.mol^{-1} is sufficient to lower the activation energy for Bcl-$_{XL}$ to undergo a conformational change that enables Bcl-$_{XL}$ to go from its soluble to membrane conformation. This would require a small change in the surface charge of Bcl-$_{XL}$ (Thudappathy *et al*., 2006a). However, Bcl-$_{XL}$ may be controlled by an isolated switch that utilises only a few residues such as that of the myristoylated alanine rich protein kinase C substrate protein or it may be controlled by changes to its conformational state generated by changing the pK_a values of many residues.

Therefore, from the evidence provided above it is not unreasonable to propose that the salt-bridges and electrostatic and hydrogen bond interactions at the domain interface of CLIC1

provide a means whereby pH is utilised to induce stability changes in the protein, ultimately priming it for membrane insertion.

4.3. Conclusion

Low pH has been demonstrated to play a role not only in altering the conformational stability and flexibility of soluble CLIC1 but also in the ability of soluble CLIC1 to interact with artificial membranes and form functional ion channels. However, pH alone has not been illustrated to trigger the conformational changes required for CLIC1 to assume its membrane-bound form. Mutating the amino acid residues Arg29 and Glu81, residues that are involved in an N-terminal domain salt-bridge and hydrogen bond network causes decreased CLIC1 and CLIC1 intermediate stability. These findings show that the Arg29-Glu81 salt-bridge and interacting hydrogen bonds are involved in stabilisation of soluble CLIC1 and its intermediate species and that altering or removing the salt-bridge and hydrogen bonds, due to protonation of Glu81 at low pH (CLIC1-WT) or by mutation of the salt-bridge residues at pH 7 (R29M and R29M/E81M) and pH 5.5 (CLIC1-R29M, E81M, R29M/E81M) decreases the stability and cooperativity (N ↔ U) of CLIC1.

Therefore, the low pH at the membrane surface appears to alter the electrostatics of the salt-bridge and surrounding hydrogen bonding interactions and thereby enables the N-terminal domain to become destabilised and more flexible.

This flexibility may promote structural rearrangements of the N-terminal domain that permit the emergence of the “trapped” membrane topology. This happens due to the lowering of the activation energy barrier between the soluble and membrane-bound form of CLIC1 initiated by changes in pH.

Finally, it can be hypothesised that the Arg29-Glu81 salt-bridge functions as part of an electrostatic network at the domain interface of CLIC1 that forms as a pH-induced stability switch.

CHAPTER 5

REFERENCES

al-Awqati, Q. (1995) Chloride channels of intracellular organelles. *Curr. Opin. Cell Biol.* **4**, 504-8.

Anderson, D.E., Becktel, W.J., Dahlquist, F.W. (1990) pH-induced denaturation of proteins: a single salt bridge contributes 3-5kcal/mol to the free energy of folding of T4 lysozyme. *Biochemistry* **29**, 2403-2408.

Anfinsen, C.B. (1973) Principles that govern the folding of protein chains. *Science* **181**, 223-30.

Arbuzova, A., Wang, L., Wang, J., Hangyas-Mihalyne, G., Murray, D., Honig, B. and McLaughlin, S. (2000) Membrane binding of peptides containing both basic and aromatic residues. Experimental studies with peptides corresponding to the scaffolding region of caveolin and the effector region MARCKS. *Biochemistry* **39**, 10330-10339.

Ashley, R.H. (2003) Challenging accepted ion channel biology: p64 and the CLIC family of putative intracellular anion channel proteins (Review). *Mol. Membr. Biol*. **20**, 1-11.

Bailey, R. W., Dunker, A. K., Brown, C. J., Garner, E. C., and Griswold, M. D. (2001) Clusterin, a binding protein with a molten globule-like region. *Biochemistry* **40**, 11828–11840.

Banerjee, T., and Kishore, N. (2005) 2,2,2-Trifluoroethanol-Induced Molten Globule State of Concanavalin A and Energetics of 8-Anilinonaphthalene Sulfonate Binding: Calorimetric and Spectroscopic Investigation. *J. Phys. Chem. B* **109**, 22655–22662.

Barlow, D. J. and Thornton, J. M. (1983). Ion-pairs in proteins. *J. Mol. Biol*. **168**, 867-885.

Beecham, J. M. (1992) Global analysis of biochemical and biophysical data. *Methods Enzymol.* **210,** 37–54.

Berry, K.L., Bulow, H.E., Hall, D.H. and Hobert, O. (2003) A C.elegans CLIC-like Protein Required for Intracellular Tube Formation and Maintenance. *Science* **302**, 2134-2137.

Berry, K.L. and Hobert, O. (2006) Mapping functional domains of chloride intracellular channel (CLIC) proteins in vivo. *J. Mol. Biol*. **359**, 1316-1333.

Berryman, M. and Bretscher, A. (2000) Identification of a novel member of the chloride intracellular channel gene family, CLIC5, associates with the actin cytoskeleton of placental microvilli. *Mol. Biol. Cell* **11**, 1509-1521.

Berryman, M., Bruno, J., Price, J. and Edwards, J.C. (2004) CLIC-5A Function as a Chloride Channel *in Vitro* and Associates with the Cortical Actin Cytoskeleton *in Vitro* and *in Vivo*. *J. Biol. Chem*. **279**, 34794-34801.

Beirzynski, A., Kim, P.S. and Baldwin, R.L. (1982) A salt bridge stabilises the helix formed by isolated C-peptide of RNase A. *Proc. Natl. Acad. Sci. U.S.A.* **79**, 2470-2474

Bilsel, O., Zitzewitz, J.A., Bowers, K.E. and Matthews, C.R. (1999) Folding mechanism of the α-subunit of tryptophan synthase, an α/β barrel protein: Global analysis highlights the interconversion of multiple native, intermediate, and unfolded forms through parallel channels. *Biochemistry* **38,** 1018-1029.

Blaber, M., Lindstrom, J.D., Gassner, N., Xu, J., Heinz, D.W. and Matthews, B.W. (1993) Energetic cost and structural consequences of burying a hydroxyl group within the core of a protein determined from Ala-->Ser and Val-->Thr substitutions in T4 lysozyme. *Biochemistry* **32**, 11363-73.

Board, P.G., Coggan, M., Chelvanayagam, G., Easteal, S., Jermiin, L.S., Schulte, G.K., Danley, D.E., Hoth, L.R., Griffor, M.C., Kamath, A.V., Rosner,M.H., Chrunyk, B.A.,

Perregaux, D.E., Gabel, C.A., Geoghegan, K.F. and Pandit, J. (2000) Identification, characterization, and crystal structure of the Omega class glutathione transferases. *J. Biol. Chem*. **275**, 24798-24806.

Bosshard, H.R., Marti, D.N., and Jelesarov, I. (2004) Protein stabilization by salt bridges: concepts, experimental approaches and clarification of some misunderstandings. *J. Mol. Recognit*. **17**, 1-16.

Bryan, P.N. and Orban, J. (2010) Proteins that switch folds. *Curr. Opin. Struct. Biol*. **20**, 482-488

Bullough, P.A., Hughson, F.M., Skehel, J.J. and Wiley, D.C. (1994) Structure of influenza haemagglutinin at the pH of membrane fusion. *Nature* **371**, 37-43.

Chamberlain, A. K., and Marqusee, S. (1998) Molten globule unfolding monitored by hydrogen exchange in urea. *Biochemistry* **37**, 1736–1742.

Chayen, N. E., Shaw Stewart, P. D., Maeder, D. L. & Blow, D. M. (1990) An automated system for micro-batch protein crystallization and screening. *J. Appl. Crystallogr*. **23**, 297–302.

Chen, V.B., Arendall III, W.B., Headd, J.J., Keedy, D.A., Immormino, R.M., Kapral, G.J., Murray, L.W., Richardson, J.S. and Richardson, D.C. (2010) MolProbity: all-atom structure validation for macromolecular crystallography. *Acta. Crystallogr., Sect. D: Biol. Crystallogr*. **D66**, 12-21.

Chung, C.T., Niemela, S.L. and Miller, R.H. (1989) One-step preparation of competent Escherichia coli: Transformation and storage of bacterial cells in the same solution. *Proc. Natl. Acad. Sci. U.S.A.* **86**, 2172-2175.

Cromer, B.A, Morton, C.J., Board, P.G. and Parker, M. (2002) From glutathione transferase to pore in a CLIC. *Eur. Biophys. J.* **31**, 359-64.

Cromer, B.A., Gorman, M.A., Hansen, G., Adams, J.J., Coggen, M., Littler, D.J., Brown, L.J., Mazzanti, M., Breit, S.N., Curmi, P.M., Dulhunty, A.F., Board, P.G. and Parker, M.W. (2007) Structure of the Janus protein human CLIC2. *J. Mol. Biol*. **374**, 719-731.

Dao-pin, S., Anderson, D. E., Baase, W. A., Dahlquist, F. W. & Matthews, B. W. (1991). Structural and thermodynamic consequences of burying a charged residue within the hydrophobic core of T4 lysozyme. *Biochemistry* **30**, 11521-11529.

Davis, I.W., Leaver-Fay, A., Chen, V.B., Block, J.N., Kapral, G.J., Wang, X., Murray, L.W., Arendall III, W.B., Snoeyink, J., Richardson, J.S. and Richardson, D.C. (2007) MolProbity: all-atom contacts and structure validation for proteins and nucleic acids. *Nucleic Acids Res*. **35**, W375-W383.

Dill, K.A. (1990) Dominant forces in protein folding. *Biochemistry* **29**, 7133-7155.

Dougherty, D. (1996) Cation-π Interactions in Chemistry and Biology: A Niew View of Benzene, Phe, Tyr and Trp. *Science* **271**, 163-168.

Dulhunty, A., Gage, P., Curtis, S., Chelvanayagam, G. and Board, P. (2001) The glutathione transferase structural family includes a nuclear chloride channel and a ryanodine receptor calcium release channel modulator. *J. Biol. Chem*. **276**, 3319-3323.

Duncan, R.R., Westwood, P.K., Boyd, A. and Ashley. R.H. (1997) Rat Brain p64H1, Expression of a New Member of the p64 Chloride Channel Protein Family in Endoplasmic Reticulum. *J. Biol. Chem*. **272**, 23880-23886.

Edwards, J.C., Tulk, B and Schlesinger, P.H. (1998) Functional expression of p64, an intracellular chloride channel protein. *J. Membr. Biol*. **163**, 119-127.

Edelhoch, H. (1967) Spectroscopic determination of tryptophan and tyrosine in proteins. *Biochemistry* **6,** 1948-1954.

Eftink, M.R. and Ghirion, C.A. (1975) Dynamics of a protein matrix revealed by fluorescence quenching. *Proc. Natl. Acad. Sci. U.S.A.* **72**, 3290-3294.

Eftink, M.R. and Ghirion, C.A. (1976) Exposure of tryptophanyl residues in proteins. Quantitive determination of fluorescence quenching studies. *Biochemistry* **15**, 672-680.

Eftink, M.R. and Ghirion, C.A. (1977) Exposure of tryptophanyl residues and protein dynamics. *Biochemistry* **16**, 5546-5551.

Eftink M.R. and Ghirion, C.A. (1981) Fluorescence Quenching Studies with Proteins. *Anal. Biochem.* **114**, 199-227.

Eftink, M.R. (1995) Use of Multiple Spectroscopic Methods to Monitor Equilibrium Unfolding of Proteins. *Methods Enzymol*. **259**, 487-512.

Emsley, P. and Cowtan, K. (2004). Coot: model-building tools for molecular graphics. *Acta Crystallogr*. **D60**, 2126-2132.

Fairman, R., Shoemaker, K.R., York, E.J., Stewart, J.M. and Baldwin, R.L. (1990) The Glu2-…Arg10+ side chain interaction in the C-peptide helix of ribonuclease A. *Biophys. Chem*. **37**, 107-119.

Fanucchi, S: Effects of the environment on the conformational stability of the chloride intracellular channel protein CLIC1. *PhD thesis*. University of the Witwatersrand, Molecular and Cell Biology; 2006.

Fanucchi, S., Adamson, R.J. and Dirr, H.W. (2008) Formation of an Unfolding Intermediate State of Soluble Chloride Intracellular Channel Protein CLIC1 at Acidic pH. *Biochemistry* **47**, 11674-11681.

Federici, L., Masulli, M., Bonivento, D., Di Matteo, A., Gianni, S., Falvaloro, B., Di Ilio, C. and Allocati, N. (2007) Role of Ser11 in the stabilization of the structure of *Ochrobactrum anthropi. Biochem. J*. **403**, 267-274.

Federici, L., Masulli, M., Gianni, S., Di Ilio, C. and Allocati, N. (2009) A conserved hydrogen-bond network stabilizes the structure of Beta class glutathione S-transfreases. *Biochem. Biophys. Res Commun.* **382**, 525-529.

Fersht, A. R. (1972). Conformational equilibria in a- and d-chymotrypsin. The energetics and importance of the salt bridge. *J. Mol. Biol*. **64**, 497-509.

Fink, A. L. (1995) Protein Stability and Folding: Theory and Practice. In *Methods in Molecular Biology* (Shirley, B. A., ed.) pp. 343-360, Humana Press, NJ.

Flanagan, M.T. and Hesketh, T.R. (1973) Electrostatic interactions in the binding of fluorescent probes to lipid membranes. *Biochim. Biophys. Acta* **298**, 535-545.

Fraczkiewicz, R. and Braun, W. (1998) Exact and Efficient Analytical Calculation of the Accessible Surface Areas and Their Gradients for Macromolecules. *J. Comp. Chem.* **19**, 319-333.

Freedom, R.B. and Radda, G.K. (1969) The interaction of 1-anilino-8-naphthalene sulfonate with erythrocyte membranes. *FEBS Lett*. **3**, 150-152.

Gasteiger E., Hoogland C., Gattiker A., Duvaud S., Wilkins M.R., Appel R.D., Baroch A. (2005) Protein Identification and Analysis Tools on the ExPASy Server. In *The Proteomics Protocols Handbook* (Walker, J.M., ed), pp. 571-607, Humana Press, New York.

Gildenhuys, S. Wallace, L.A., Dirr, H.W. (2008) Stability of Reduced *Escherichia coli* Glutaredoxin 2: A Monomeric Structural Homologue of the Glutathione Transferase Family. *Biochemistry* **47**, 10801-10808.

Goodchild, S.C., Howell, M.W., Cordina, N.M., Littler, D.R., Breit, S.N., Curmi, P.M.G. and Brown, L.J. (2009) Oxidation promotes insertion of the CLIC1 chloride intracellular channel into the membrane. *Eur. Biophys. J.* **39**, 129-138.

Green, R.F.Jr., and Pace, C.N. (1973) Urea and guanidine hydrochloride denaturation of ribonuclease, lysozyme, α-chymotrypsin and β-lactoglobulin. *J. Biol. Chem.* **249,** 5388-5393

Green, M.R. (1986) Pre-mRNA splicing. *Annu. Rev. Genet*. **20**, 671-708.

Greenfield, N. (1999) Applications of circular dichroism in protein and peptide analysis. *TrAC, Trends Anal. Chem.* **18**, 236-244.

Guex, N. and Peitsch, M.C. (1997) SWISS-MODEL and the Swiss-Pdb viewer: an environment for comparative protein modelling. *Electrophoresis.* **18**, 2714-2723.

Harrop S.J., DeMaere, M.Z., Fairle, W.D., Reztsova, T., Valenzuela, S.M., Mazznti, M., Tonini, R., Qui, M.R., Jankova, L., Warton, K., Bauskin, A.R., Wu, W.M., Pankhurst, S., Campbell, T.J., Breit, S.N. and Curmi PMG (2001) Crystal structure of the soluble form of the intracellular chloride ion channel CLIC1 (NCC27) at 1.4 Å resolution. *J. Biol. Chem*. **276**, 44993-45000.

Hendsch, Z.S. and Tidor, B. (1994) Do salt bridges stabilize proteins – a continuum electrostatic analysis. *Protein Sci*. **3**, 211-2226.

Hoh, F., Cavé, A., Strub, M.P., Banères, J.L. and Padilla, A. (2009) Removing the invariant salt bridge of parvalbumin increases flexibility in the AB-loop structure. *Acta Crystallogr., Sect. D: Biol.Crystallogr*. **D65**, 733-743

Honig, B. H. and Hubell, W. L. (1984). Stability of “salt bridges" in membrane proteins. *Proc. Natl. Acad. Sci. U.S.A.* **81**, 5412-5416.

Hornby, J.A., Luo, J.K., Stevens, J.M., Wallace, L.A., Kaplan, W., Armstrong, R.N. and Dirr, H.W. (2000) Equilibrium folding of dimeric class mu glutathione transferases involves a stable monomeric intermediate. *Biochemistry* **39**, 12336-12344.

Horovitz, A. and Fersht, A. R. (1992). Co-operative interactions during protein folding. *J. Mol. Biol*. **224**, 733-740.

Howell, S., Duncan, R.R. and Ashley, R.H. (1996) Identification and characterisation of a homologue of p64 in rat tissues. *FEBS Lett.* **390**, 207-210.

Iurca-Mustata, G., Van Belle, D., Prevost, M. and Rooman, M. (2001) Role of Salt Bridges in Homeodomains Investigated by Structural Analyses and Molecular Dynamics Simulations. *Biopolymers* **59**, 145-159.

Jamin, M., Antalik, M., Loh, S. N., Bolen, D. W., and Baldwin, R. L. (2000) The unfolding enthalpy of the pH 4 molten globule of apomyoglobin measured by isothermal titration calorimetry. *Protein Sci.* **9**, 1340–1346.

Jentsch, T.J. and Gunther, W. (1997) Chloride channels: an emerging molecular picture. *BioEssays*. **19**, 117–126.

Kahn, P. (1979) The interpretation of near-ultraviolet circular dichroism. *Methods Enzymol.* **61**, 339−378.

Kajander, T., Khan, P.C., Passila, S.H., Cohen, D.C., Lethio, L., Adolfsen, W., Wawicker, J., Schell, U. and Goldeman, A. (2000) Buried charged surface in proteins. *Structure* **8**, 1203-1214.

Kazumasa, S. and Goto, Y. (2000) Manipulating Monomer-Dimer Equilibrium of Bovine β-Lactoglobulin by Amino Acid Substitution. *J. Biol. Chem*. **277**, 25735-25740.

Kelly, S.M. and Price, N.C. (1997) The application of circular dichroism to studies of protein folding and unfolding. *Biochim. Biophys. Acta* **1338**, 161-185.

Kelly, S.M. and Price, N.C. (2000) The use of Circular Dichroism in the Investigation of Protein Structure and Function. *Curr. Protein Pept. Sci.* **1**, 349-384.

Kim, J., Blackshear, P.J., Johnson, J.D. and McLaughlin, S. (1994) Phosphorylation reverses the membrane association of peptides that correspond to the basic domains of MARCKS and neuromodulin. *Biophys. J.* **67**, 227-237.

Knutson, J.R., Beechman, J.M. and Brand, L. (1983) Simultaneous analysis of multiple fluorescence decay curves: A global approach. *Chem. Phys. Lett.* **102**, 501-507.

Kumar, S and Nussinov, R. (1999) Salt bridge stability in monomeric proteins. *J. Mol. Biol.* **293**, 1241-55.

Kumar, S., Tsai, C. J., Ma, B. and Nussinov, R. (2000). Contribution of salt bridges toward protein thermostability. *J. Biomol. Struct. Dyn.* **11**, 79-85.

Kuwajima, K. (1989) The molten globule state as a clue for understanding the folding and cooperativity of globular-protein structure. *Proteins **6***, 87–103.

Lacroix, E., Viguera, A. R., and Serrano, L. (1998) Elucidating the folding problem of α-helices: Local motifs, long range electrostatics, ionic strength, dependence and prediction of NMR parameters. *J. Mol. Biol.* **284**, 173–191.

Laemmli, U.K. (1970) Cleavage of structural proteins during the assembly of the head of bacteriophage T4. *Nature* **227**, 680-685

Lakowicz, J.R and Weber, G. (1973) Quenching of fluorescence by oxygen: Detection of structural fluctuations in proteins on the nanosecond time scale. *Biochemistry* **12**, 4171-4179

Lakowicz, J. R. (1999) Principles of fluorescence spectroscopy. pp 11-14, 188, 237-249, 447-449. Plenum Press, New York.

Landry, D., Sullivan, S., Nicolaides, M., Redhead, C., Edelman, A., Field, M., Al-Awqati, Q and Edwards, J. (1993) Molecular cloning and characterization of p64, a chloride channel protein from kidney microsomes. *J. Biol. Chem.* **268**, 14948-14955.

Li, H., Robertson, A.D., and Jensen, J. H. (2005) Very fast empirical prediction and rationalization of protein pKa values. *Proteins* **61**, 704-721.

Li, Y.F., Li, D.F., Zeng, Z. and Wang, D.C. (2006) Trimeric structure of the wild soluble chloride intracellular ion channel CLIC4 observed in crystals. *Biochem. Biophys. Res. Commun*. **343**, 1272-1278.

Littler. D.R., Harrop, S.J., Fairlie, W.D., Brown, L.J., Pankhurst, G.J., Pankhurst, S., Campbell, T.J., Bauskin, A.R., Tonini, R., Mazzanti, M., Breit, S.N. and Curmi, P.M. (2004) The intracellular chloride channel protein CLIC1 undergoes a redox-controlled structural transition. *J. Biol. Chem*. **279**, 9298-9305.

Littler, D.R., Assaad, N.N., Harrop, S.J., Brown, L.J., Pankhurst, G.J., Luciano, P., Aguilar, M.I., Mazzanti, M., Berryman, M.A., Breit, S.N. and Curmi, P.M. (2005) Crystal structure of the soluble form of the redox-regulated chloride ion channel protein CLIC4. *FEBS J*. **272**, 4996-5007.

Littler, D.R., Harrop, S.J., Brown, L.J., Pankhurst, G.J., Mynott, A.V., Luciani, P., Mandyam, R.A., Mazzanti, M., Tanda, S., Berryman, M.A., Breit, S.N. and Curmi, P.M. (2008) Comparison of vertebrate and invertebrate CLIC proteins: the crystal structures of Caenorhabditis elegans EXC-4 and Drosophila melanogaster DmCLIC. *Proteins* **71**, 364-378.

Littler, D.R., Harrop, S.J., Goodchild, S.C., Phang, J.M., Mynott, A.V., Jian, L., Valenzuela, S.M., Mazzanti, M., Brown, L.J., Breit, S.N. and Curmi, P.M.G. (2010) The enigma of the CLIC proteins: Ion channels, redox proteins, enzymes, scaffolding proteins? *FEBS Lett*. **584**, 209-2101.

Littler, D.R., Brown, L.J., Breit, S.N., Perrakis, A. and Curmi, P.M.G. (2010b) Structure of human CLIC3 at 2 Å resolution. *Proteins* **78**, 1594-1600.

Lloyd, S.E., Pearce, S.H., Fisher, S.E., Steinmeyer, K., Schwappach, B., Scheinman, S.J., Harding, B., Bolino, A., Devoto, M., Goodyer, P., Rigden, S.P., Wrong, O., Jentsch, T.J., Craig, I.W. and Thakker, R.V. (1996) A common molecular basis for three inherited kidney stone diseases. *Nature* **379**, 445-449.

Lounnis, V. and Wade, R.C. (1997) Exceptionally Stable Salt Bridges in Cytochrome P450cam Have Functional Roles. *Biochemistry* **36**, 5402-5417.

Ma, J.C. and Dougherty, D.A. (1997) The cation-π interaction. *Chem. Rev*. **97**, 1303-1324.

Marqusee, S. and Sauer, R. T. (1994). Contribution of a hydrogen bond/salt bridge network to the stability of secondary and tertiary structures in lambda repressor. *Protein Sci*. **3**, 2217-2225

Matthews, B. W. (1968) Solvent content of protein crystals. *J. Mol. Biol.* **33**, 491–497.

Matsuyama, S., Llopis, J., Deveraux, Q.L., Tsien, R.Y and Reed, J.C. (2000) Changes in intramitochondrial and cytosolic pH: early events that modulate caspase activation during apoptosis. *Nature Cell. Biol*. **2**, 318-325.

McCoy, A.J., Grosse-Kunstleve, R.W., Adams, P.D., Winn, M.D., Storoni, L.C. and Read, R.J. J. (2007) Phaser crystallographic software. *J. Appl. Crystallogr*. **40**, 658-674.

McLaughlin, S and Aderem, A. (1995) The myristoyl-electrostatic switch: a modulator of reversible protein-membrane interactions. *Trends Biochem. Sci*. **20**, 272-276.

Mi, W., Liang, Y.H., Lanfen, L. and Su, X.D. (2008) The crystal structure of human chloride intracellular channel protein 2: A disulfide bond with functional implications. *Proteins* **71**, 509-513.

Mottonen, J., Strand, A., Symersky, J., Sweet, R.M., Danley, D.E., Geoghegan, K.F., Gerard, R.D. and Goldsmith, E.J. (1992) Structural basis of latency in plasminogen activator inhibitor-1. *Nature* **355**, 270-273.

Muga, A., Gonzalez-Manas, J.M., Lakey, J.H., Pattus, F. and Surewicz, W.K. (1993) pH-dependent stability and membrane interaction of the pore-forming domain of colicin A. *J. Biol. Chem.* **268**, 1553-7.

Murshudov, G.N., Vagin, A.A. and Dodson, E.J. (1997) Refinement of Macromolecular Structures by the Maximum-Likelihood method. *Acta Crystallogr., Sect. D: Biol. Crystallogr.* **D53**, 240-255.

Murzin, A.G. (2008) Biochemistry. Metamorphic proteins. *Science* **320**, 1725-1726.

Musafia, B., Buchner, V. and Arad, D. (1995). Complex salt bridges in proteins: statistical analysis of structure and function. *J. Mol. Biol*. **254**, 761-770.

Neuefeind T, Huber R, Dasenbrock H, Prade L, Bieseler B (1997) Crystal structure of herbicide-detoxifying maize glutathione S-transferase-I in complex with lactoylglutathione: evidence for an induced-fit mechanism. *J. Mol. Biol.* **274**, 446-453.

Nishizawa, T., Nagao, T., Iwatsubo, T., Forte, J.G. and Urushidani, T. (2000) Molecular Cloning and Characterization of a Novel Chloride Intracellular Channel-related Protein, Parchorin, Expressed in Water-secreting Cells. *J. Mol. Chem*. **275**, 11164-11173.

Pace, C.N. (1986) Determination and analysis of urea and guanidine hydrochloride denaturation curves. *Methods Enzymol.* **131**, 266-280.

Pace, C.N. and J.M. Scholtz (1996) Measuring the conformational stability of a protein. In Protein Structure: A Practical Approach (Creighton, T. E., ed) pp. 299-321, IRL Press, Oxford.

Pace, C.N., Grimsley, G.R. and Scholtz, J.M. (2009) Protein ionizable groups: pK values and their contribution to protein stability and solubility. *J. Biol. Chem*. **284**, 13285-13289.

Papworth. C., Bauer, J.C., Braman, J. and Wright, D.A. (1996) Site-directed mutagenesis using double-stranded plasmid DNA templates. *Strategies* **9**, 3-4.

Parker, M.W. and Feil, S.C. (2005) Pore-forming protein toxins: from structure to function. *Prog. Biophys. Mol. Biol*. **88**, 91-142.

Paul, C.H. (1982) Building models of globular protein molecules from their amino acid sequences. 1. Theory. *J. Mol. Biol.* **155**, 53-62.

Perkins, S.J. (1986) Protein volumes and hydration effects. *Eur. J. Biochem.* **319**, 749-754.

Perutz, M. F. (1970). Stereochemistry of cooperative effects in haemoglobin. *Nature* **228**, 726-739.

Perutz, M.F., Gronenborn, A.M., Clore, G.M., Fogg, J.H. and Shih, D.T. (1985) The pKa values of two histidine residues in human haemoglobin, the Bohr effect, and the dipole moments of a-helices. *J Mol. Biol.* **183**, 491-498.

Pervushin, K., Billeter, M., Siegal, G. and Wuthrich, K. (1996). Structural role of a buried salt bridge in the 434 repressor DNA-binding domain. *J. Mol. Biol*. **264**, 1002-1012.

Piromjitpong J, Wongsantichon J, Ketterman AJ (2007) Differences in the subunit interface residues of alternatively spliced glutathione transferases affects catalytic and structural functions. *Biochem. J.* **401**, 635–644.

Ptitsyn, O. B. (1995) Molten globule and protein folding. *Adv. Protein Chem.* ***47***, 83–229.

Rico, M., Nieto, J.L., Santoro,J., Bermejo, F.J., Herrandz, J. and Gallego, E. (1983) Low-Temperature 1H-NMR evidence of the folding of isolated ribonuclease S-peptide. *FEBS Lett*. **162**, 314-319.

Riordan, J.R., Rommens, J.M., Kerem, B., Alon, N., Rozmahel, R., Grzelczak, Z., Zielenski, J., Lok, S., Plasvic, N., Chou, J.L., Drumm, M.L., Ianuzzi, M.C., Collins, F.S. and Tsui, L.C. (1998) Identification of the cystic fibrosis gene: cloning and characterisation of complementary DNA. *Science* **245**, 1066-1073.

Rodionova, N.A., Semisotnov, G.V., Kytyshenko, V.N., Uverskym, I.A., Bolotina, V.E. and Ptitsyn. (1989) Staged equilibrium of carbonic anhydrase unfolding in strong denaturants. *Mol. Biol. (Mosk)* **23**, 683-692.

Sanchez-Ruiz, J.M. and Makhatadze, G.I. (2001) To charge or not to charge? *Trends Biotechnol.* **19**, 132–135.

Sandvig, K. and Olsnes, S. (1980) Diphtheria toxin entry into cells is facilitated by low pH. *J. Cell Biol.* **87**, 828-32.

Schmid, F.X. (1997) Optical spectroscopy to characterise protein conformation. In Protein structure – a practical approach (2nd Ed.) (Creighton, T.E., ed.), pp. 261-297, Oxford University Press, UK.

Scholtz, J.M. and Baldwin, R.L. (1992) The mechanism of α-helix formation by peptides. *Annu. Rev. Biophys. Biomol. Struct.* **21**, 9-118.

Scrutton, N.S. and Raine, A.R.C. (1996) Cation-pi bonding and amino-aromatic interactions in the bimolecular recognition of substituted ammonium ligands. *Biochem. J*. **319**, 1-8.

Semisotnov, G.V., Rodionova, N.A., Razgulyaev, O.I., Uversky, Y.N., Gripas, A.F. and Gilmanshin, R.I. (1991) Study of the “molten globule” intermediate state in protein folding by a hydrophobic fluorescent probe. *Biopolymers* **3**, 119-128.

Serrano, L., Horovitz, A., Avron, B., Bycroft, M. and Fersht, A. R. (1990). Estimating the contribution of engineered surface electrostatic interactions to protein stability by using double mutant cycles. *Biochemistry* **29**, 9343-9352.

Seykora, J.T., Myat, M.M., Allen, L.A., Ravetch, J.V. and Aderem, A. (1996) Molecular determinants of the myristoyl-electrostaitic switch of MARCKS. *J. Biol. Chem.* **271**, 18797-18802.

Shai, Y. (1999) Mechanism of the binding, insertion and destabilization of phospholipid bilayer membranes by α-helical antimicrobial and cell non-selective membrane-lytic peptides. *Biochim. Biophys. Acta*. **1462**, 55-70.

Shanks, R.A., Larocca, M.C., Berryman, M., Edwards, J.C., Urushidani, T., Navarre, J. and Goldenring, J.R. (2002) AKAP350 at the Golgi apparatus. II. Association of AKAP350 with a novel chloride intracellular channel (CLIC) family member. *J. Mol. Chem*. **277**, 40973-40980.

Shoemaker, K.R., Kim, P.S., Brems, D.N., Marqusee, S., York, E.J., Chaiken, I.M., Stewart, J.M. and Baldwin, R.L. (1985) Nature of the charged-group effect on the stability of the C-peptide helix. *Proc. Natl. Acad. Sci. U.S.A.* **82**, 2349–2353.

Shorning, B.Y., Wilson, D.B., Meehan, R.R. and Ashley. R.H. (2003) Molecular cloning and development expression of Chloride Intracellular Channel (CLIC) genes in *Xennopus laevis. Dev. Genes Evol*. **213**, 514-518.

Simpkins, I. (2000) General principles of biochemical investigations, In Principles and Techniques of Practical Biochemistry (Wilson, K and Walker, J. ed.), pp. 1-7, Cambridge University Press, U.K.

Simon, D.B., Bindra, R.S., Mansfield, T.A., Nelson-Williams, C., Mendonca, E., Stone, R., Schurman, S., Nayir, A., Alply, H., Bakkaloglu, A., Rodriguez-Soriano, J., Morales, J.M., Taylor, C.M., Pilz, D., Brem, A., Trachtman, H., Griswold, W., Richard, G.A., John, E. and

Lifton, R.P. (1997) Mutations in the chloride channel gene *CLCNKB* cause Bartter's syndrome type III. *Nat. Genet.* **17**, 171-178.

Singh, U. C. (1988). Probing the salt bridge in the dihydrofolate reductase methotrexate complex by using the coordinate-coupled free energy perturbation method. *Proc. Natl Acad. Sci. US.A.* **85**, 4280-4284.

Singh, H and Ashley, R.H. (2006) Redox Regulation of CLIC1 by Cysteine Residues Associated with the Putative Channel Pore. *Biophys. J.* **90**, 1628-38.

Singh, H. and Ashley, R.H. (2007) CLIC4 (p64H1) and its putative transmembrane domain form poorly selective, redox regulated ion channels. *Mol. Membr. Biol*. **24**, 41-52.

Singh, H., Cousin, M.A. and Ashely, R.H. (2007) Functional reconstitutiom of mammalian "chloride intracellular channels" CLIC1, CLIC4 and CLIC5 reveals differential regulation by cytoskeletal actin. *FEBS J*. **274**, 6306-6316.

Sinha, N., Kumar, S. and Nussinov, R. (2001a) Inter-Domain Interactions in Hinge-Bending Transitions. *Structure* **9**, 1165-1181.

Sinha. N. and Nussinov, R. (2001b) Point mutations and sequence variability in proteins: Redistributions of pre existing populations. *Proc. Natl. Acad. Sci. U.S.A.* **98**, 3139-3144.

Sinha, N., Tsai, C.J. and Nussinov, R. (2001c) Building blocks, hinge-bending motions and protein topology. *J. Biomol. Struct. Dyn.* **19**, 369-380.

Soulages, J.L. (1998) Chemical Denaturation: Potential Impact of Undetected Intermediates in the Free Energy of Unfolding and *m*-Values Obtained from a Two-State Assumption. *Biophys. J*. **75**, 484-492.

Stoychev, S: The role of the domain interface in the stability, folding and function of CLIC1. *PhD thesis***.** University of the Witwatersrand, Molecular and Cell Biology; 2006.

Stoychev, S.H., Nathaniel, C., Fanucchi. S., Brock, M., Li, S., Asmus, K., Woods, V.L. and Dirr, H.W. (2009) Structural Dynamics of Soluble Chloride Intracellular Channel Protein CLIC1 Examined by Amide Hydrogen-Deuterium Exchange Mass Spectrometry. *Biochemistry* **48**, 8413-8421.

Strange, K., Emma, F. and Jackson, P.S. (1996) Cellular and molecular physiology of volume-sensitive anion channels. *Am. J. Physiol.* **270**, C711-C730.

Strickland, E.H. (1974) Aromatic contributions to circular dichroism spectra of proteins. *Crit. Rev. Biochem.* **2**, 113-175.

Stryer, L.S. (1965) The interaction of a naphthalene dye with apomyoglobin and apohemoglobin. A fluorescent probe of non-polar binding sites *J. Mol. Biol*. **13**, 482-495.

Sun, D. P., Sauer, U., Nicholson, H. and Matthews, B. W. (1991). Contributions of engineered surface salt bridges to the stability of T4 lysozyme determined by directed mutagenesis. *Biochemistry* **30**, 7142-7153.

Takano, K., Sholtz, J.M., Sacchettini, J.C., and Pace, C.N. (2003) The contribution of polar group burial to protein stability is strongly context-dependent. *J. Biol. Chem*. **278**, 31290-31795.

Tanford, C. (1970) Protein denaturation. *Adv. Protein Chem.* **24**, 1-95.

The Collaborative Computational Project, Number 4 Suite: Programs for Protein Crystallography. *Acta Cryst.* **D50**, 760-763.

Thompson J.D., Higgins, D.G. and Gibson, T.J. (1994) CLUSTAL W: improving the sensitivity of progressive multiple sequence alignment through sequence weighting, position specific gap penalties and weight matrix choice. *Nucleic Acids Res*. **22**, 4673-80.

Thuduppathy, G. R., Terrones, O., Craig, J. W., Basa~nez, G., and Hill, R. B. (2006) The N-terminal domain of Bcl-XL reversibly binds membranes in a pH-dependent manner. *Biochemistry* **45**, 14533–14542.

Thudappathy, G.R., Craig, J.W., Kholodenko, V., Schon, A. and Hill, R.B. (2006a) Evidence that Membrane Insertion of the Cytosolic Domain of Bcl-XL is Governed by an Electroststic Mechanism. *J. Mol. Biol.* **359**, 1045-1058.

Thurkill, R.L., Grimsley, G.R. Scholtz, J.M. and Pace, C.N. (2006) Hydrogen bonding markedly reduces the pK of buried carboxyl groups in proteins. *J. Mol. Biol.* **362**, 594-604.

Tuinstra, R.L., Peterson, F.C., Kutlesa, S., Elgin, E.S., Kron, M.A. and Volkman, B.F. (2008) Interconversion between two unrelated protein folds in the lymphotactin native state. *Proc. Natl. Acad. Sci. U.S.A.* **105**, 5057-5062.

Tonini, R., Ferroni, A., Valenzuela, S.M., Warton, K., Campbell, T.J., Breit, S.N. and Mazzanti, M. (2000) Characterisation of the NCC27 nuclear ion channel: Comparison of its electrophysiological properties on the nuclear and plasma membranes and inhibition of its conductance in transfected CHO-K1 cells by antibody blockade. *FASEB J*. **14**, 1171-1178.

Towell, J.F. and Manning, M.C. (1994) Analysis of protein structure spectroscopy, In Techniques and Instrumentation in Analytical Chemistry (Purdie, N and Brittain, H.G., ed.), pp. 175-205, Elsevier Science B. V., New York.

Tulk, B.M., Schlesinger, P.H., Kapadia, S.A. and Edwards, J.C. (2000) CLIC-1 functions as a chloride channel when expressed and purified from bacteria. *J. Biol. Chem.* **275**, 269866-26998.

Tulk, B.M., Kapadia, S. and Edwards, J.C. (2002) CLIC1 inserts from the aqueous phase into phospholipids membranes, where it functions as an anion channel. *Am. J. Physiol. Cell Physiol.* **282**, C1109-C1112.

Uversky, V.N., Winter, S. and Lober, G. (1998) Self-association of 8-anilino-1-naphthalene-sulfonate molecules: spectroscopic characterization and application to the investigation of protein folding. *Biochim. Biophys. Acta* **1388**, 133-142.

Van der Goot, F.G., Gonzalez-Manas, J.M., Lakey, J.H. and Pattus, F. (1991) A "molten-globule" membrane-insertion intermediate of the pore-forming domain of colicin A. *Nature* **354**, 408-410.

Valenzuela, S.M., Martin, D.K., Por, S.B., Robbins, J.M., Warton, K., Bootcov, M.R., Schofield, P.R., Campbell, T.J. and Breit, S.N. (1997) Molecular cloning and expression of chloride ion channel of cell nuclei. *J. Biol. Chem*. **272**, 12575-12582.

Waldburger, C.D., Schildbach, J.F., Sauer, R.T. (1995) Are buried salt bridges important for protein stability? *Nat. Struct. Biol*. **2**, 122-128.

Wallace, A.C., Laskowski, R.A. and Thornton, J.M. (1995) LIGPLOT: a program to generate schematic diagrams of protein-ligand interactions. *Protein Eng.* **8**, 127-134.

Wallace, L. A., Sluis-Cremer, N., and Dirr, H. W. (1998) Equilibrium and kinetic unfolding properties of dimeric human glutathione transferase A1-1. *Biochemistry* **37**, 5320–5328.

Wallace, L.A., Burke, J. and Dirr, H.W. (2000) Domain-domain interface packing at conserved Trp-20 in class alpha glutathione transferase impacts on protein stability. *Biochim. Biophys. Acta* **1478**, 325-332.

Wang, Y., Geer, L. Y., Chappey, C., Kans, J. A. and Bryant, S. H. (2000) Cn3D: sequence and structure views for Entrez. *Trends Biochem. Sci.* **25**, 300-302.

Warton, K., Tonini, R., Fairlie, W.D., Mathews, J.M., Valenzuela, S.M., Qui, M.R., Wu, W.M., Pankhurst, S., Bauskin, A.R., Harrop, S.J, Campbell, T.J., Curmi, P.M.G., Breit,S.N. and Mazzanti, M (2002) Recombinant CLIC1 (NCC27) assembles in lipid bilayers via a pH-dependent two-state process to form chloride ion channels with identical characteristics to

those observed in Chinese hamster ovary cells expressing CLIC1. *J. Biol. Chem.* **277**, 26003-26011.

Weber, G. and Young, L. B. (1964). Fragmentation of Bovine Serum Albumin by Pepsin. I. the Origin of the Acid Expansion of the Albumin Molecule. *J. Biol. Chem.* **239**, 1415-23.

Winayanuwattikun,P and Ketterman, A.J. (2005) An Electron-sharing Network Involved in the Catalytic Mechanism is Functionally Conserved in Different Glutathione Transferase Classes. *J. Biol. Chem*. **280**, 31776-31782.

White, S. H., and Wimley, W. C. (1999) Membrane protein folding and stability: Physical principles. *Annu. Rev. Biophys. Biomol. Struct.* **28**, 319–365.

Whitten, S.T., and García-Moreno, B.E. (2000) pH dependence of stability of staphylococcal nuclease: evidence of substantial electrostatic interactions in the denatured state. *Biochemistry* **39**, 14292-14304.

Woody, R.W. (1995) Circular dichroism. *Methods Enzymol.* **246**, 34-71.

Xu, D., Lin, S. L. and Nussinov, R. (1997). Protein binding versus protein folding: the role of hydrophilic bridges in protein associations. *J. Mol. Biol*. **265**, 68-84.

Xu, D., Tsai, C. J. and Nussinov, R. (1997a). Hydrogen bonds and salt bridges across protein-protein interfaces. *Protein Eng*. **10**, 999-1012.

Yamasaki, M., Li, W., Johnson, D.J. and Huntington, J.A. (2008) Crystal structure of a stable dimer reveals the molecular basis of serpin polymerization. *Nature*. **455**, 1255-1258.

Zitzewitz, J.A., Bilsel, O., Luo, J., Jones, B.E. and Matthews, C.R. (1995) Probing the folding mechanism of a leucine zipper peptide by stopped-flow circular dichroism spectroscopy. *Biochemistry* **34,** 12812-12819.

CHAPTER 6

APPENDIX

Table A: Data-collection and refinement statistics…….....118

Figure A: Ribbon representation of the superimposed crystal structures of CLIC1-WT and CLIC1-R29M/E81M…….…...119

Figure B: Ramachandran plots of CLIC1-WT and CLIC1-R29M/E81M……..……..120

Determination of the crystal structure of CLIC1-R29M/E81M

I would like to acknowledge Dr Fanucchi and Dr Achilonu from the Protein Structure-Function Research Unit, School of Molecular and Cell Biology, University of the Witwatersrand and Dr Fernandes, School of Chemistry, University of the Witwatersrand for their hard work obtaining the crystal structure of CLIC1 R29M/E81M.

6.1. Purification of CLIC1-R29M/E81M

CLIC1 R29M/E81M was purified as described in Chapter 2, section 2.2.4. Possible impurities were removed via size exclusion chromatography using a G-75 sephadex column.

6.2. R29M/E81M crystal structure

6.2.1. Crystallisation of CLIC1-R29M/E81M

The crystallisation of CLIC1-R29M/E81M was performed by Dr Ikechukwa Achilonu, University of the Witwatersrand, Johannesburg, South Africa. Crystals were grown by the hanging-drop vapour diffusion method at 293 K using a 24-well microplate. Each hanging drop consisted of equal volumes of protein (10 mg/ml in 0.1 M Tris-HCl, 5 mM DTT and 0.02% NaN_3, pH 6.5) and reservoir buffer consisting of 0.1 M Bis-Tris, 25% (w/v) PEG 2000 monomethyl ether, 0.02% NaN_3 and 1 mM DTT, pH 6.5. The reservoir volume used was 1.5 ml and consisted of 1 mL reservoir buffer and 0.5 mL oil (silicon oil : paraffin oil, 1:1) for favourable conditions for the growth of large crystals by slowing evaporation and supersaturation in the wells (Chayen *et al*., 1990).

The crystals were harvested, briefly soaked in reservoir buffer and mounted on a cryo-loop. X-ray diffraction data was collected on a Bruker X8 Proteum system with a Microstar copper rotating-anode generator with Montel 200 optics, a PLATINUM 135 CCD detector and an Oxford Cryostream Plus system. Crystals were cooled in a stream of nitrogen to 113 K during data collection and images were collected covering an oscillation angle of 0.5 ^{o} per image. Data were processed using the programs SAINT and APEX (Bruker AXS Inc, Madison, Wisconsin, USA) by Professor Manuel Fernandez, University of the Witwatersrand, Johannesburg, South Africa.

6.2.2. Structure solution

The CLIC1-R29M/E81M crystal structure was solved by Dr Sylvia Fanucchi, University of the Witwatersrand, Johannesburg, South Africa. The protein structure was solved by molecular replacement using PHASER (McCoy *et al*., 2007), as implemented in the CCP4 suite of programs using CLIC1-M32A (PDB entry 3O3T) as the search model. The structure was refined using TLS and restrained refinement as implemented in the program REFMAC5 (Murshudov *et al*., 1997). Addition of waters and real space refinement were performed using COOT (Emsley and Cowten, 2004). The model was validated using MolProbity (Chen *et al*., 2010, Davis *et al*., 2007).

6.3. Crystal structure of R29M/E81M

As mentioned previously, the crystal structure of CLIC1-R29M/E81M was solved by Drs Ikechukwa Achilonu, Manuel Fernandes and Sylvia Fanucchi, University of the Witwatersrand, Johannesburg, South Africa. The details of the structure are reported here and are used to further interpret the structural and stability data obtained in this study.

The structure of human CLIC1-R29M/E81M was determined to a resolution of 1.78 Å and the data-collection and refinement statistics are shown in Table A (http://www.rcsb.org/pdb/explore/explore.do?structureId=3P8W). The Matthews coefficient (V_M; Matthews, 1968) for the crystal was calculated using the *CCP4* suite of programs (Collaborative Computational Project, Number 4, 1994). A V_M value of 2.13 $Å^3$ Da^{-1} was obtained with associated solvent content of 42.23% indicating that the crystal contained 1 molecule in the asymmetric unit. The electron density of the final model is well defined for residues 6-241.

The electron densities for residues 29 and 81 in the R29M/E81M mutant are consistent with a methionine residue. The replacement of Arg29 and Glu81 by methionine does not alter the backbone structure as indicated by an rmsd of 2.22 Å between the backbone C^{α} of the CLIC1-WT and R29M/E81M proteins (Figure A). The Ramachandran plots for the WT and R29M/E81M mutant proteins are shown in Figure B and indicate that the backbone conformation of R29M/E81M mutant is not significantly different to that of the WT.

Table A: Data-collection and refinement statistics

	R29M/E81M CLIC1
PDB code	3P8W
Wavelength (Å)	1.518
Space Group	P 2_1 2_1 2_1
Unit Cell Parameters (Å, °)	a=42.39 b=64.61 c=82.98 α=β=γ=90
Wilson plot *B* factor (Å^2)	17.376
Solvent content (%)	42.23
Resolution Range (A)	50.98 – 1.78
No. of observed reflections	15972
Completeness %	98.2
$\langle I/\sigma(I) \rangle$	12.41
R_{sym}	0.27
Final overall *R* factor	0.2141
R_{work}	0.2104
R_{free}	0.2815
No. of protein atoms	1850
Matthews coefficient V_M (Å^{3}Da^{-1})	2.13
Average *B* value (Å^2)	16.29
rmsd in bond length (Å)	0.019
rmsd in bond angles (°)	1.758
Ramachandran statistics **Most allowed (%)** **Allowed (%)**	 97.6 99.6
Asymmetric unit content	Monomer



Figure A: Ribbon representation of the superimposed crystal structures of CLIC1-WT and CLIC1-R29M/E81M.

CLIC1-WT (black) and CLIC1-R29M/E81M (grey) proteins. This image was generated using Swiss PDB Viewer (Guex and Peitsch, 1997) using PDB codes 1k0m (Harrop *et al.*, 2001) and 3P8W (http://www.rcsb.org/pdb/explore/explore.do?structureId=3P8W).

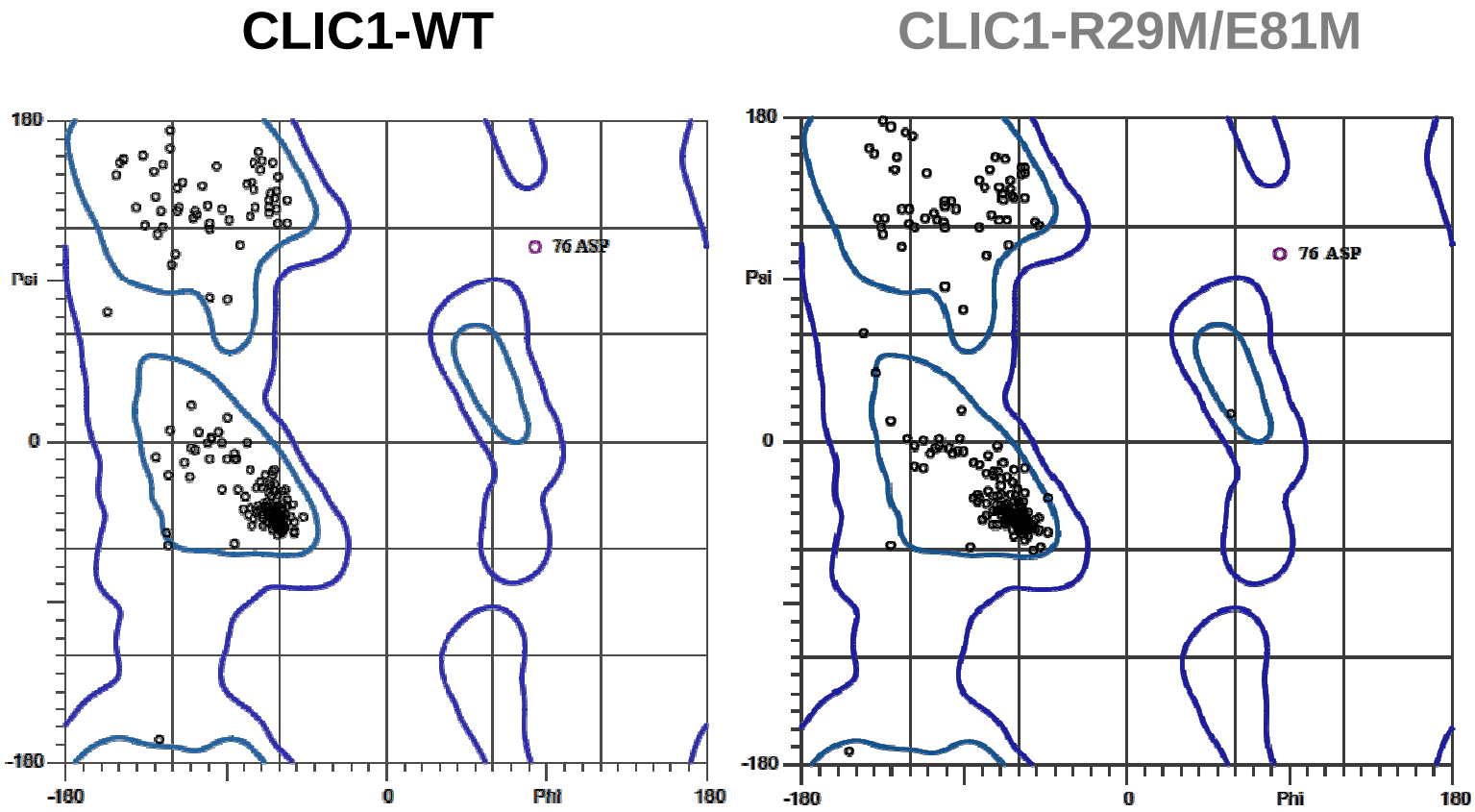


Figure B: Ramachandran plots of CLIC1-WT and CLIC1-R29M/E81M

The most allowed region of the Ramachandran plots consisted of 97.6% of residues for CLIC1-WT and R29M/E81M. The allowed region consisted of 99.6% and 99.4% of the residues for CLIC1-WT and R29M/E81M, respectively. This image was generated using Swiss PDB Viewer (Guex and Peitsch, 1997) using PDB codes 1K0M (wild type) (Harrop *et al.*, 2001) and 3P8W (R29M/E81M) (http://www.rcsb.org/pdb/explore/explore.do?structureId=3P8W).